Statistical Analysis of Surface-Water-Quality Data in and near the Coal-Mining Region of Southwestern Indiana, 1957–80

United States Geological Survey Water-Supply Paper 2291

Statistical Analysis of Surface-Water-Quality Data in and near the Coal-Mining Region of Southwestern Indiana, 1957–80

By JEFFREY D. MARTIN and CHARLES G. CRAWFORD

U.S. GEOLOGICAL SURVEY WATER-SUPPLY PAPER 2291

DEPARTMENT OF THE INTERIOR
DONALD PAUL HODEL, Secretary

U.S. GEOLOGICAL SURVEY
Dallas L. Peck, Director

UNITED STATES GOVERNMENT PRINTING OFFICE: 1987

For sale by the Books and Open-File Reports Section, U.S. Geological Survey,
Federal Center, Box 25425, Denver, CO 80225

Library of Congress Cataloging in Publication Data

Martin, Jeffrey D.
Statistical analysis of surface-water-quality data in and near the coal-mining region of southwestern Indiana, 1957–80.

(U.S. Geological Survey water-supply paper ; 2291)
Bibliography: p.
Supt. of Docs. no.: I 19.13:2291
1. Water quality—Indiana—Statistical methods. 2. Coal mines and mining—Environmental aspects—Indiana. I. Crawford, Charles G. II. Title. III. Series: Geological Survey water-supply paper ; 2291.
TD224.I6M37 1986 628.1'6832 85–600284

CONTENTS

FIGURES

TABLES [Tables are at end of paper]

ABBREVIATIONS

a	Regression intercept coefficient
a_c	Corrected intercept coefficient in the exponential form of the log-log model
Alk	Total alkalinity concentration, in milligrams per liter as calcium carbonate
b	Regression slope coefficient
CL	Upper or lower confidence limit
CL lower	Lower confidence limit
CL upper	Upper confidence limit
CV	Coefficient of variation, in percent
DS	Dissolved-solids concentration, in milligrams per liter
Ep	Standard error of regression, in percent
Es	Standard error of regression
f	Confidence limit factor equal to 1 for the predicted individual response or equal to 0 for the predicted mean or median response
°F	Degree Fahrenheit
Fe	Total iron concentration, in micrograms per liter
ft^3/s	Cubic foot per second
$ft^3/s/mi^2$	Cubic foot per second per square mile
h	Positive constant in the hyperbolic model
in	Inch
$\log_{10}$	Base-10 logarithm
M	Mean
mg/L	Milligram per liter
mg/L as $CaCO_3$	Milligram per liter as calcium carbonate
mi^2	Square mile
Mn	Total manganese concentration, in micrograms per liter
n	Number of data pairs
N.	North
NS	Relation is not significant at $p<0.05$
p	Probability of obtaining a statistically significant relation where, in fact, there is no relation
$p<0.01$	Probability is less than 1 percent
$p<0.05$	Probability is less than 5 percent
Q	Streamflow, in cubic foot per second
$\bar{Q}$	Mean streamflow, in cubic foot per second
R	Residual error
R-square	Coefficient of determination
S	Standard deviation
SC	Specific conductance, in microsiemens per centimenter at 25 degrees Celsius
SO_4	Sulfate concentration, in milligrams per liter
SS	Suspended-solids concentration, in milligrams per liter
Sxx	Sum of squares of the independent variable
$t_{\alpha/2}$	Critical value of the t distribution with n–2 degrees of freedom and $100(1-\alpha)$ percent probability
W.	West
x	A value of a water-quality variable that is transformed to a value of the independent variable (X)
X	A value of the independent variable
$\bar{X}$	Mean of the independent variable
y	A value of a water-quality variable that is log-transformed to a value of the dependent variable (Y)
Y	A value of the dependent variable
$\hat{Y}$	Predicted response of the dependent variable for a value of the independent variable
Z	Characteristic of the base-10 logarithm of mean streamflow
α	(1–P/100), where P is the desired percent probability for the confidence limit
Σ	Summation
µg/L	Microgram per liter
µS/cm at 25°C	Microsiemens per centimeter at 25 degrees Celsius
–	In tables 29 and 30 only, a negative relation
+	In table 30 only, a positive relation
*	Relation is significant at $p<0.05$
**	Relation is significant at $p<0.01$

Statistical Analysis of Surface-Water-Quality Data in and near the Coal-Mining Region of Southwestern Indiana, 1957–80

By Jeffrey D. Martin *and* Charles G. Crawford

Abstract

The Surface Mining Control and Reclamation Act of 1977 requires that applications for coal-mining permits contain information about the water quality of streams at and near a proposed mine. To meet this need for information, streamflow, specific conductance, pH, and concentrations of total alkalinity, sulfate, dissolved solids, suspended solids, total iron, and total manganese at 37 stations were analyzed to determine the spatial and seasonal variations in water quality and to develop equations for predicting water quality.

The season of lowest median streamflow was related to the size of the drainage area. Median streamflow was least during fall at 15 of 16 stations having drainage areas greater than 1,000 square miles but was least during summer at 17 of 21 stations having drainage areas less than 1,000 square miles. In general, the season of lowest median specific conductance occurred during the season of highest streamflow except at stations on the Wabash River. Median specific conductance was least during summer at 9 of 9 stations on the Wabash River, but was least during winter or spring (the seasons of highest streamflow) at 27 of the remaining 28 stations.

Linear, inverse, semilog, log-log, and hyperbolic regression models were used to investigate the functional relations between water-quality characteristics and streamflow. Of 186 relations investigated, 143 were statistically significant. Specific conductance and concentrations of total alkalinity and sulfate were negatively related to streamflow at all stations except for a positive relation between total alkalinity concentration and streamflow at Patoka River near Princeton. Concentrations of total alkalinity and sulfate were positively related to specific conductance at all stations except for a negative relation at Patoka River near Princeton and for a positive and negative relation at Patoka River at Jasper. Most of these relations are good, have small confidence intervals, and will give reliable predictions of the water-quality variables listed above. The poorest relations are typically at stations in the Patoka River watershed. Suspended-solids concentration was positively related to streamflow at all but two stations on the Patoka River. These relations are poor, have large confidence intervals, and will give less reliable predictions of suspended-solids concentration.

Predictive equations for the regional relations between dissolved-solids concentration and specific conductance and between sulfate concentration and specific conductance, and the seasonal patterns of water quality, are probably valid for the coal-mining regions of Illinois and western Kentucky.

INTRODUCTION

Background

Coal deposits have been identified in 20 counties in southwestern Indiana (fig. 1). The effects of coal mining on water quality in this region have been documented in the literature (Corbett and Agnew, 1968; Corbett, 1969; Wilber and others, 1980; Peters, 1981; Wangsness and others, 1981a, 1981b, 1983; Zogorski and others, 1981). These investigations showed that specific conductance and concentrations of dissolved solids, acidity, sulfate, iron, manganese, and aluminum were generally higher in mined areas than in unmined areas, whereas pH and concentrations of total alkalinity were generally lower in mined areas than in unmined areas.

The Surface Mining Control and Reclamation Act of 1977 (Public Law 95–87) addresses water-quality problems associated with coal mining. The act requires an assessment of the probable hydrologic consequences of mining and reclamation on the hydrologic regime and the quantity and quality of water at and near the proposed mine. Hydrologic information for the area near the mine, referred to as "the general area" by the act, must be provided by an appropriate Federal or State agency. The general area is defined as "the topographic and ground water basin surrounding a mine plan area which is of sufficient size, including areal extent and depth, to include one or more watersheds containing perennial streams and ground water zones and to allow assessment of the probable cumulative impacts on the quality and quantity of surface and ground water systems in the basin" (Office of Surface Mining, 1979, p. 15349). The regulatory program implementing the act requires that mining-permit applications "***include water quality data to identify the characteristics of surface waters in, discharging into, or which will receive flows from surface or ground water from affected areas within the proposed mine plan area, sufficient to identify seasonal variations***" (Office of Surface Mining, 1979, p. 15355).

The minimum water-quality data required by the act include pH and concentrations of total dissolved solids, total suspended solids, acidity, dissolved iron, total iron, and total manganese. These data will be used, in part, by operators or consultants in preparing mining-permit applications and in estimating the probable hydrologic effects of mining, and by the regulatory authority in reviewing permit applications, determining cumulative hydrologic effects, and recommending procedures for mitigating damage to the environment.

The U.S. Geological Survey has designed a water-quality-data network to obtain the information required for the general area. Water-quality data at 293 reconnaissance sites and 84 network sites in the coal-mining region have been collected from March 1979 through August 1981 (Renn and others, 1980; U.S. Geological Survey, 1982, p. 65–67, 125–128, 134–137, 145–148, 206–209, 277–280, 391–398; Renn, 1983). Data collected include measurements of streamflow, temperature, specific conductance, and pH; concentrations of major cations and anions, dissolved oxygen, metals, nutrients, organic carbon, suspended sediment, and elements adsorbed on streambed materials; and populations of benthic invertebrates and periphytic algae. Network data have been analyzed. Surface-water quality is discussed by Wilber and others (1980), concentrations of selected elements adsorbed on streambed materials are discussed by Wilber and Boje (1982), and stream biota are discussed by Wangsness (1982).

In addition to data obtained from the network operated by the U.S. Geological Survey, other data that can supplement the network and provide useful information on the water quality of southwestern Indiana are available. Most of the additional data have been collected by the Indiana State Board of Health as part of a statewide water-quality-monitoring program established in 1957. The period of record for this program is the longest in the coal-mining region.

Purpose and Scope

Streamflow and water-quality data at 21 Indiana State Board of Health stations and streamflow and specific conductance data at 16 U.S. Geological Survey gaging stations were analyzed to provide information on surface-water quality in and near the coal-mining region of southwestern Indiana. This report (1) summarizes streamflow and water-quality data collected at these stations and examines the spatial and seasonal variations in streamflow and water quality, and (2) investigates the form and significance of the functional relations between water-quality variables and develops equations for predicting water quality.

Statistics of central tendency and dispersion were calculated for streamflow, specific conductance, pH, total alkalinity, sulfate, suspended solids, total iron, and total manganese data collected from 1957 to 1980 at the 37 stations in and near the coal-mining region of Indiana mentioned above. Statistics also were calculated for winter, spring, summer, and fall to enable an examination of seasonal variations.

Linear, inverse, semilog, log-log, and hyperbolic regression models were used to investigate the functional relations between water-quality variables. For statistically significant functional relations, equations were developed for predicting specific conductance, pH, and concentrations of alkalinity, sulfate, dissolved solids, suspended solids, total iron, and total manganese from values of streamflow, specific conductance, and (or) suspended-solids concentration. Regression models and the methods used to select the best model are described in detail. Information is provided for use in assessing the slope and goodness-of-fit of a relation and in estimating confidence limits for predicted water quality. Examples of the procedure used to calculate confidence limits are given to allow the user to assess the reliability of a predicted water-quality value.

Results of the study are presented in tables and figures. The tables provide specific numerical data for a water-quality station and are intended to be used in applications for coal-mining permits or for other site-specific uses. The tables are placed together at the end of the report. The figures provide a comparative view of water quality and are intended to be used in assessing cumulative hydrologic effects of mining or for interpreting water quality. Although comparisons of water quality among stations are contained throughout the report, it is beyond the scope of this report to interpret the surface-water quality of the coal-mining region. Interpretation of the causes, effects, or mechanisms responsible for the differences or similarities in water quality is left to the reader.

DESCRIPTION OF STUDY AREA

The coal-mining region of Indiana consists of 20 counties in southwestern Indiana whose recoverable reserves of coal are estimated to be 17 billion short tons (Weir, 1973, p. 33). Indiana counties contiguous to those in the coal-mining region were included in the study area so that water quality in the coal-mining region could be compared with water quality upstream from the coal-mining region (fig. 1). A comprehensive description of the

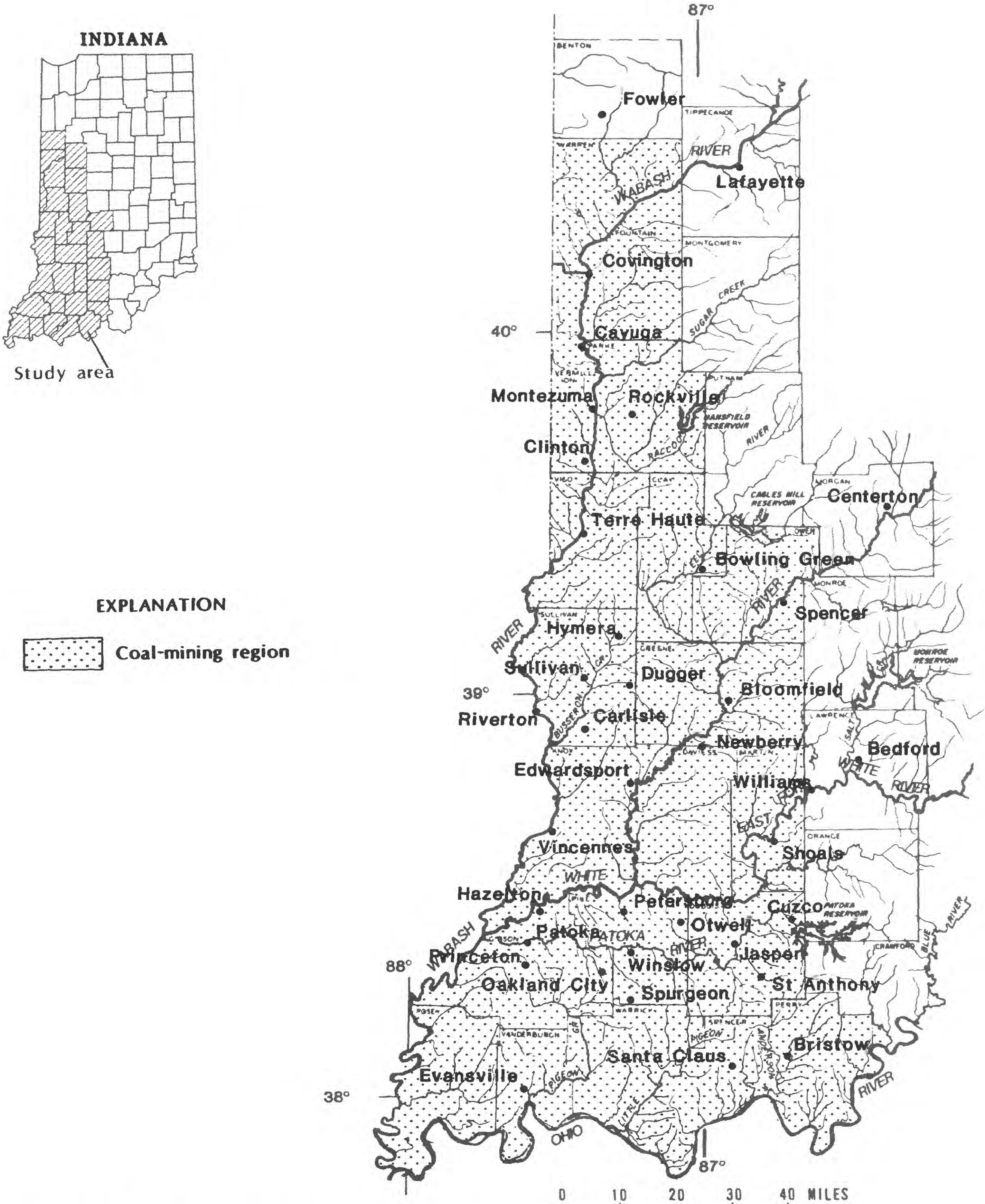

Figure 1. Study area and coal-mining region, southwestern Indiana.

coal-mining region is presented in a series of coal-hydrology reports by Wangsness and others (1981a, 1981b, 1983).

Geology

Rocks of Pennsylvanian and Mississippian age are the major bedrock units. Rocks of the Pennsylvanian System are primarily a cyclic sequence of shale, siltstone, and sandstone interbedded with thin strata of coal, clay, black shale, and limestone (Gray, 1979, p. K1). All of Indiana's commercial coal deposits are in the Pennsylvanian rocks that crop out in the central part of southwestern Indiana (fig. 2). Mississippian rocks, predominantly composed of limestone and cyclic sequences of sandstone, shale, and limestone (Gray, 1979, p. K3), underlie Pennsylvanian rocks and crop out in the east.

At least three glacial advances have covered parts of the study area, and all but the southeastern part have been glaciated at least once (fig. 2). The result of these glacial advances is a deposit of drift ranging in thickness from less than 50 ft in the south to more than 300 ft in the north (Purdue University Water Resources Research Center and Geosciences Research Associates, Inc., 1980, pl. 6).

Extensive till deposits cover the glaciated north and abut the unglaciated south. Sand and gravel outwash deposits and modern flood-plain deposits occur along the major rivers and streams. Between the outwash deposits along the Wabash River and the till to the east is a wide band of windblown loess and sand. All the major valleys in the south are filled with glacial lake deposits composed of clay, silt, and sand (Wayne, 1966, p. 33).

Geomorphology

The five geomorphic units (fig. 3) are strongly influenced by glacial and bedrock geology (Schneider, 1966, p. 41, 42). The Norman Upland consists of long, steep slopes and narrow valleys and ridgetops that have formed on resistant Mississippian siltstone in the east. The Mitchell Plain, west of the Norman Upland, has formed on Mississippian limestone and is a well-developed karst plain containing numerous sinkholes. West of the Mitchell Plain is the Crawford Upland, which corresponds to the area where rocks of Early Mississippian age crop out (figs. 2, 3). The Crawford Upland is a maturely dissected, westward-sloping plateau composed of resistant sandstone and limestone. The Wabash Lowland is west of the Crawford Upland; it is an area of broad valleys and rolling plains formed from rocks of Pennsylvanian age. The Wabash Lowland contains most of the strip-mined land in Indiana (fig. 4). The Tipton Till Plain is a nearly flat glacial plain that caps the northern counties and forms a sharp boundary with the other geomorphic units (Schneider, 1966, p. 49).

Climate

Southwestern Indiana has a continental climate. The average annual temperature ranges from 52°F in the north to 56°F in the south (Clark, 1980, p. 10). Prevailing winds are from the southwest most of the year. Average annual precipitation ranges from 36 inches in the north to 44 inches in the south. Approximately one-third of the annual rainfall runs off, mainly during cool weather (Schaal, 1959, p. 109). Average monthly precipitation is greatest in May (4.5 in) and June (4.3 in) and least in February (2.5 in) and October (2.6 in). The averages are based on data for 1941–70 obtained at precipitation stations in Evansville, Fowler, Princeton, Rockville, Terre Haute, and Vincennes (fig. 1) (National Oceanic and Atmospheric Administration, 1973).

Surface-Water Hydrology

The major rivers draining the coal-mining region of southwestern Indiana are the East Fork White River, White River, Patoka River, Wabash River, and Ohio River (fig. 5). Streamflow in all of the rivers and in many of the streams is partially regulated by reservoirs. Streamflow in the East Fork White River, White River, Wabash River, and Ohio River is well sustained by ground water. Streamflow in the Patoka River, as in the intermittent streams, has been zero at several times during the period of recorded streamflow (table 1). (All tables are at the end of the report.)

Streamflow in the Patoka River watershed can be affected by spoil from surface coal mines. During the drought of 1964, mined watersheds produced an average streamflow of 0.27 $ft^3/s/mi^2$ of spoil where unmined watersheds were dry (Corbett, 1965, p. 3). Corbett concluded that mined watersheds are a significant source of streamflow to the Patoka River during droughts.

Variation in streamflow is the result of many factors, some of which interact. Examples of factors affecting streamflow are trends in climate, patterns of precipitation, amount of ground-water seepage, drainage-basin characteristics, and water use. Examination of seasonal changes is perhaps the most useful way of explaining temporal variation in streamflow. Mean monthly streamflow for most of the gaging stations in the coal-mining region is greatest in April or March and least in September or October (Horner, 1976). Winter and spring are the seasons of greatest flood frequency (Schaal, 1959, p. 109).

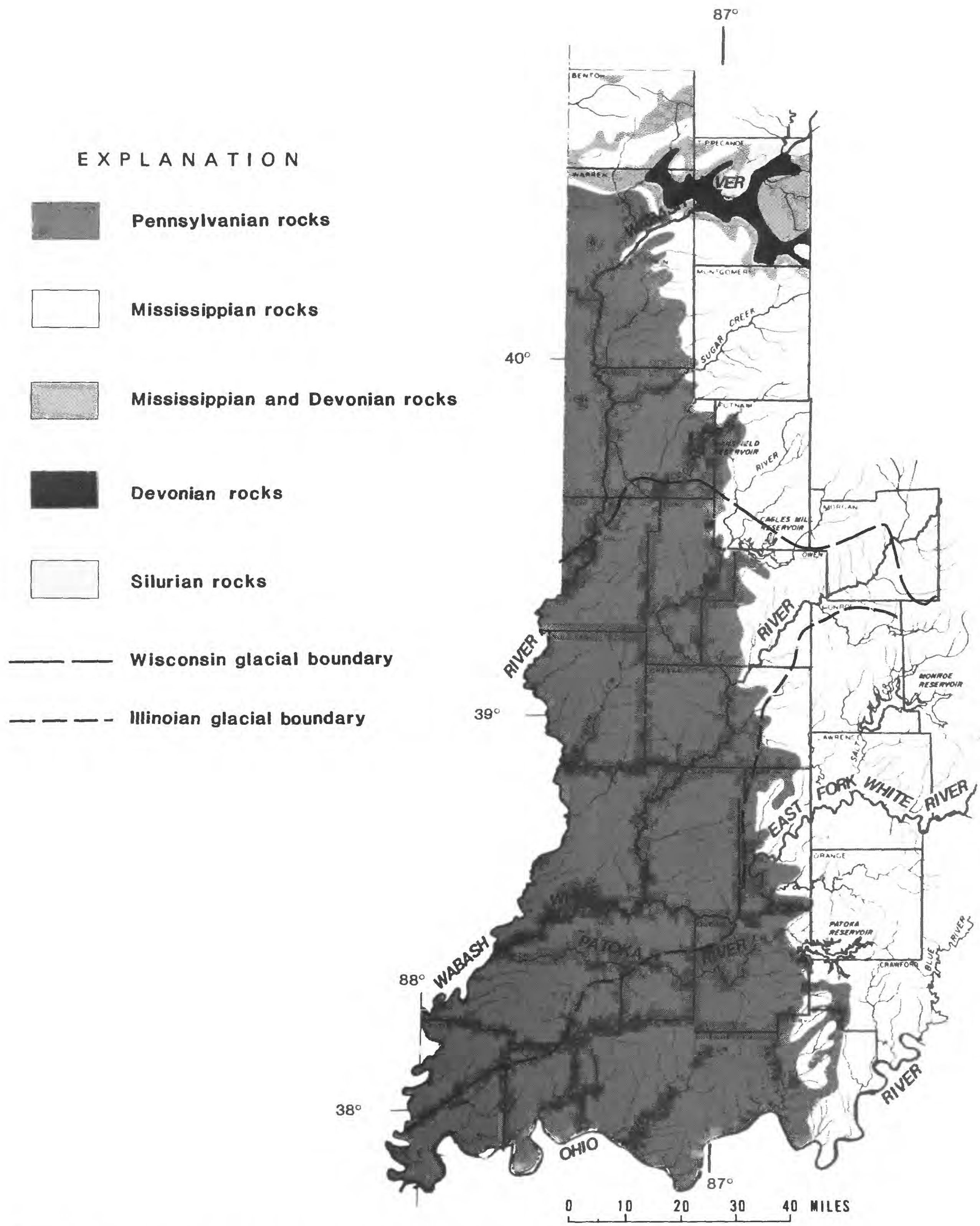

Figure 2. Generalized bedrock geology. (Modified from Gutschick, 1966, p. 5.)

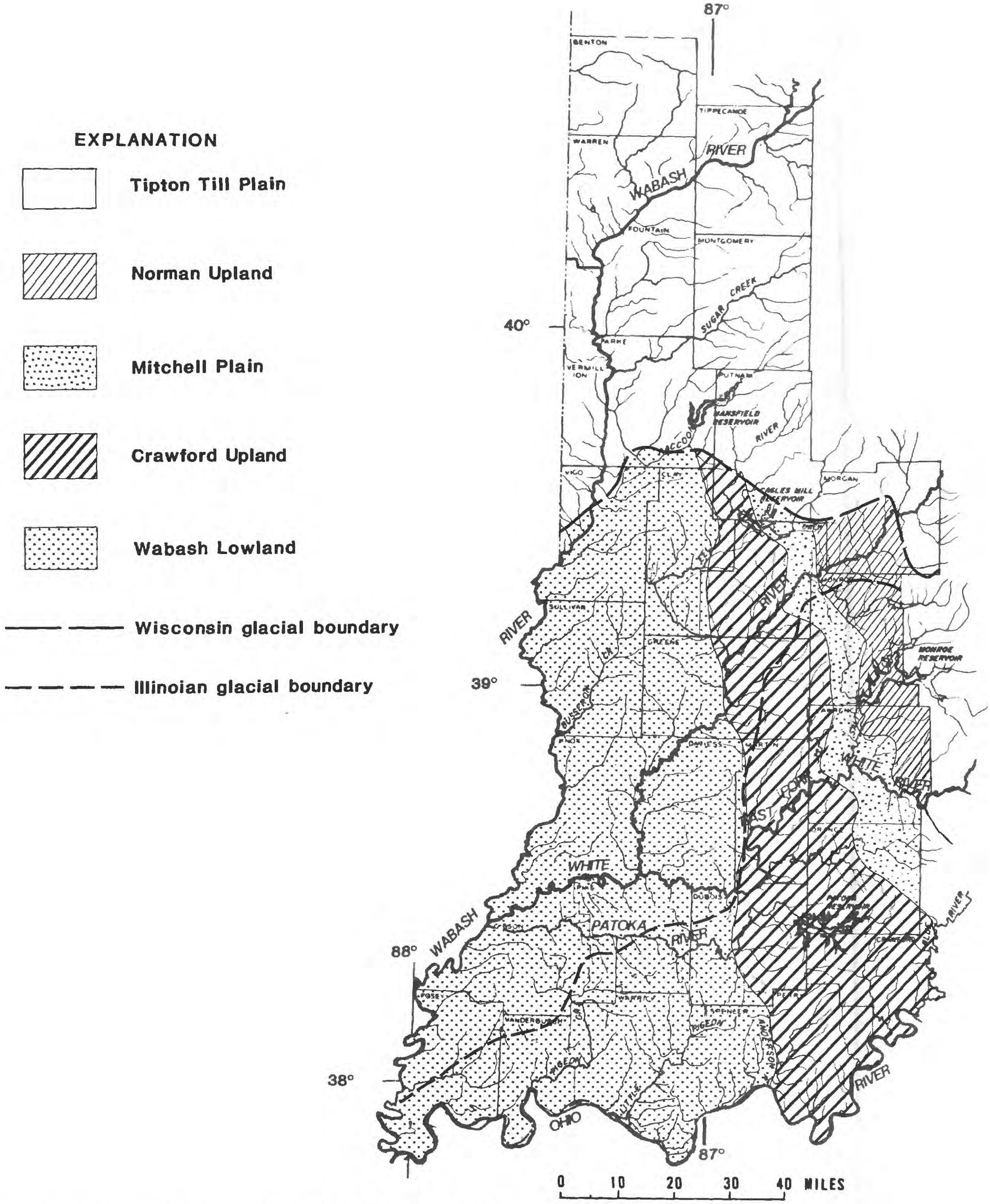

Figure 3. Geomorphic units. (Modified from Schneider, 1966, p. 41.)

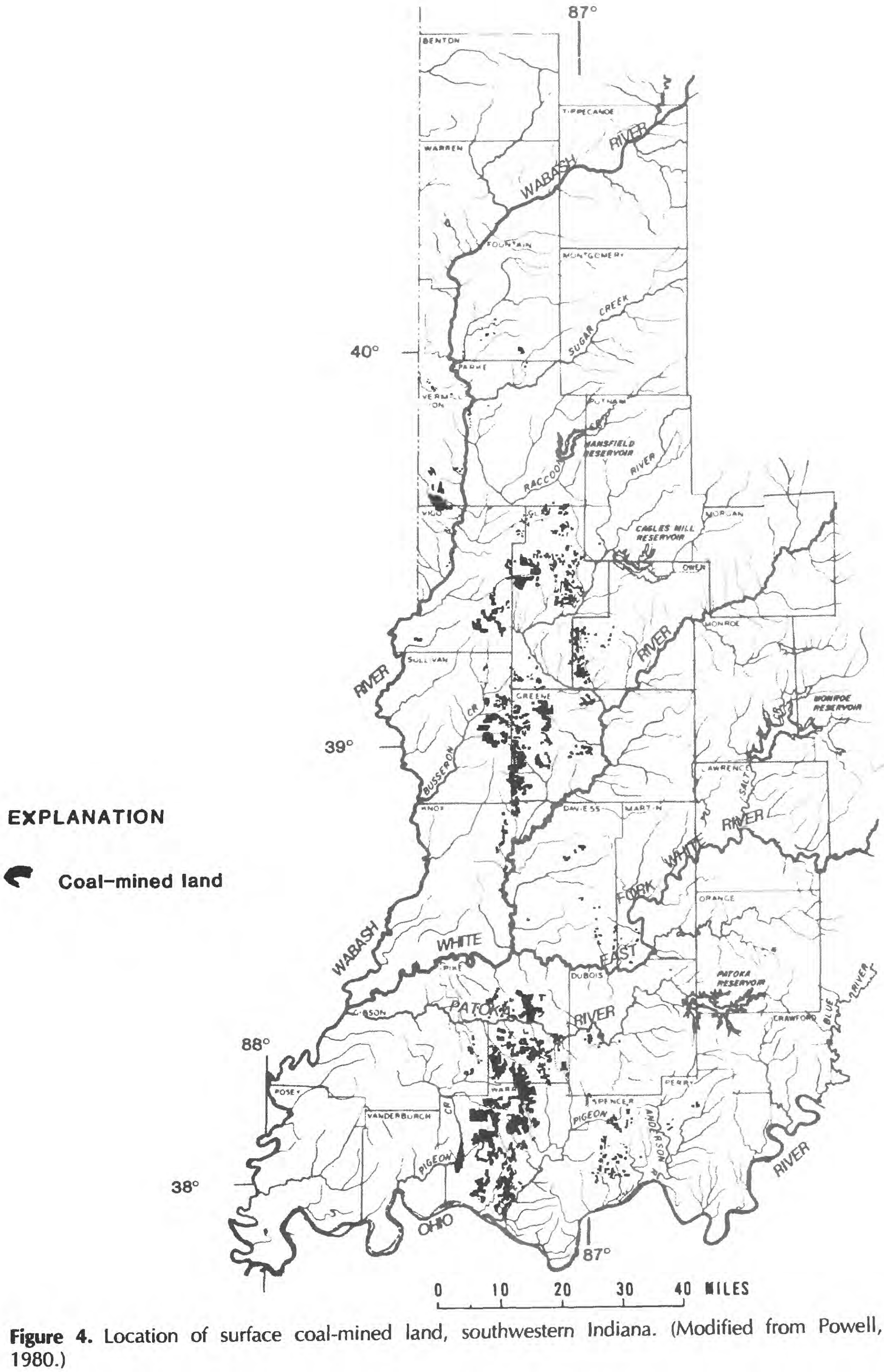

Figure 4. Location of surface coal-mined land, southwestern Indiana. (Modified from Powell, 1980.)

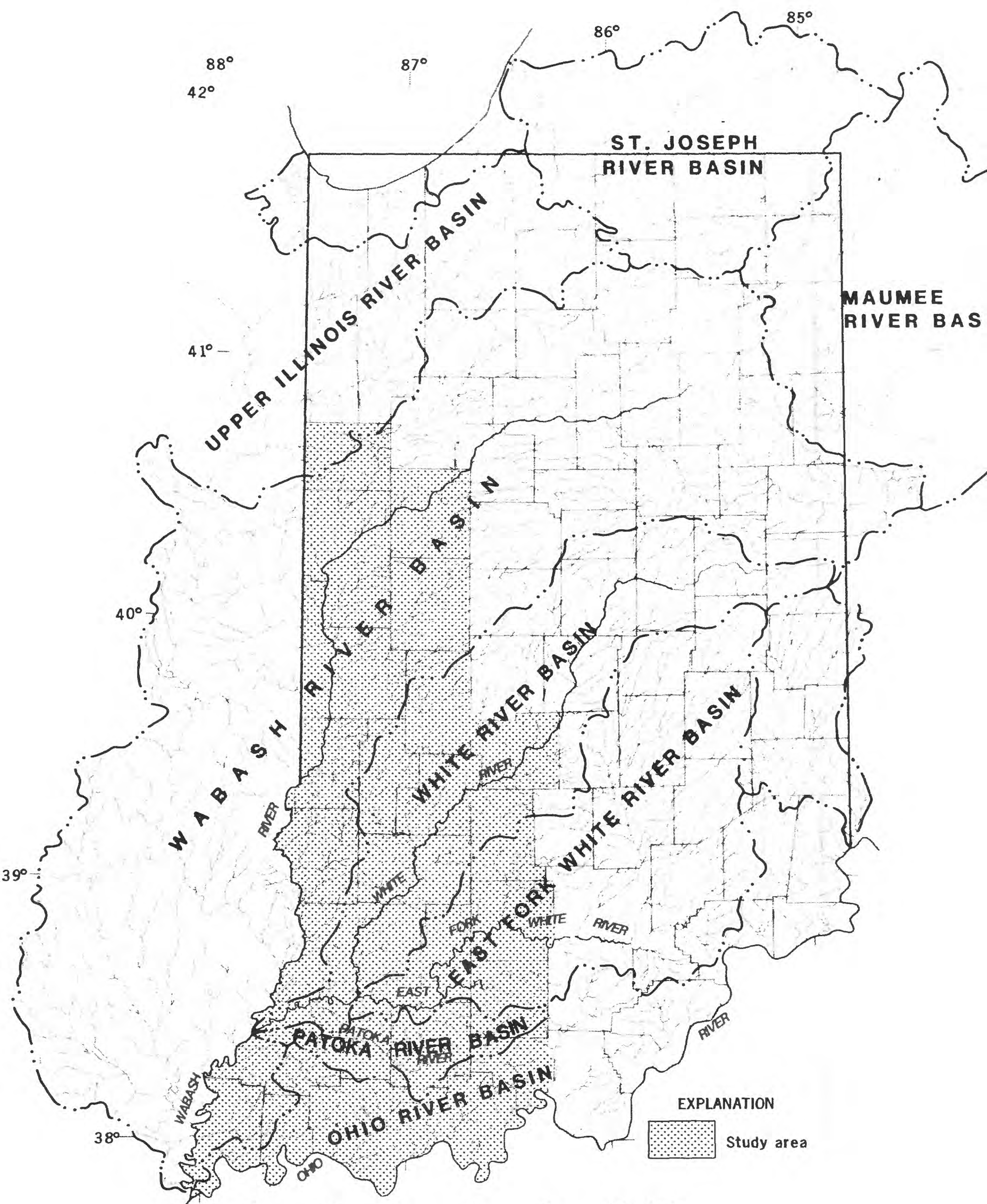

Figure 5. Locations of the major drainage basins in and near the study area.

The principal causes of floods are prolonged periods of rainfall and rainfall on snow cover or frozen soil.

Streamflow and related hydrologic information for selected U.S. Geological Survey gaging stations in and near the coal-mining region are presented in table 1. Locations of the gaging stations are shown in figures 6*A* and 6*B*.

SOURCES AND DESCRIPTION OF DATA

The U.S. Geological Survey and the Indiana State Board of Health have collected surface-water-quality data in the coal-mining region (figs. 6*A* and 6*B*). Data that have been collected and that are required by the Surface Mining Control and Reclamation Act include pH and concentrations of suspended solids, dissolved solids, total iron, and total manganese. In addition, streamflow, specific conductance, concentrations of alkalinity and sulfate, and other water-quality constituents and properties have been measured.

U.S. Geological Survey Data

The U.S. Geological Survey collected specific conductance data approximately monthly from 1969 through 1975 at 16 streamflow gaging stations in the coal-mining region. The method described by Skougstad and others (1979, p. 545–547) was used to measure specific conductance. The number of specific conductance measurements and related information at the 16 gaging stations is presented in table 2. An explanation of the station-numbering system and additional information on station location is given elsewhere (U.S. Geological Survey, 1982, p. 10).

Eleven of 16 gaging stations receive drainage from surface coal mines (table 2). Surface-mined land accounts for a large percentage of the drainage area for most of these stations. None of the following stations receive drainage from surface coal mines (figs. 4, 6*A*, 6*B*): Patoka River at Jasper (station 03375500), Middle Fork Anderson River at Bristow (station 03303300), Busseron Creek near Hymera (station 03342100), Eel River at Bowling Green (station 03360000), and Hall Creek near St. Anthony (station 03375800).

Water-quality data from local and regional water-resources investigations are stored in the U.S. Geological Survey's national water-data storage and retrieval system (WATSTORE). Measurements of specific conductance, dissolved solids, and sulfate were retrieved for all counties in the coal-mining region. The retrieval produced 505 measurements at 132 stations (excluding specific conductance measurements at the 16 stations mentioned in the preceding paragraph). The small amount of additional data from the 132 stations did not warrant individual analysis by station. These data were used to investigate the regionwide relations between dissolved-solids concentration and specific conductance and between sulfate concentration and specific conductance. The methods of Skougstad and others (1979, p. 501, 577, 615) were used to measure the concentrations of dissolved solids and sulfate. A graphical analysis of water quality in the coal-mining region, based on data from WATSTORE, is presented by Wangsness and others (1981a, 1981b, 1983).

Indiana State Board of Health Data

The Indiana State Board of Health has collected water-quality samples at 21 river stations in southern Indiana as part of a statewide monitoring program. Samples were collected approximately biweekly from 1957 through 1970 and have been collected approximately monthly since then. Specific conductance and pH were measured in the field. The Indiana State Board of Health used standard methods described in American Public Health Association and others (1975) in analyzing the water-quality samples.

Of the water-quality properties and constituents monitored by the Indiana State Board of Health, only specific conductance, pH, and concentrations of alkalinity, sulfate, suspended solids, total iron, and total manganese were used in the analysis of surface-water quality. Only data published through 1980 were used. The number of water-quality measurements and related information for Indiana State Board of Health stations is shown in table 3. Information on the State monitoring network is given in Indiana State Board of Health (1957–1980). An explanation of the station-numbering system and additional information on station location is given in Indiana State Board of Health (1980, p. 12–18).

Fourteen of 21 water-quality stations receive drainage from surface coal mines (table 3). The proportion of coal-mined land in the drainage area of these stations varies from a small percentage for stations on the White River and the Wabash River to a large percentage for some stations on the Patoka River. None of the following stations receive drainage from surface coal mines (figs. 4, 6*A*, 6*B*): Wabash River at Lafayette (station WB301), Wabash River at Covington (station WB260), White River at Spencer (station WR166), East Fork White River at Williams (station EW77), East Fork White River at Shoals (station EW56), Patoka River at Jasper (station P86), and Patoka River near Jasper (station P76).

The Indiana State Board of Health does not collect streamflow data in its monitoring program. However, 8 of its 21 stations are at U.S. Geological Survey gaging stations. For the other 13 stations, it was necessary to estimate streamflow from the daily mean streamflow at nearby U.S. Geological Survey gages. The ratio of the drainage area at the Indiana State Board of Health station to the drainage area at the U.S. Geological Survey gage was

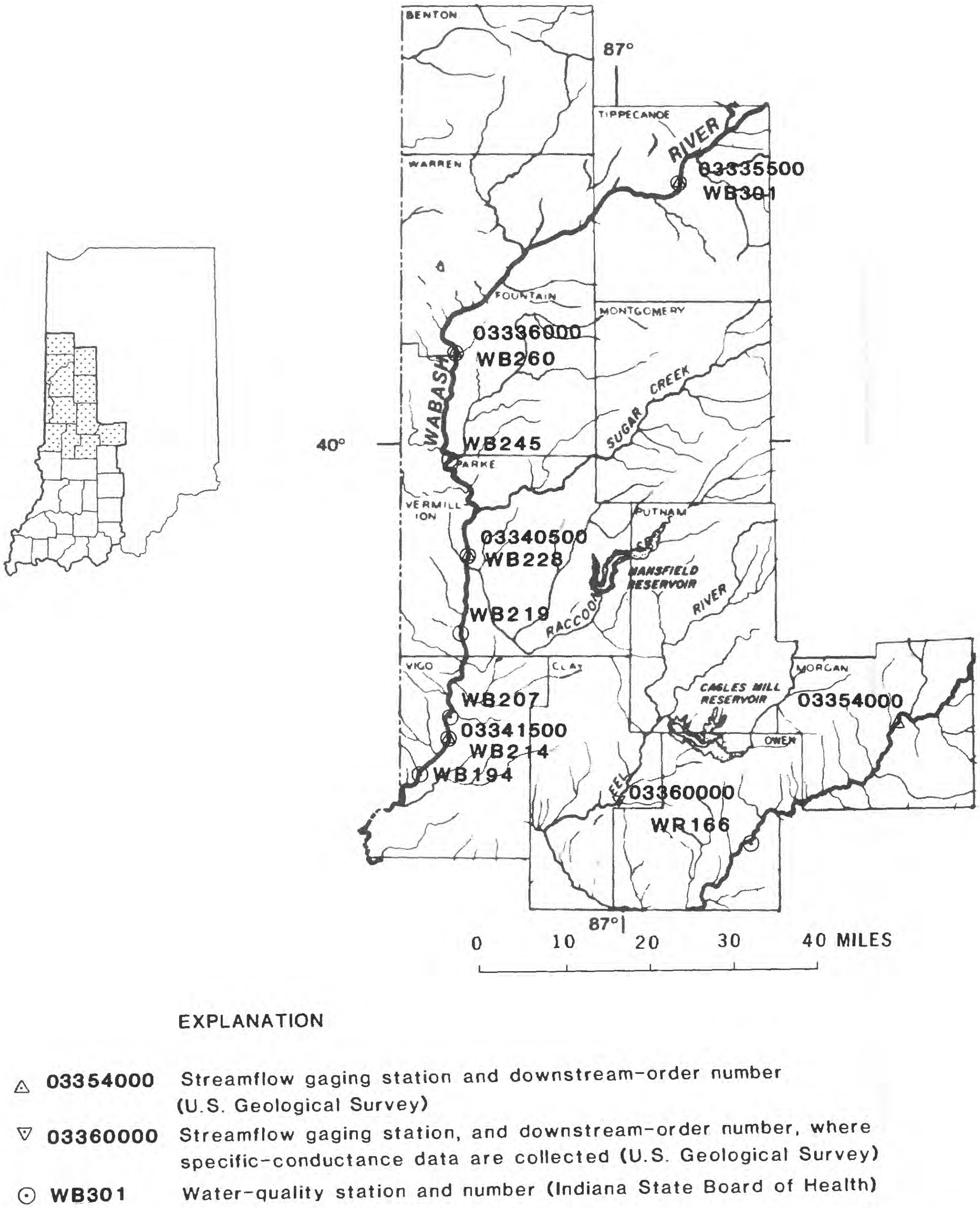

Figure 6*A*. Locations of U.S. Geological Survey gaging stations and Indiana State Board of Health water-quality stations in the northern part of the study area.

multiplied by the daily mean streamflow to estimate streamflow at the water-quality station. This method should provide useful estimates of streamflow because most Indiana State Board of Health stations are at or near a U.S. Geological Survey gage (figs. 6*A*, 6*B*).

Of the 13 stations that required estimates of streamflow, the drainage areas of 4 were within 2 percent of the drainage area of the closest U.S. Geological Survey gage, 8 were within 5 percent, and 11 were within 11 percent. The most uncertain estimates of streamflow are for White River at Spencer (station WR166) and Patoka River near Jasper (station P76). Drainage areas of these stations were within 37 and 66 percent of the drainage area of the closest U.S. Geological Survey gage.

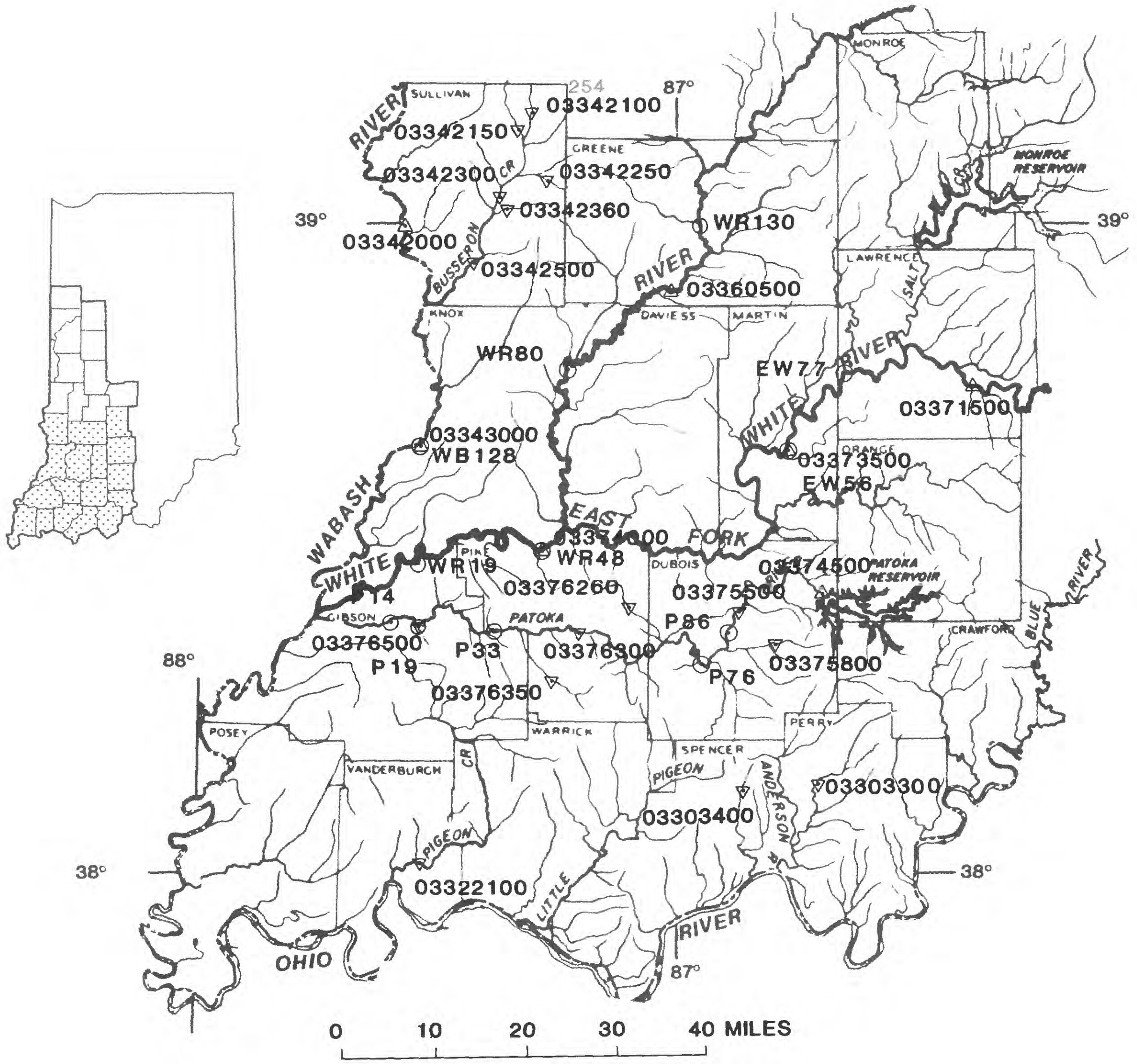

EXPLANATION

△ **03371500** Streamflow gaging station and downstream-order number (U.S. Geological Survey)

▽ **03322100** Streamflow gaging station, and downstream-order number, where specific-conductance data are collected (U.S. Geological Survey)

⊙ **WB128** Water-quality station and number (Indiana State Board of Health)

Figure 6*B*. Locations of U.S. Geological Survey gaging stations and Indiana State Board of Health water-quality stations in the southern part of the study area.

Except for table 1 and the section "Surface-Water Hydrology," streamflow data summarized and discussed in this report refer only to daily mean streamflow (or to estimates of daily mean streamflow) on days when water-quality measurements were made. These data (tables 4, 6; figs. 8*A*, 8*C*, 9*A*, 9*C*) are included in the report to facilitate comparisons and interpretations of water quality. Comprehensive hydrologic data are published annually for gaging stations in Indiana in "U.S. Geological Survey Water-Data Reports."

STATISTICAL ANALYSIS OF SURFACE-WATER-QUALITY DATA

Statistical Methods

The Statistical Analysis System[1] was used for all statistical analyses (SAS Institute Inc., 1982a, 1982b). PROC UNIVARIATE (SAS Institute Inc., 1982a, p. 575) was used to calculate statistics of central tendency (mean and median) and dispersion (minimum, maximum, and standard deviation) for streamflow and water-quality data. The coefficient of variation is reported rather than the standard deviation because the coefficient of variation can be used to compare the variability of samples having different means (Sokal and Rohlf, 1969, p. 62). The coefficient of variation is the standard deviation of a sample expressed as a percentage of the mean:

$$CV = (S/M)100, \qquad (1)$$

where
CV = the coefficient of variation,
S = the standard deviation, and
M = the mean.

TELLAGRAF (Integrated Software Systems Corporation, 1983) was used to plot side-by-side schematic plots of streamflow and water-quality data by station. A schematic plot is a box-and-whisker plot modified to show more detail near the extremes of the data. It is a useful tool for visually examining the central tendency and dispersion of a group of data and is especially useful for comparing two or more groups of data.

Construction and use of schematic plots are discussed in chapter 2 of Tukey (1977). First, the median value is plotted as a horizontal line. The 25th and 75th percentiles (called "hinges") are used to draw a box. The box represents the interquartile range. A value called the "step" is set equal to 1.5 times the interquartile range. Four "fences" are defined in terms of the step. The inner fences are one step from the hinges and the outer fences are two steps from the hinges. Values between the inner fences and the hinges are called "adjacent" values and are shown by a vertical line. Values between the inner and outer fences are called "outside" values and are shown as "+." Values beyond the outer fences are considered "far out" values and are shown as "0." An example of a schematic plot is shown in figure 7.

DISSPLA (Integrated Software Systems Corporation, 1981) was used to plot seasonal median values of streamflow and water-quality characteristics by station. This type of plot shows seasonal variations at a station and differences among stations.

[1]Any use of brand, firm, or trade names or trademarks in this publication is for descriptive purposes only and does not constitute endorsement by the U.S. Geological Survey.

Summaries and Plots of Statistical Analyses

Statistical summaries in tables 4–13 give number of measurements, minimum and maximum values, mean, median, and coefficient of variation for streamflow and water-quality data by station and by season for each station. The seasons are: winter (December 21–March 20), spring (March 21–June 20), summer (June 21–September 20), and fall (September 21–December 20). Summary statistics of water-quality variables are presented as follows: for U.S. Geological Survey gaging stations, streamflow (table 4) and specific conductance (table 5); and for Indiana State Board of Health stations, streamflow (table 6), specific conductance (table 7), pH (table 8), total alkalinity (table 9), sulfate (table 10), suspended solids (table 11), total iron (table 12), and total manganese (table 13).

Schematic plots of streamflow and water-quality data are shown by station in figures 8*A*–*J*. Schematic plots of water-quality variables are shown as follows: for U.S. Geological Survey gaging stations, streamflow (fig. 8*A*) and specific conductance (fig. 8*B*); and for Indiana State Board of Health stations, streamflow (fig. 8*C*), specific conductance (fig. 8*D*), pH (fig. 8*E*), total alkalinity (fig. 8*F*), sulfate (fig. 8*G*), suspended solids (fig. 8*H*), total iron (fig. 8*I*), and total manganese (fig. 8*J*).

Seasonal median plots of streamflow and water-quality characteristics are shown by station in figures 9*A*–*J*. Seasonal medians of water-quality variables are shown as follows: for U.S. Geological Survey gaging stations, streamflow (fig. 9*A*) and specific conductance (fig. 9*B*); and for Indiana State Board of Health stations, streamflow (fig. 9*C*), specific conductance (fig. 9*D*), pH (fig. 9*E*), total alkalinity (fig. 9*F*), sulfate (fig. 9*G*), suspended solids (fig. 9*H*), total iron (fig. 9*I*), and total manganese (fig. 9*J*).

Spatial Variations in Water Quality

Spatial variations in water quality can be determined by comparing ranges and median or mean values of water-quality characteristics by station (tables 4–13). Spatial variations can also be determined by comparing schematic plots of water-quality data by station (figs. 8*A*–*J*). Differences in streamflow characteristics (tables 1, 4, 6), period of record (tables 2, 3), and other factors should be considered in comparisons and interpretations of water quality.

Distributions of streamflow when samples were collected were similar at stations on the East Fork White River, White River, and Wabash River (fig. 8*C*). Streamflow tended to increase downstream, but this trend was not consistent. Streamflow at stations on the Patoka River was smaller than at other Indiana State Board of Health stations. Distributions of streamflow at U.S. Geological Survey gaging stations were diverse (fig. 8*A*) and show

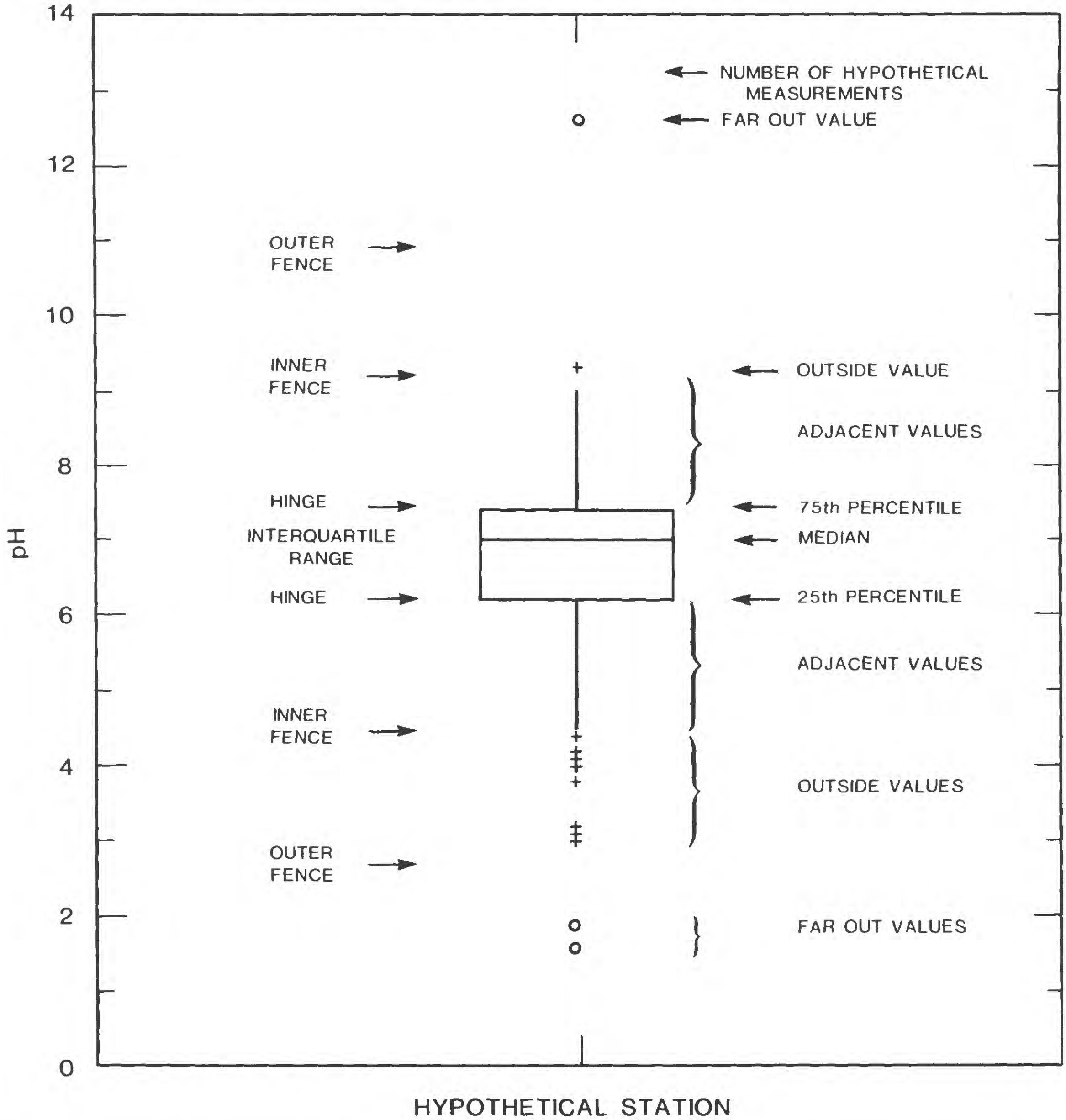

Figure 7. Example of a schematic plot.

the effect of drainage area (table 2) on streamflow. Streamflow ranged from 0.00 ft^3/s at Crooked Creek near Santa Claus (station 03303400), Hall Creek near St. Anthony (station 03375800), Flat Creek near Otwell (station 03376260), and Patoka River at Jasper (station P86) to 105,000 ft^3/s at White River at Hazelton (station WR19) (tables 4, 6). Median streamflow ranged from 2.0 ft^3/s at Crooked Creek near Santa Claus to 9,330 ft^3/s at White River at Petersburg (station WR48).

Specific conductance was similar at all stations on the Wabash River but decreased downstream at stations on the White River (fig. 8*D*). Distributions of specific conductance at stations on the Patoka River were variable (figs. 8*B*, 8*D*). Specific conductance at stations on the Patoka River at and upstream from Winslow (stations 03376300, P76, P86, and 03375500) was lower than that at stations downstream from Winslow (stations P33, P19, 03376500, and P14). Specific conductance at U.S. Geological Survey gaging stations was highest at stations that received drainage from surface coal mines (fig. 8*B*, table 2). Specific conductance ranged from 90 μS/cm at 25° C at Patoka River at Jasper (station 03375500) to 21,200 μS/cm at 25° C at Patoka River near Princeton (station P19) (tables 5, 7). Median specific conductance ranged from 170 μS/cm at 25° C at Middle Fork Anderson River at Bristow (station 03303300) to 3,000 μS/cm at 25° C at South Fork Patoka River near Spurgeon (station 03376350).

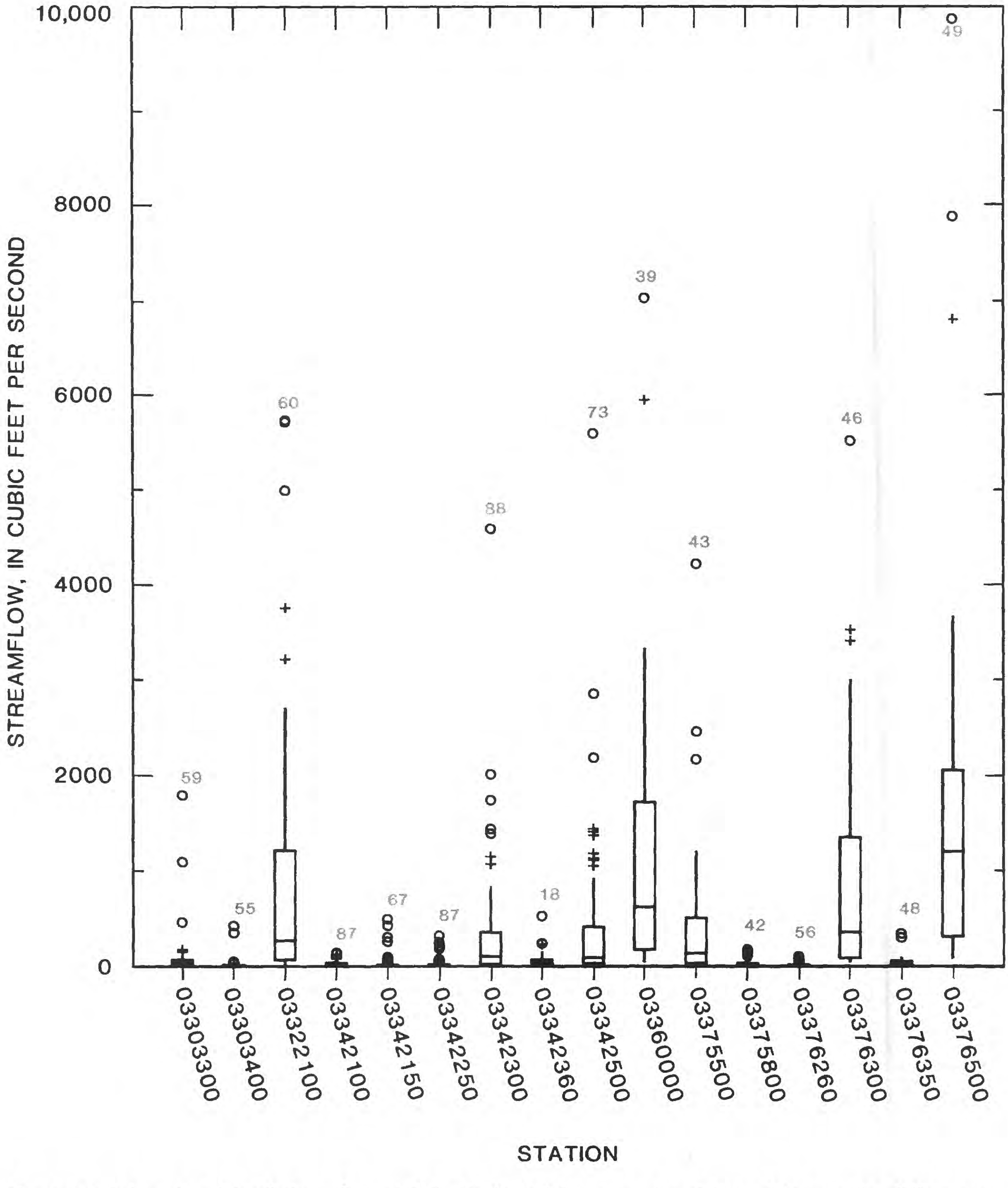

Figure 8*A*. Schematic plots of streamflow at U.S. Geological Survey gaging stations. Data are the daily mean streamflows on days when water-quality measurements were made. The number of streamflow measurements is shown near the top of each plot.

Distributions of pH were similar at stations on the East Fork White River, White River, and Wabash River (fig. 8*E*). Values of pH at stations on the Patoka River were less than those at other Indiana State Board of Health stations. Many measurements of pH at Patoka River near Princeton (station P19) were less than 5.5. Values of pH ranged from 3.0 at Patoka River near Princeton to 9.8 at White River at Bloomfield (station WR130), Wabash River at Montezuma (station WB228), and Wabash River at Vincennes (station WB128) (table 8). Median pH ranged from 7.0 at Patoka River near Oakland City (station P33) to 8.0 at White River at Bloomfield, Wabash

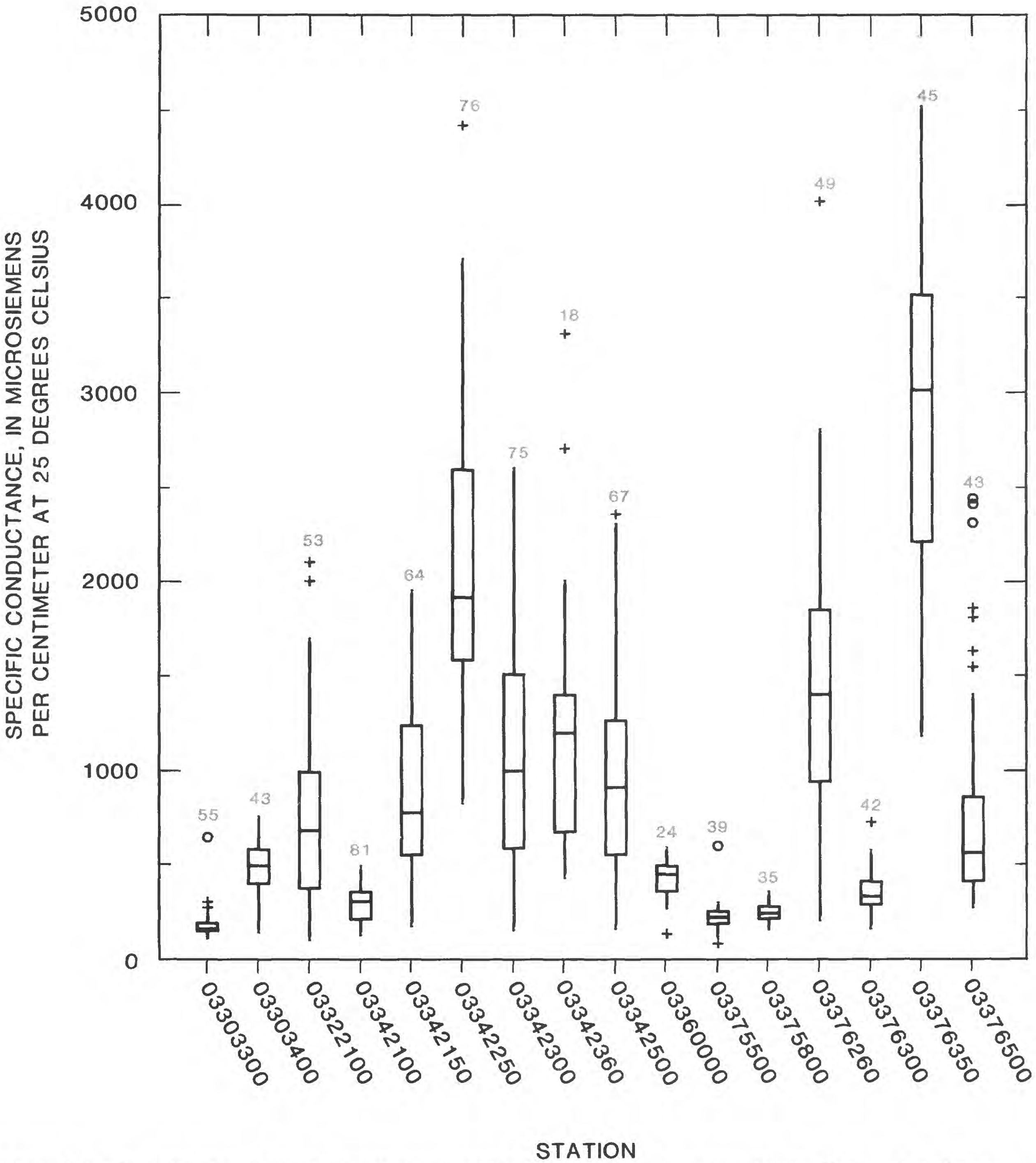

Figure 8*B*. Schematic plots of specific conductance at U.S. Geological Survey gaging stations. The number of measurements is shown at the top of each plot.

River at Terre Haute (station WB214), and Wabash River near Terre Haute (station WB194).

Total alkalinity concentration was less at stations on the Patoka River than at all other Indiana State Board of Health stations (fig. 8*F*). Distributions of total alkalinity were similar at all stations on the Wabash River but decreased downstream at stations on the White River. Total alkalinity concentration ranged from 0 mg/L as $CaCO_3$ at Patoka River near Princeton (station P19) to 590 mg/L as $CaCO_3$ at Wabash River at Terre Haute (station WB214) (table 9). Median total alkalinity concentration ranged from 30 mg/L as $CaCO_3$ at Patoka River near Princeton

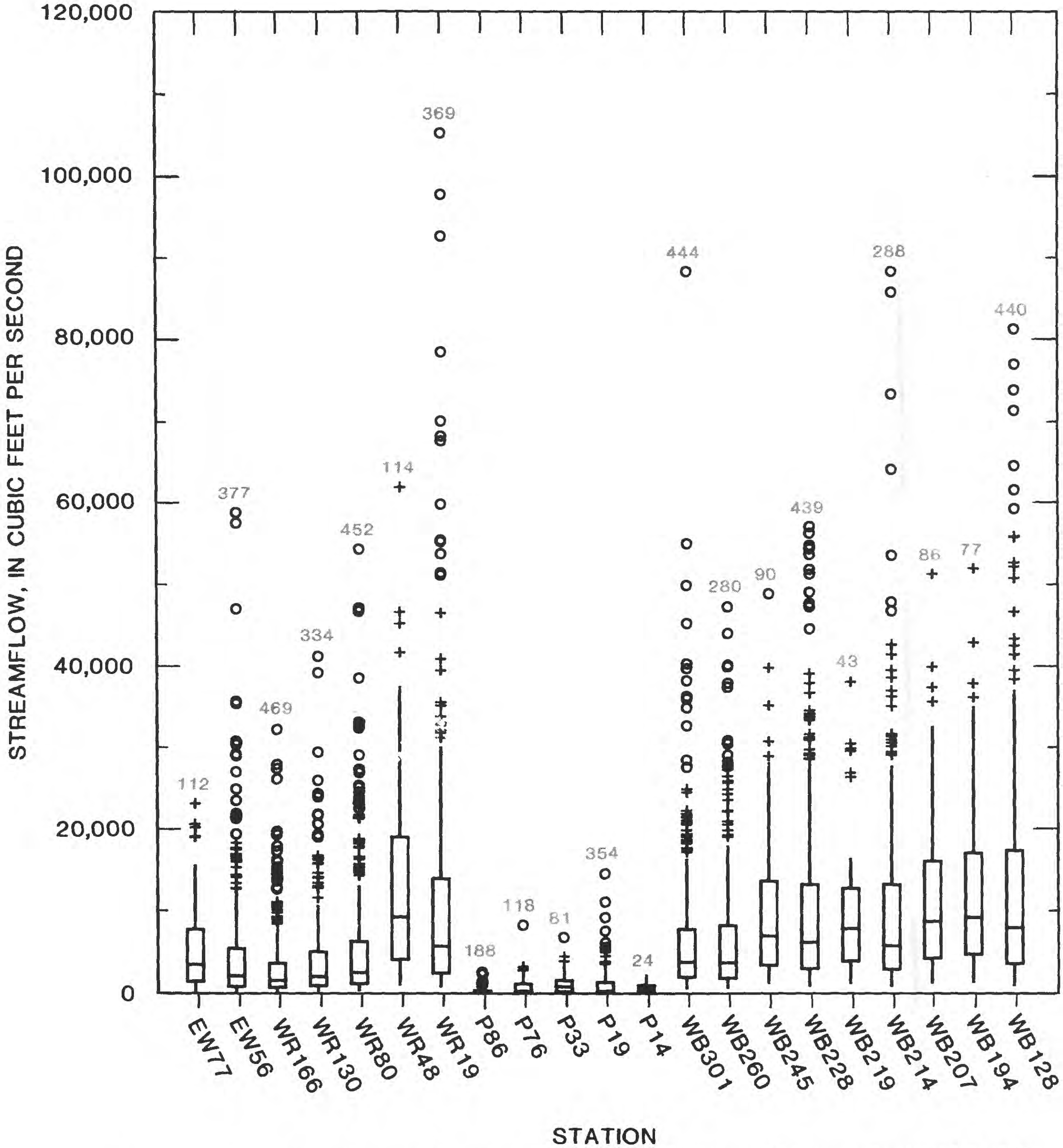

Figure 8C. Schematic plots of streamflow at Indiana State Board of Health stations. Data are estimates of the daily mean streamflows on days when water-quality measurements were made. The number of streamflow measurements is shown at the top of each plot.

to 230 mg/L as $CaCO_3$ at White River at Spencer (station WR166).

Distributions of sulfate concentration were similar at stations on the White River and Wabash River (fig. 8*G*). Sulfate concentration ranged from 16 mg/L at Patoka River near Jasper (station P76) to 1,000 mg/L at Patoka River near Oakland City (station P33) (table 10). Median sulfate concentration ranged from 36 mg/L at East Fork White River at Williams (station EW77) and Patoka River near Jasper to 150 mg/L at Patoka River near Oakland City.

Distributions of suspended-solids concentration were similar at all Indiana State Board of Health stations (fig. 8*H*). Suspended-solids concentration ranged from 1

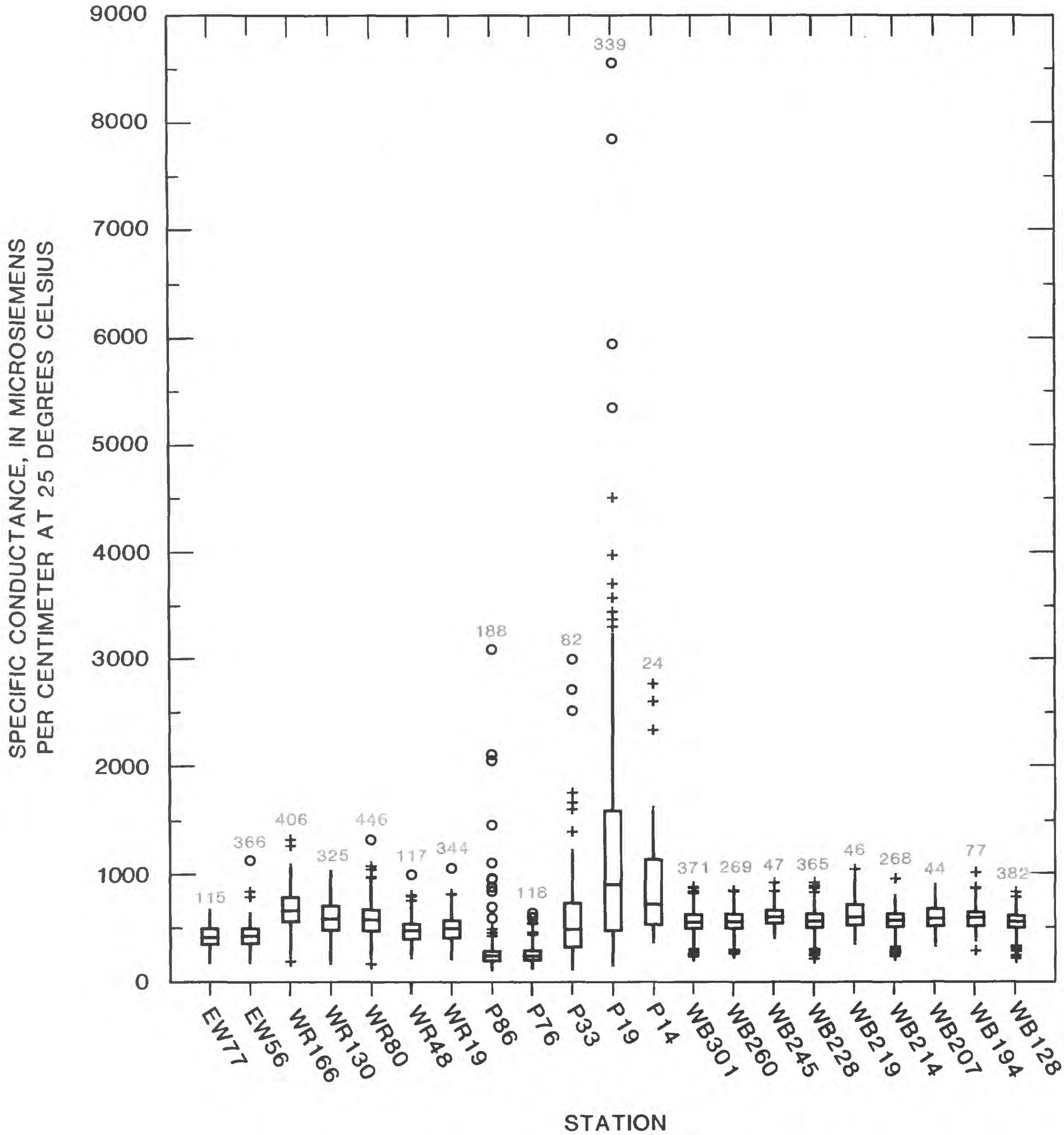

Figure 8*D*. Schematic plots of specific conductance at Indiana State Board of Health stations. The number of specific conductance measurements is shown near the top of each plot. Specific conductance of 19,500 and 21,200 μS/cm at 25°C at station P19 is not shown.

mg/L at East Fork White River at Shoals (station EW56), White River at Spencer (station WR166), Patoka River at Jasper (station P86), Patoka River near Princeton (station P19), Wabash River at Lafayette (station WB301), and Wabash River at Vincennes (station WB128) to 3,400 mg/L at Patoka River near Princeton (table 11). Median suspended-solids concentration ranged from 25 mg/L at Patoka River at Jasper to 84 mg/L at Patoka River near Jasper (station P76).

No pattern in the distributions of total iron concentration is apparent in figure 8*I*. Total iron concentration ranged from 200 μg/L at East Fork White River at Williams (station EW77), Wabash River at Clinton (station WB219), and Wabash River at Vincennes (station

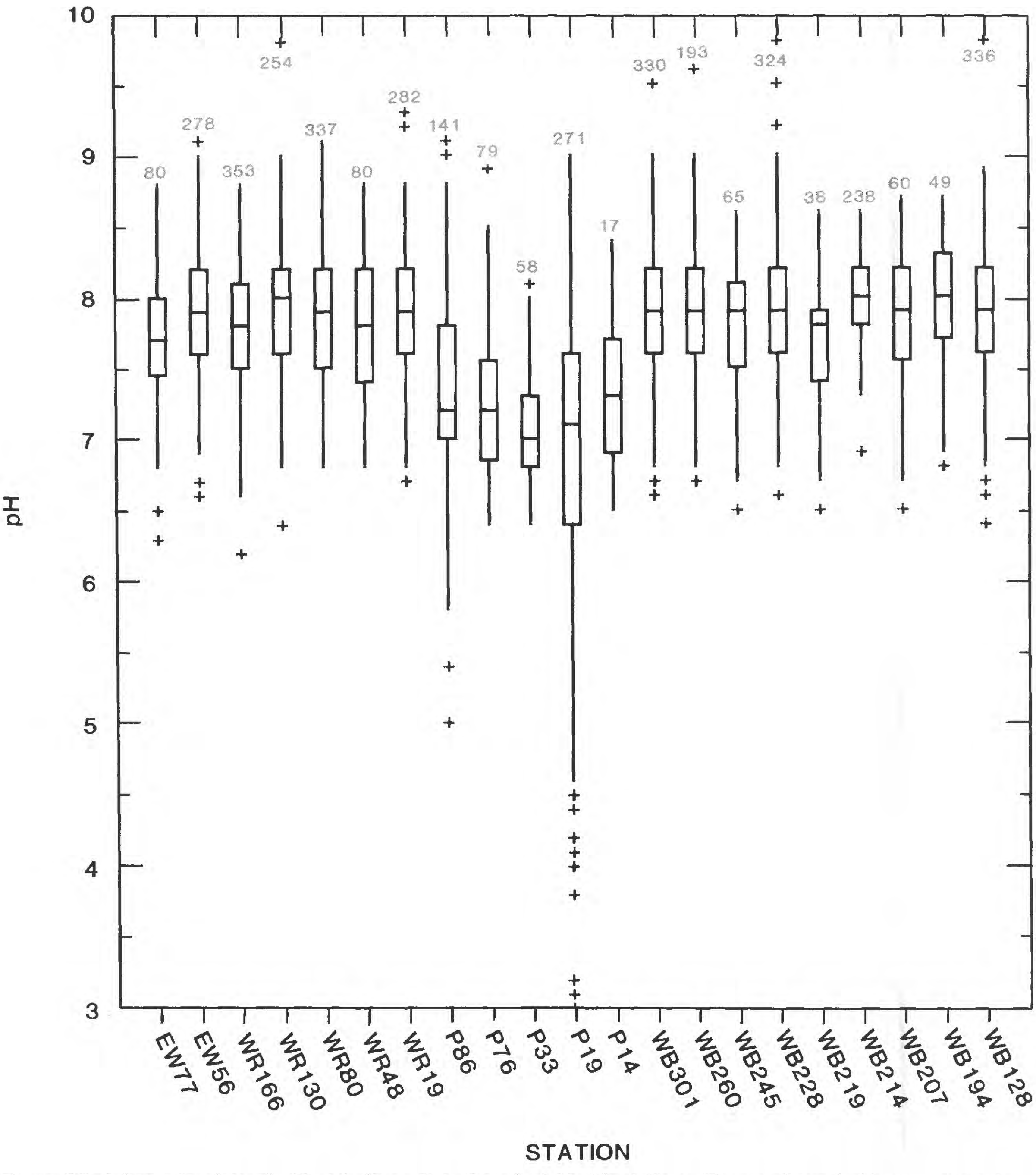

Figure 8*E*. Schematic plots of pH at Indiana State Board of Health stations. The number of pH measurements is shown near the top of each plot.

WB128) to 9,600µ)g/L at Wabash River at Vincennes (table 12). Median total iron concentration ranged from 600 µg/L at East Fork White River at Williams to 2,000 µg/L at Patoka River near Oakland City (station P33).

Total manganese concentration was greatest at stations on the Patoka River (fig. 8*J*). Distributions of total manganese concentration were similar at the other Indiana State Board of Health stations. Total manganese concentration ranged from 40 µg/L at East Fork White River at Williams (station EW77) to 7,700 µg/L at Patoka River near Oakland City (station P33) (table 13). Median total manganese concentration ranged from 120 µg/L at East Fork White River at Williams to 1,700 µg/L at Patoka River near Oakland City.

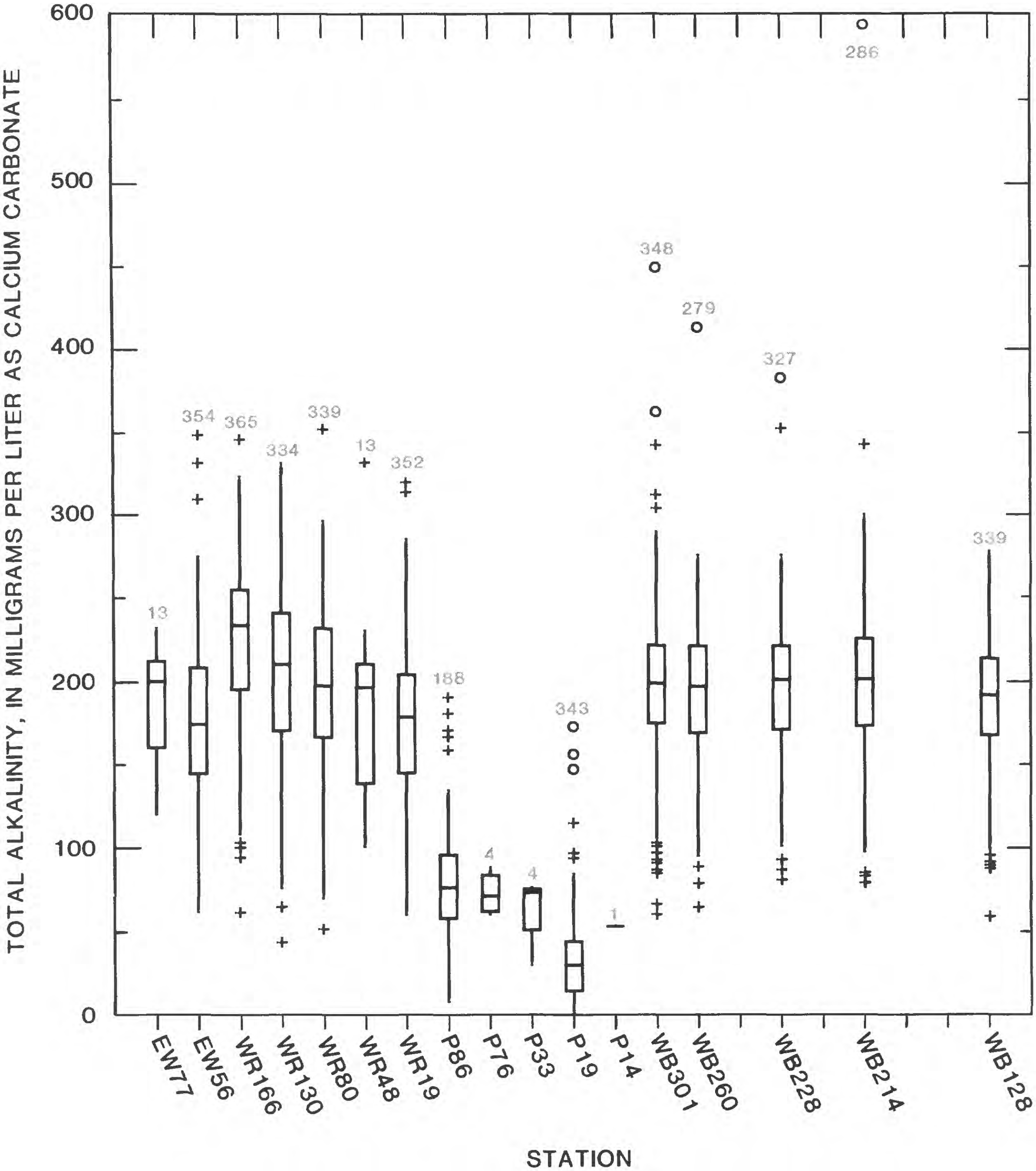

Figure 8*F*. Schematic plots of total alkalinity concentration at Indiana State Board of Health stations. The number of total alkalinity measurements is shown near the top of each plot.

Seasonal Variations in Water Quality

Seasonal variations and long-term trends are two kinds of temporal variations in water quality. Long-term trends were not considered in this report. Seasonal variations can be determined by comparing coefficients of variation and seasonal medians or means for water-quality characteristics (tables 4–13, figs. 9*A*–*J*). Stations with fewer than three measurements in any season are not considered in this discussion.

Median streamflow when samples were collected was greatest during spring or winter and least during fall or summer at all stations (figs. 9*A*, 9*C*). The season of lowest median streamflow was related to the size of the

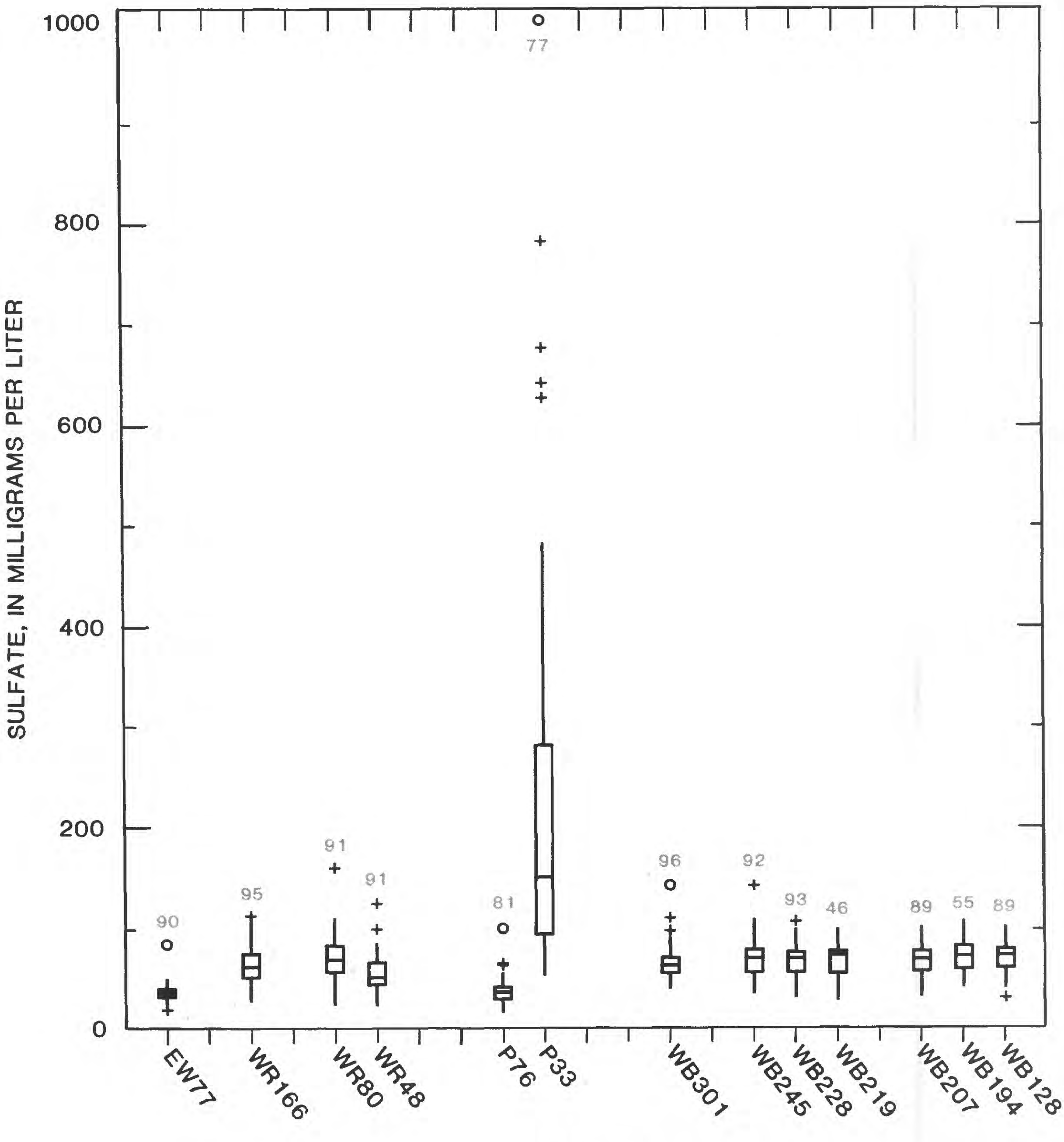

Figure 8*G*. Schematic plots of sulfate concentration at Indiana State Board of Health stations. The number of sulfate measurements is shown near the top of each plot.

drainage area. Median streamflow was least during fall at 15 of 16 stations having drainage areas greater than 1,000 mi^2 but was least during summer at 17 of 21 stations having drainage areas less than 1,000 mi^2. Streamflow was highly variable, as shown by the large coefficients of variation. Coefficients of variation ranged from 82 percent at Wabash River near Terre Haute (station WB194) to 365 percent at Crooked Creek near Santa Claus (station 03303400) (tables 4, 6). Typically, streamflow was least variable during winter or spring and most variable during fall or summer.

Specific conductance was related seasonally to streamflow and, at stations on the Wabash River, to station location. Median specific conductance was greatest

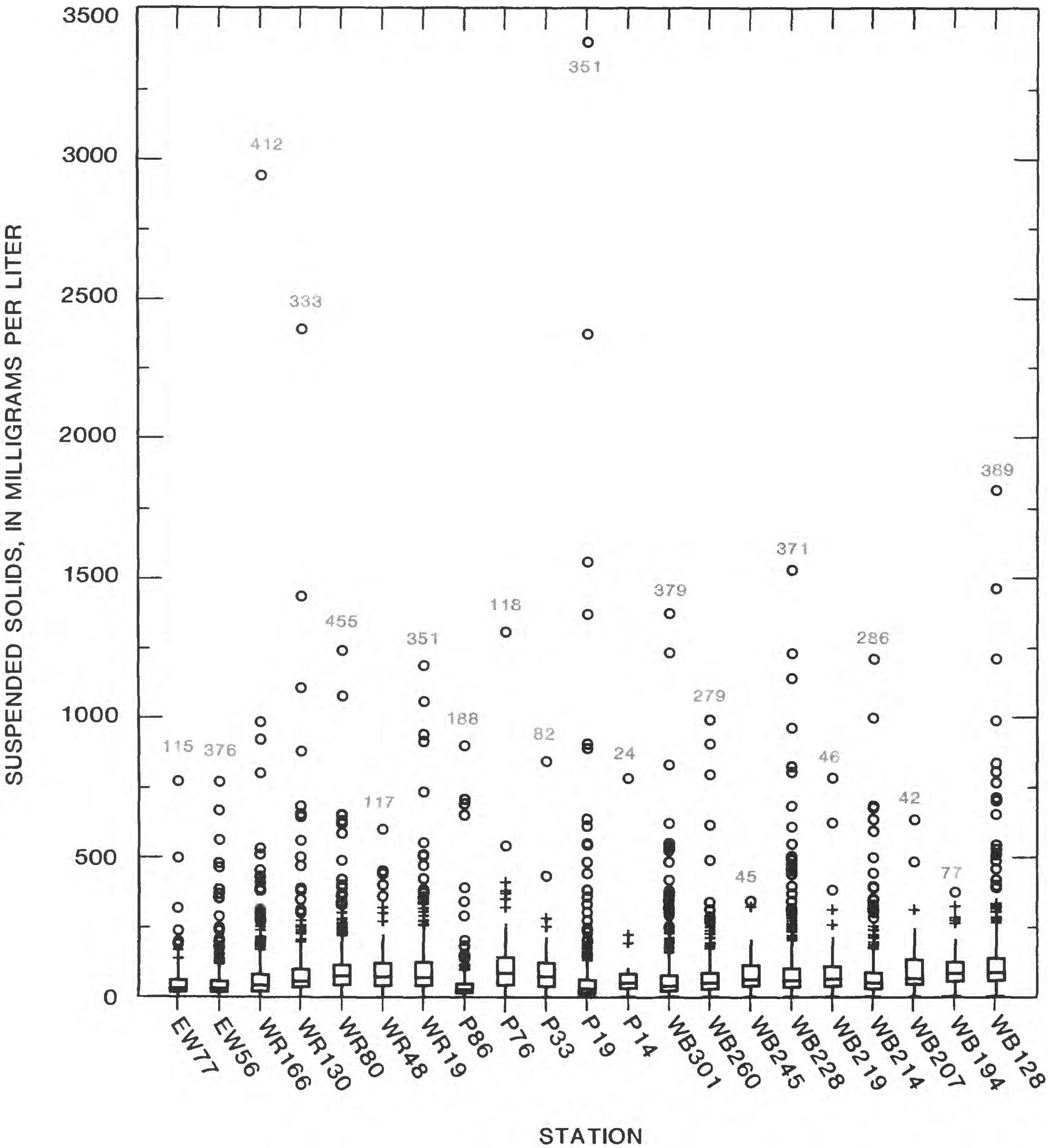

Figure 8*H*. Schematic plots of suspended-solids concentration at Indiana State Board of Health stations. The number of suspended-solids measurements is shown near the top of each plot.

during fall or summer (seasons of least streamflow) at 35 of 37 stations (figs. 9*B*, 9*D*), was greatest during fall at 15 of 16 stations on the East Fork White River, White River, and Wabash River, but was greatest during summer at 14 of the remaining 21 stations. Median specific conductance was least during summer at 9 of 9 stations on the Wabash River, but was least during winter or spring (the seasons of greatest streamflow) at 27 of the remaining 28 stations.

Specific conductance was most variable at stations in the Patoka River and the Busseron Creek watersheds and least variable at stations on the Wabash River. Specific conductance was most variable during winter at all stations on the East Fork White River, White River,

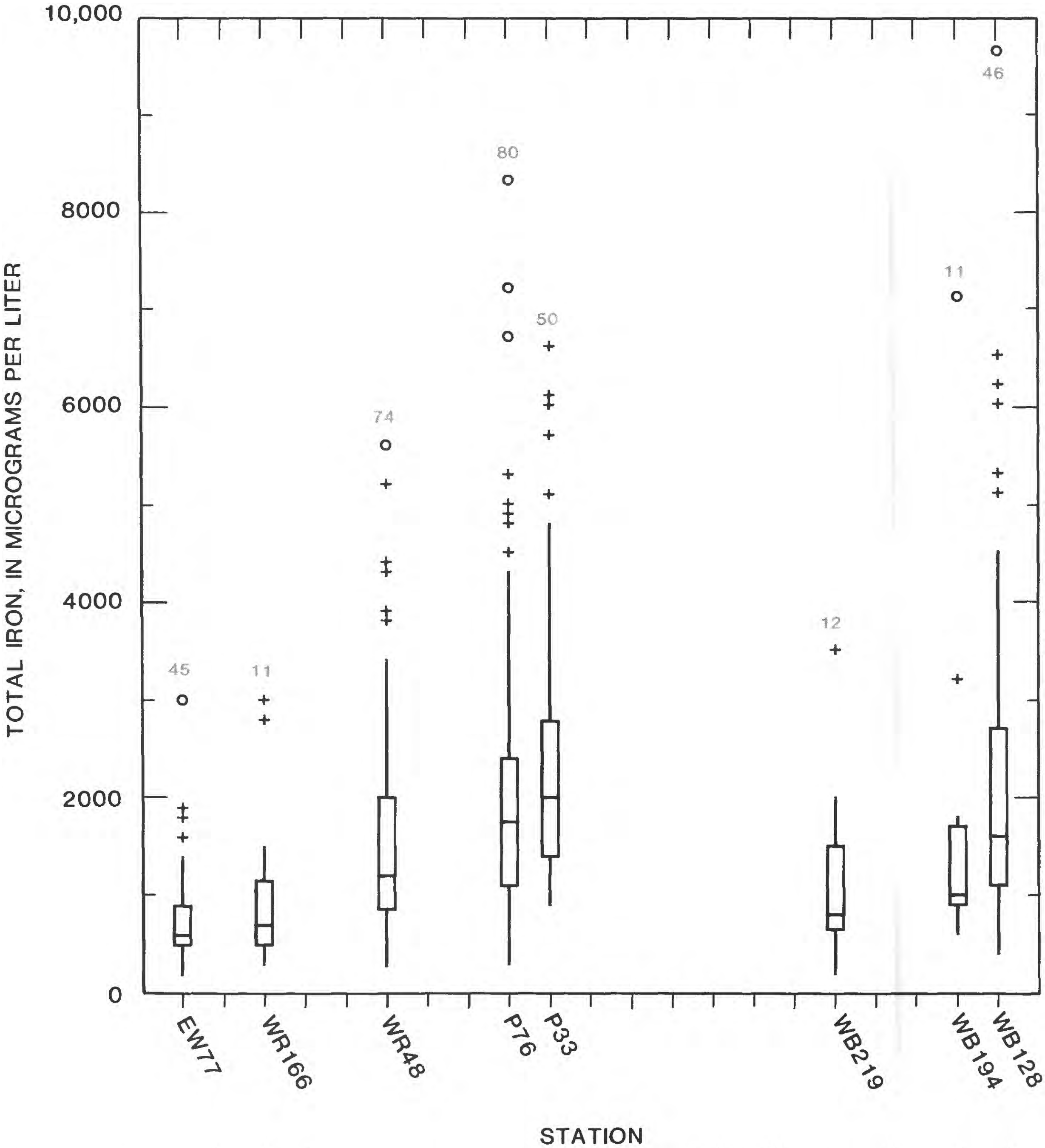

Figure 8*I*. Schematic plots of total iron concentration at Indiana State Board of Health stations. The number of total iron mearsurements is shown at the top of each plot.

and Wabash River. Coefficients of variation ranged from 18 percent at Hall Creek near St. Anthony (station 03375800) to 135 percent at Patoka River near Princeton (station P19) (tables 5, 7).

Median pH was related seasonally to station location (fig. 9*E*). Median pH was greatest during spring and least during fall at 3 of 4 stations on the Patoka River, was greatest during summer at 9 of the 16 remaining stations, and was least during winter at 14 of the 16 remaining stations. Coefficients of variation for pH ranged from 4 percent at Wabash River at Terre Haute (station WB214) to 17 percent at Patoka River near Princeton (station P19) (table 8).

Median total alkalinity concentration was greatest during fall and least during spring at all stations on the East Fork White River, White River, and Wabash River

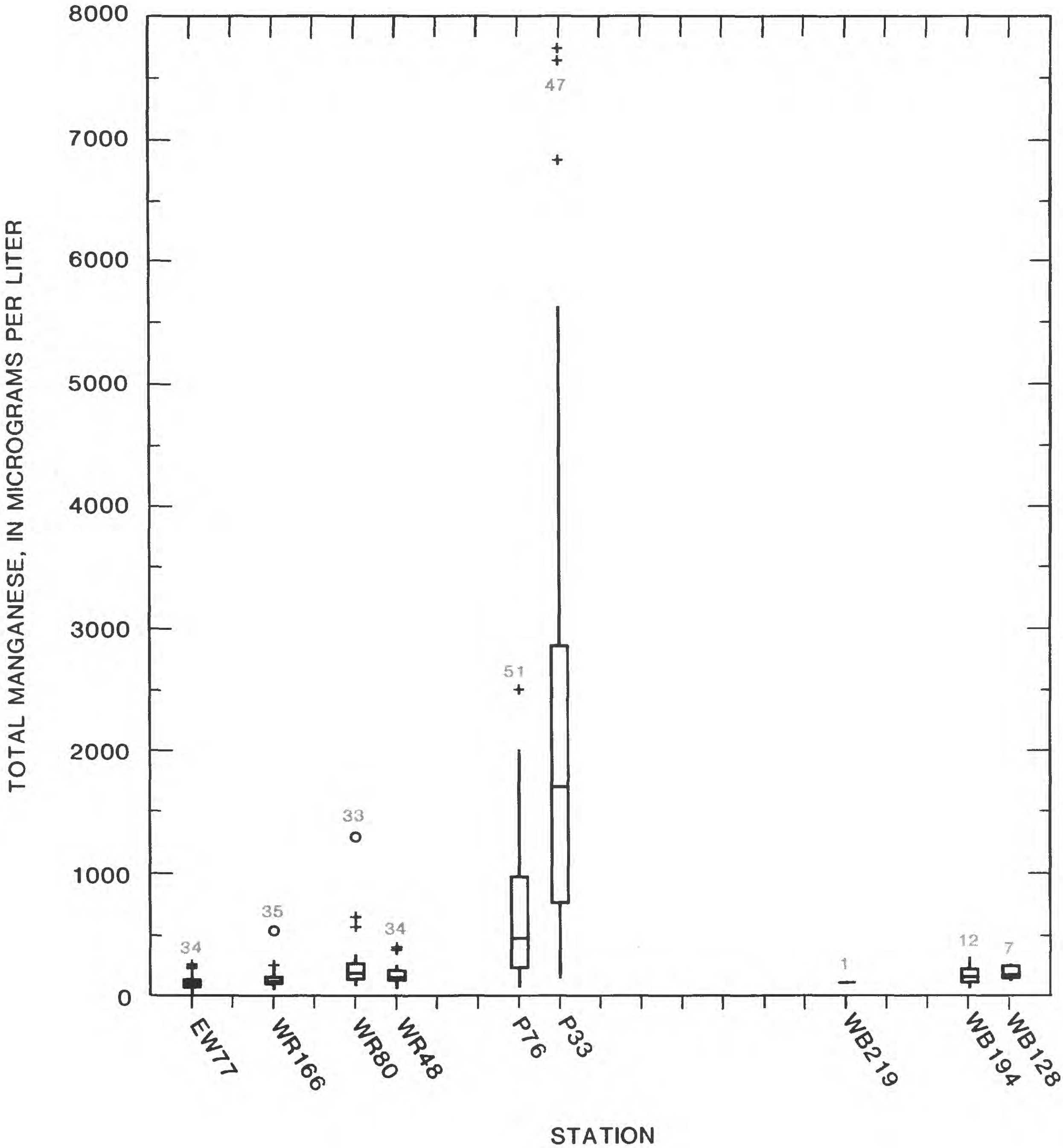

Figure 8*J*. Schematic plots of total manganese concentration at Indiana State Board of Health stations. The number of total manganese measurements is shown near the top of each plot.

except Wabash River at Montezuma (station WB228), where median total alkalinity concentration was least during summer (fig. 9*F*). No seasonal pattern was apparent at stations on the Patoka River. Coefficients of variation ranged from 20 percent at White River at Spencer (station WR166) to 73 percent at Patoka River near Princeton (station P19) (table 9). Total alkalinity concentration at stations on the East Fork White River, White River, and Wabash River was generally most variable during winter and least variable during fall.

Median sulfate concentration was greatest during fall at 9 of 10 stations on the White River and Wabash

(Text continues on p. 34)

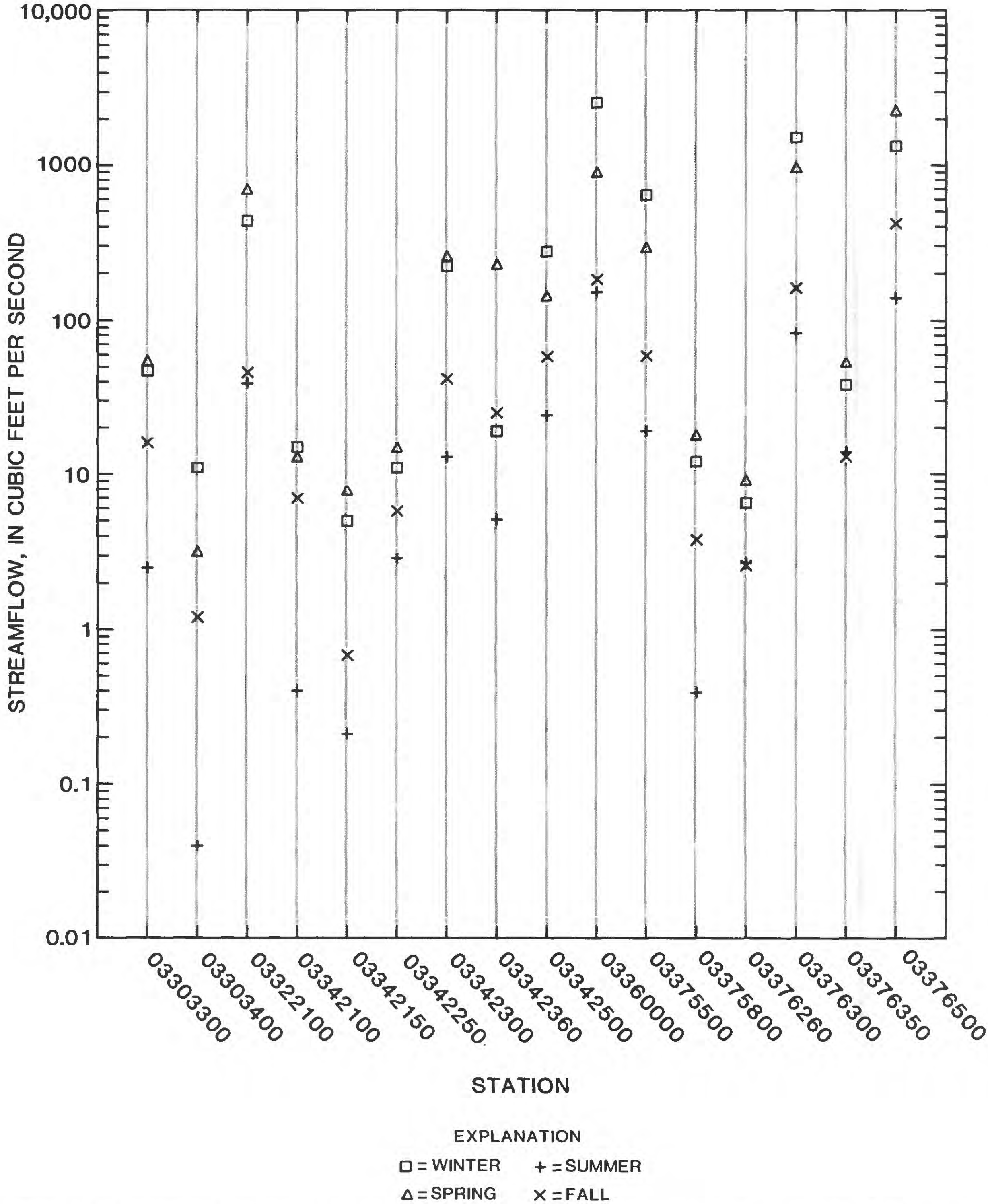

Figure 9*A*. Seasonal median streamflow at U.S. Geological Survey gaging stations. Data are the daily mean streamflows on days when water-quality measurements were made.

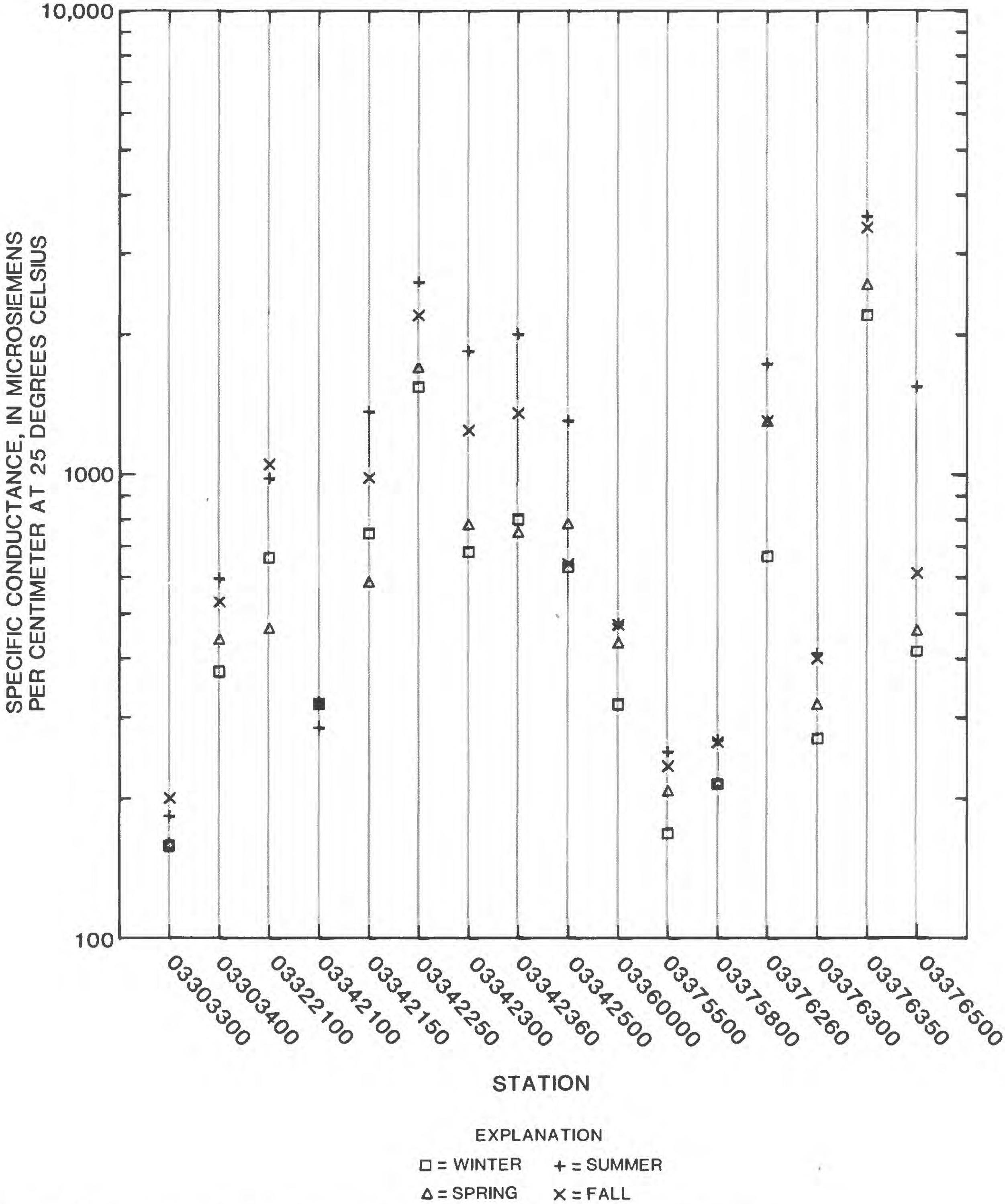

Figure 9*B*. Seasonal median specific conductance at U.S. Geological Survey gaging stations.

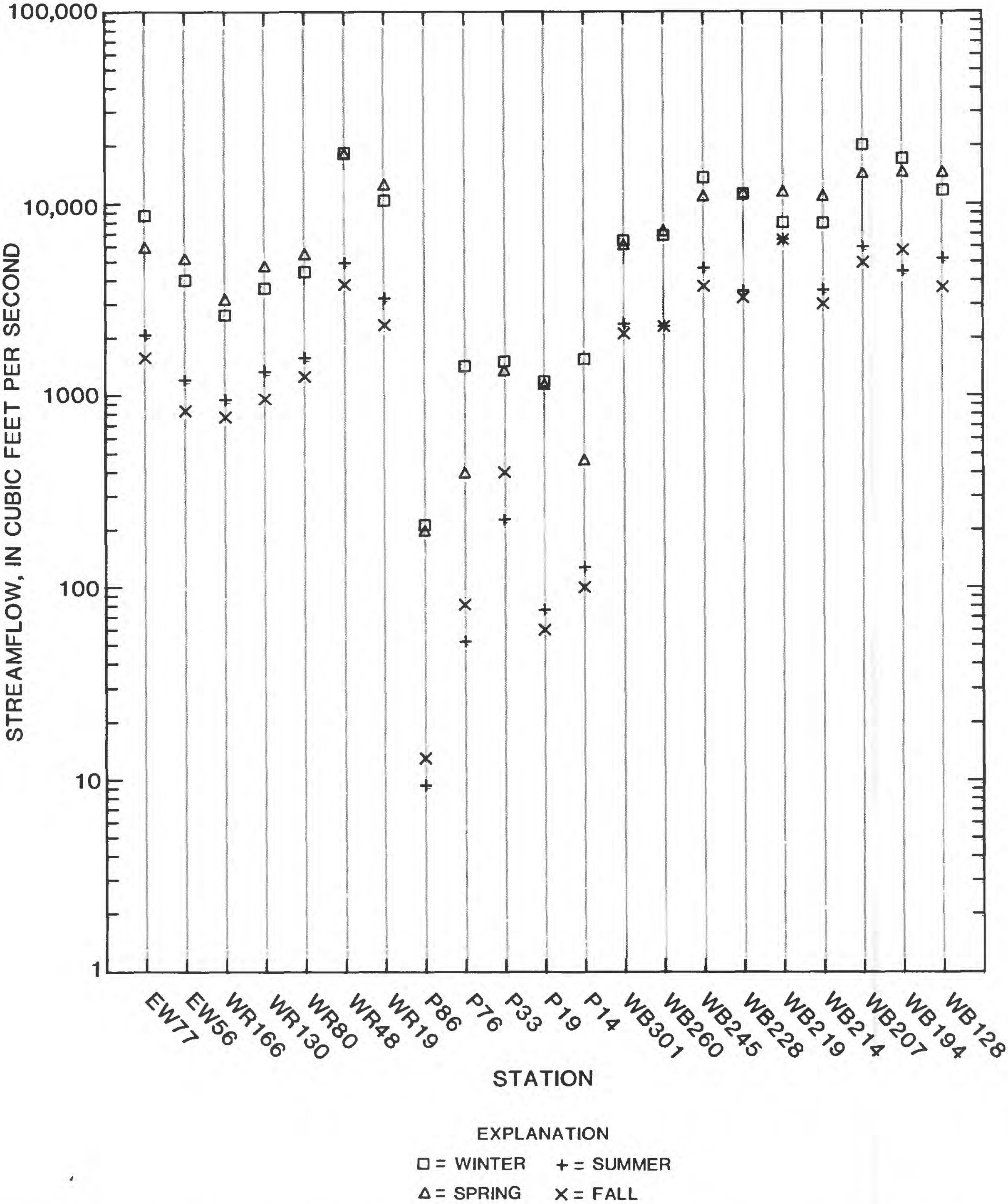

Figure 9C. Seasonal median streamflow at Indiana State Board of Health stations. Data are estimates of the daily mean streamflow on days when water-quality measurements were made.

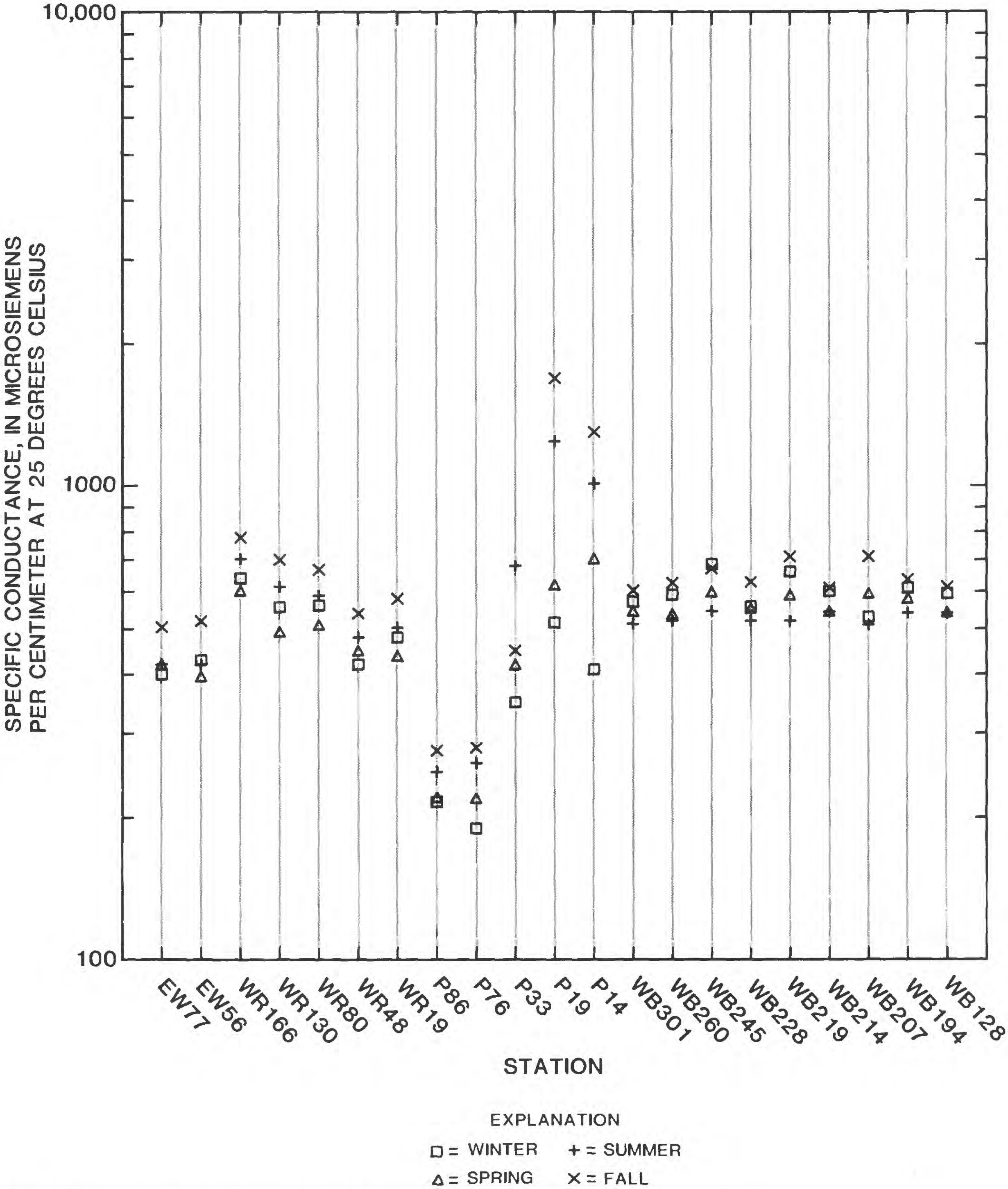

Figure 9*D*. Seasonal median specific conductance at Indiana State Board of Health stations.

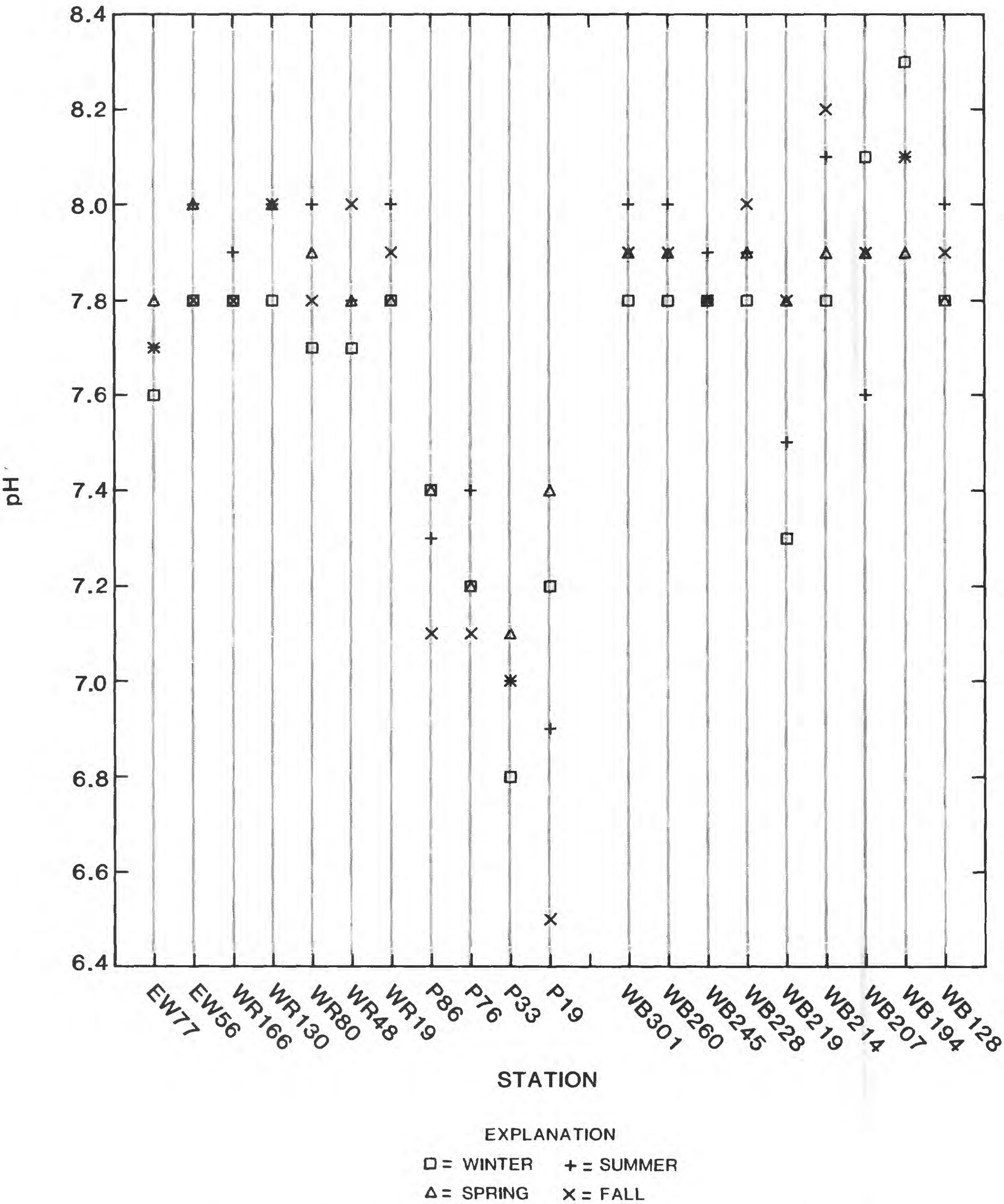

Figure 9*E*. Seasonal median pH at Indiana State Board of Health stations. Stations with fewer than three measurements in any season are not shown.

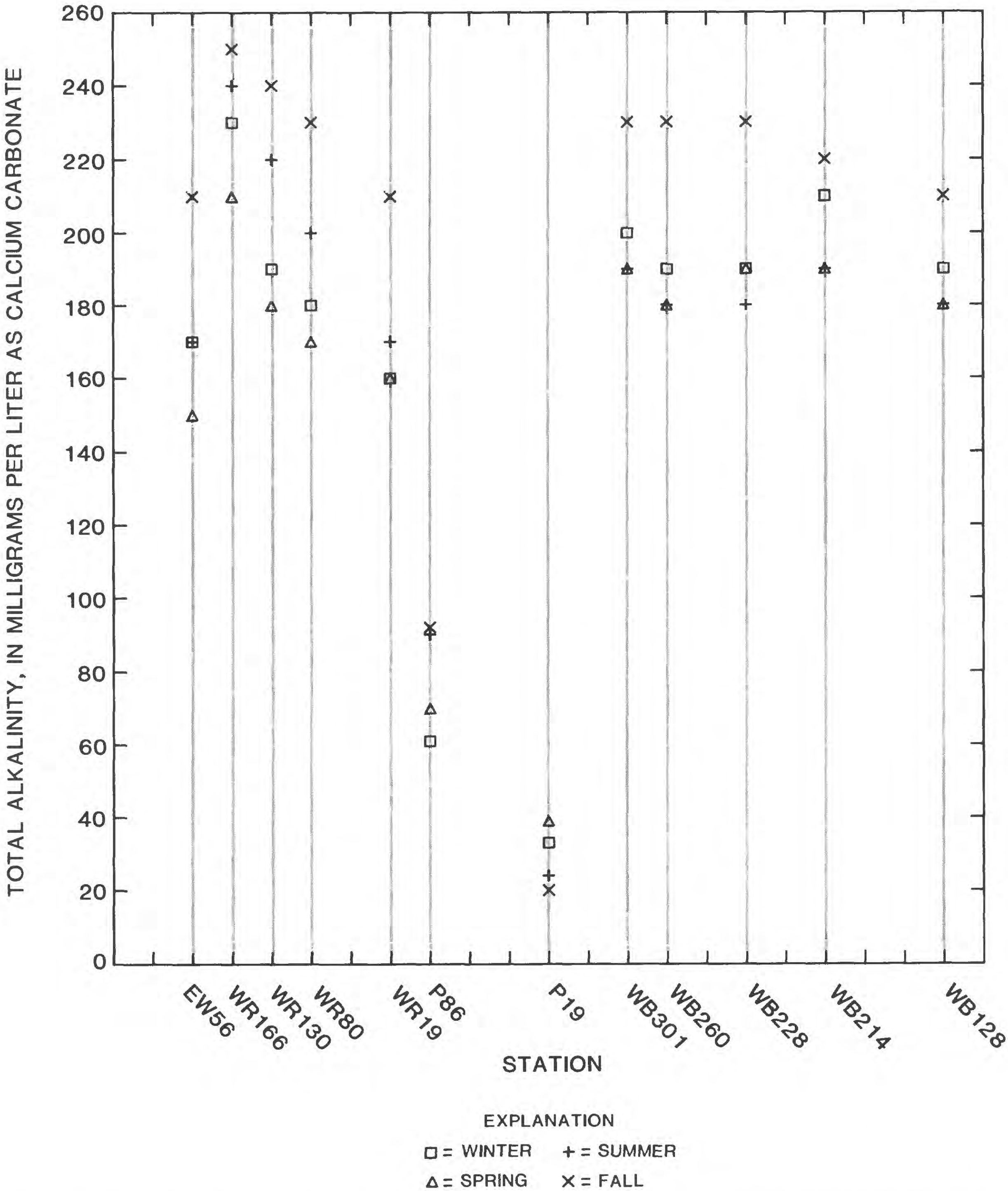

Figure 9*F*. Seasonal median total alkalinity concentration at Indiana State Board of Health stations. Stations with fewer than three measurements in any season are not shown.

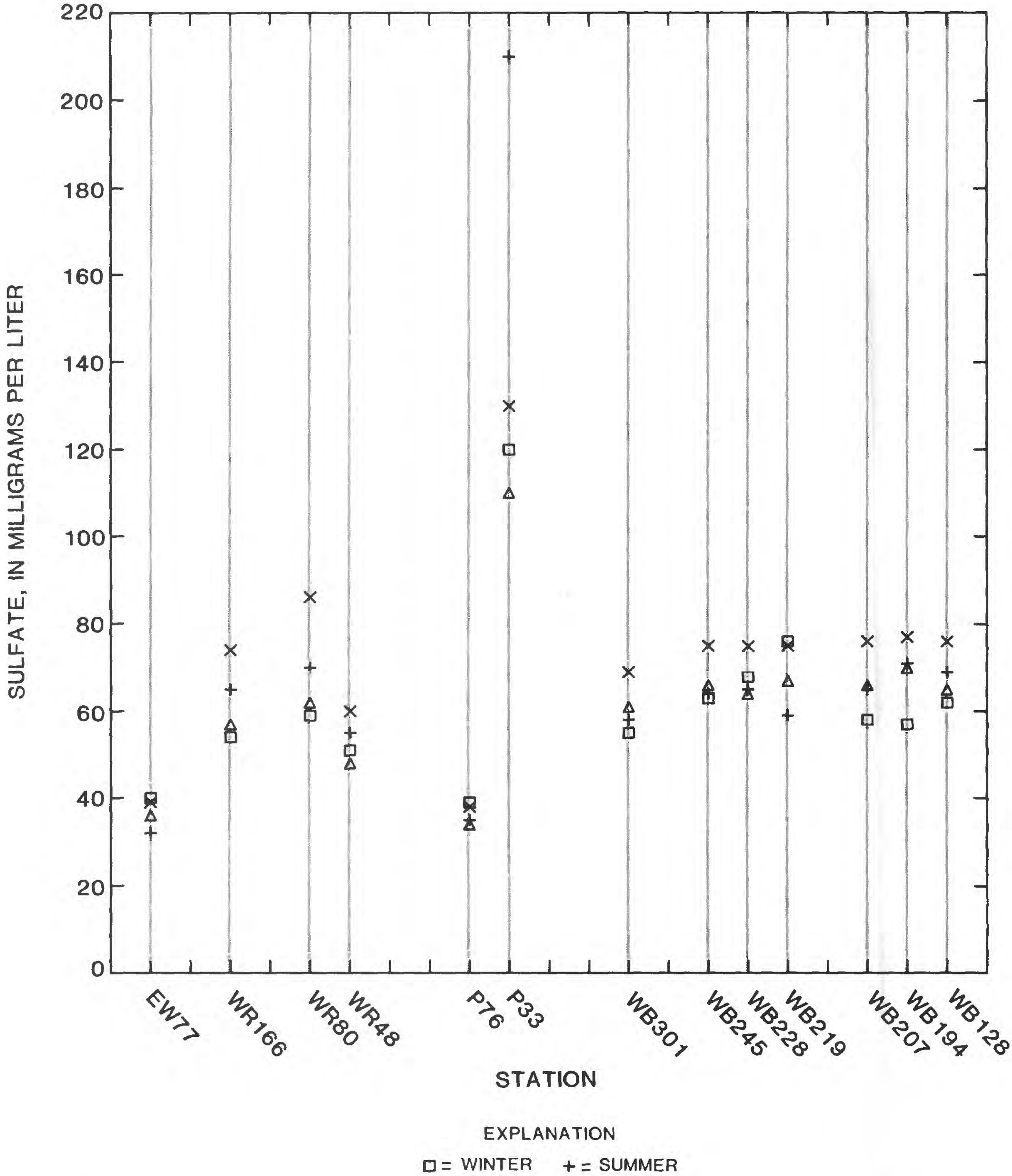

Figure 9G. Seasonal median sulfate concentration at Indiana State Board of Health stations. Stations with fewer than three measurements in any season are not shown.

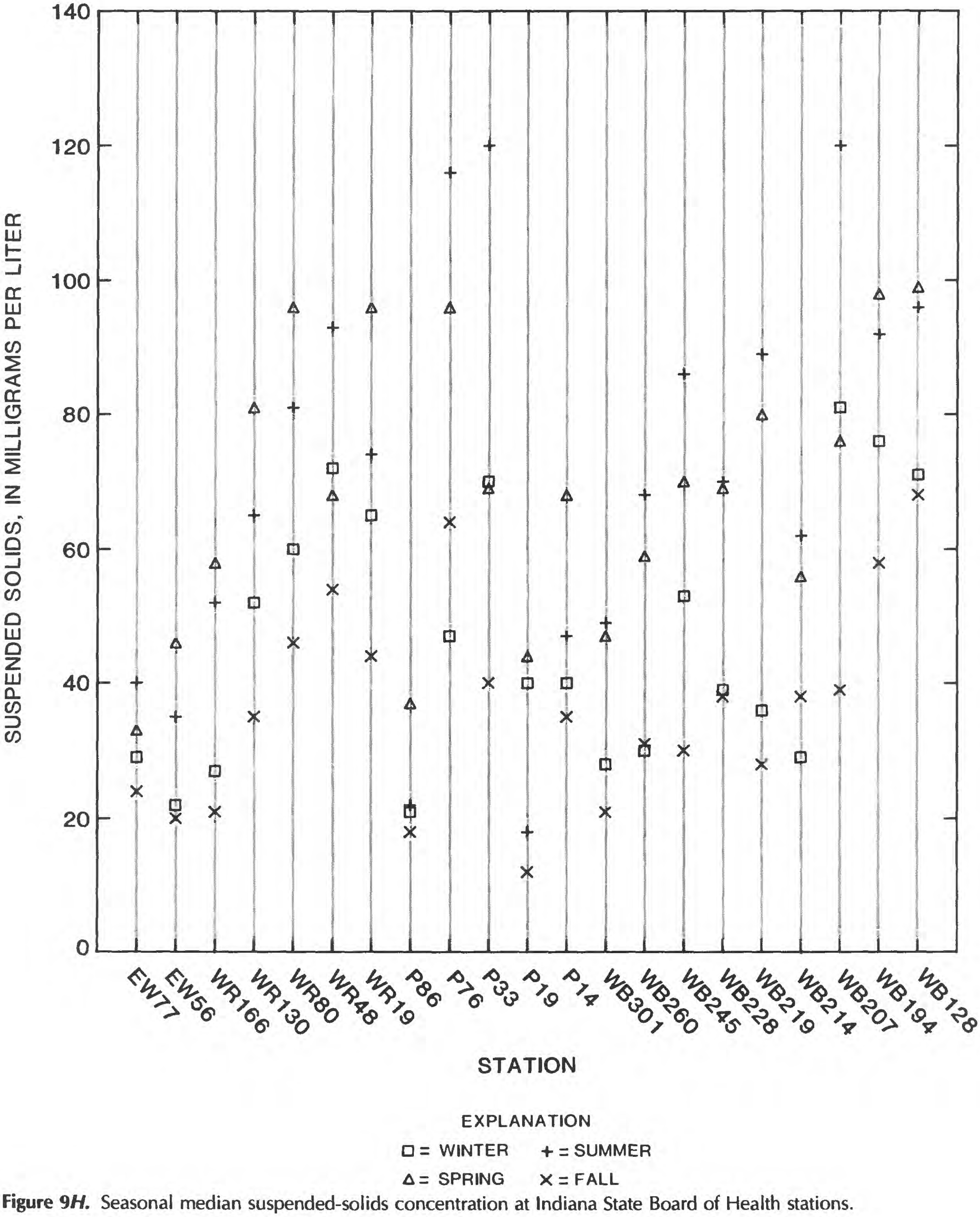

Figure 9*H*. Seasonal median suspended-solids concentration at Indiana State Board of Health stations.

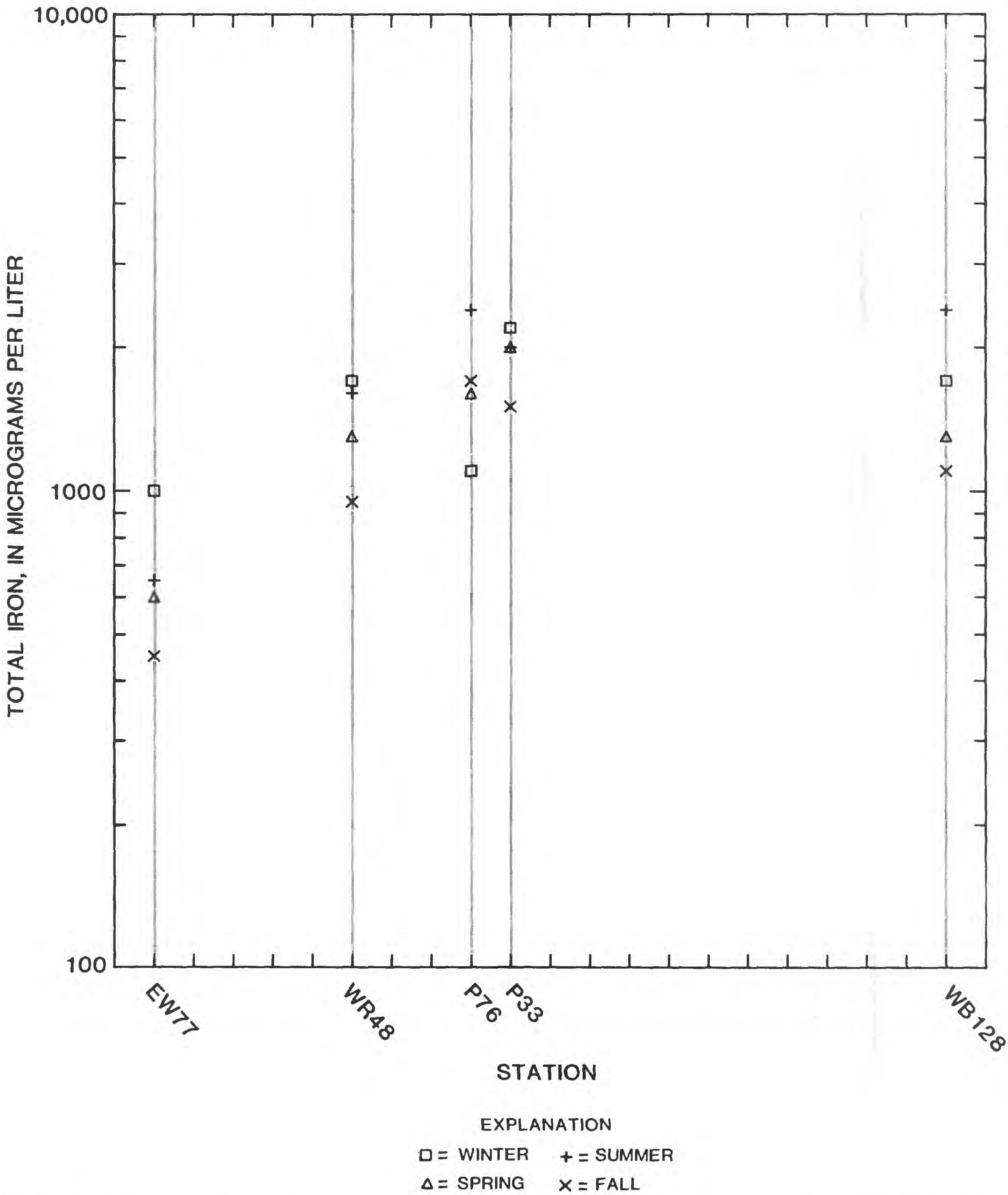

Figure 9*l*. Seasonal median total iron concentration at Indiana State Board of Health stations. Stations with fewer than three measurements in any season are not shown.

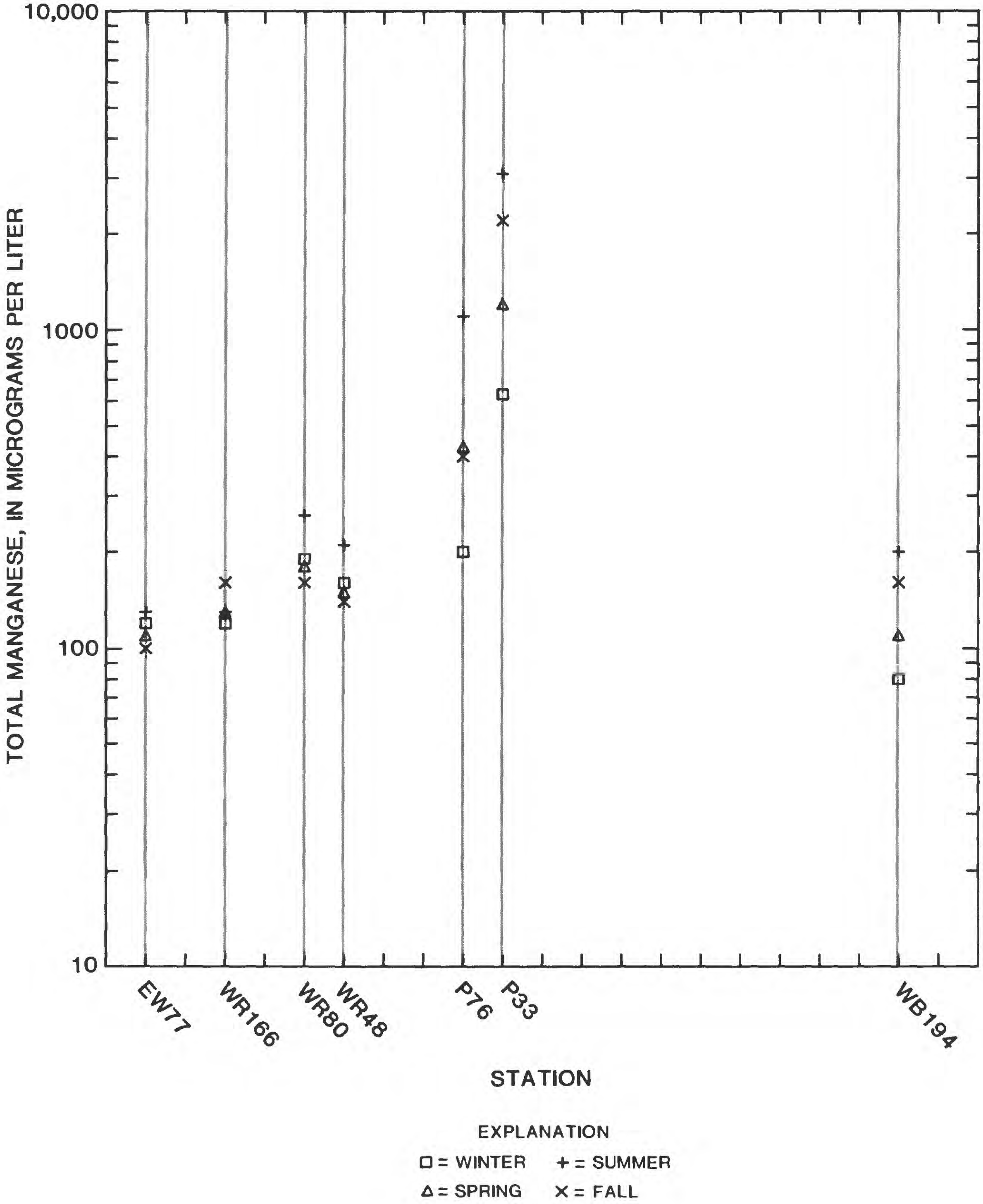

Figure 9J. Seasonal median total manganese concentration at Indiana State Board of Health stations. Stations with fewer than three measurements in any season are not shown.

River (fig. 9*G*). Coefficients of variation ranged from 20 percent at Wabash River at Vincennes (station WB128) to 89 percent at Patoka River near Oakland City (station P33) (table 10). Sulfate concentration was most variable during winter at all stations on the Wabash River.

Median suspended-solids concentration was least during fall at 18 of 21 Indiana State Board of Health stations, but was greatest during summer (11 stations) or spring (10 stations) (fig. 9*H*). Suspended-solids concentration was highly variable at all stations. Coefficients of variation ranged from 74 percent at Wabash River near Terre Haute (station WB194) to 308 percent at Patoka River near Princeton (station P19) (table 11).

Median total iron concentration was greatest during winter or summer at 5 of 5 stations, and was least during fall at 4 of 5 stations (fig. 9*I*). Coefficients of variation ranged from 62 percent at Patoka River near Oakland City (station P33) to 86 percent at Wabash River at Vincennes (station WB128) (table 12).

Median total manganese concentration was greatest during summer at 6 of 7 stations and least during winter or fall at 7 of 7 stations (fig. 9*J*). Coefficients of variation ranged from 40 percent at White River near Petersburg (station WR48) to 87 percent at Patoka River near Jasper (station P76) and Patoka River near Oakland City (station P33) (table 13).

WATER-QUALITY FUNCTIONAL RELATIONS AND PREDICTIVE EQUATIONS

Functional Relations

Surface-water quality is controlled or influenced by a variety of factors related to hydrology, geology, chemistry, biology, and land use (Hem, 1970, p. 12; Rickert and Hines, 1975, p. A6). The objective of many scientific studies is to determine the cause-and-effect relations between these factors and water quality. Rigorous application of the scientific method is required to investigate the processes and mechanisms that determine if a relation truly is one of cause and effect.

An objective of this study, however, is to investigate the form and significance of the functional relations between water-quality variables. A functional relation is a statistical relation that allows one to predict values of a variable on the basis of known values of a different variable (Sokal and Rohlf, 1969, p. 405). Knowledge of the processes and mechanisms necessary to establish a cause-and-effect relation is not required to establish a functional relation. Functional relations are based on probability. An understanding of the functional relations between variables (particularly between water quality and streamflow) is helpful in interpreting water-quality data.

The functional relation between two water-quality variables may be good, poor, or nonexistent. If a relation exists, the slope of the regression line defining the relation can be positive, negative, or both (Smith and others, 1982, p. 6). The mechanisms or processes causing the functional relation may be simple, complex, or unknown. For example, the slope of the line defining the relation between the concentration of a chemical constituent and streamflow would be negative (high concentrations at low flows and low concentrations at high flows) if the primary process is dilution of a constant source by runoff. The slope of the line defining the relation would be positive (low concentrations at low flows and high concentrations at high flows) if the primary process is erosion and large amounts of the constituent are brought to the stream by overland runoff. The slope of the line defining the relation could be both positive and negative if both processes are occurring (one process dominant at low flows and the other process dominant at high flows). Examples of stations where the relation between total alkalinity concentration and specific conductance is positive, negative, and both positive and negative are given in figures 10*A–C*.

Regression Methods Used To Investigate Functional Relations and Develop Predictive Equations

PROC REG (SAS Institute Inc., 1982b, p. 39) was used to calculate least squares regressions for the functional relations between water-quality constituents and properties and streamflow, specific conductance, and (or) suspended-solids concentration. Streamflow, specific conductance, and suspended-solids concentration were selected as independent variables in the regressions because other investigators have found them to be correlated with water quality (Knapton and Ferreira, 1980, p. 27; Wentz and Steele, 1980, p. 26–29; Smith and others, 1982, p. 13; Engberg, 1983, p. 5) and because data for these variables are more often available or are more easily obtained than data for the chemical constituents.

The concentrations of many water-quality constituents vary with streamflow; therefore, all water-quality constituents and properties were regressed against streamflow. Specific conductance is related to the concentration of ionic constituents in the dissolved phase (Hem, 1970, p. 96). Consequently, pH, total alkalinity, sulfate, dissolved solids, and total manganese were regressed against specific conductance. Total iron, primarily in the colloidal or suspended phase of surface water (Hem, 1970, p. 121), was regressed against suspended-solids concentration.

Regression Models

The functional relation between a dependent and an independent variable is expressed in the general equation for simple linear regression:

$$Y = a+bX, \quad (2)$$

where

Y = a value of the dependent variable,
X = a value of the independent variable,
a = the intercept coefficient, and
b = the slope coefficient.

Four simple linear regression models were used to investigate the functional relations between water-quality variables at each station. A function (transformation) of a water-quality variable is used as the independent variable in the inverse, semilog, and log-log models. The base-10 logarithm of a water-quality variable is used as the dependent variable in the log-log model. Equations for the models are as follows:

Model	*Equation*	
Linear	$Y = a+bX,$	(3)
Inverse	$Y = a+b(1/x),$	(4)
Semilog	$Y = a+b(\log_{10} x),$	(5)
Log-log	$\log_{10} y = a+b(\log_{10} x),$	(6)

where

x = a value of a water-quality variable that is transformed to a value of the independent variable (X),
y = a value of a water-quality variable that is log-transformed to a value of the dependent variable (Y), and
X, Y, a, and b are as previously defined.

For example, let x be a value of streamflow (x = 937 ft^3/s). Then the value of the independent variable (X) is 937 ft^3/s for the linear model, 1.07×10^{-3} s/ft^3 for the inverse model, and 2.97 $\log_{10}$ ft^3/s for the semilog and log-log models.

For regressions against streamflow, an additional model was used:

Model	*Equation*	
Hyperbolic	$Y = a+b[1/(1+hx)],$	(7)

where h is a positive constant, and Y, x, a, and b are as previously defined.

The hyperbolic model used for regression analysis was chosen from eight possible hyperbolic models that differed only in the value of h. Values of h were calculated for each hyperbolic model by using the procedure of Smith and others (1982, p. 8) as follows:

1. For a given station, the mean streamflow, $\bar{Q}$, was calculated.
2. The integer part (characteristic) of $\log_{10} \bar{Q}$, arbitrarily called Z here, was determined.
3. The constant h was assigned the value of $10^{(-2.5-Z)}$. This is the value of h for the first hyperbolic model.
4. The value of h was increased by multiplying by $10^{0.5}$. This is the value of h for the second hyperbolic model.
5. The values of h for the next six hyperbolic models were calculated by multiplying the previous value of h by $10^{0.5}$.

Eight values of h were used to calculate eight different independent variables for the hyperbolic models. PROC CORR (SAS Institute Inc., 1982a, p. 501) was used to calculate Spearman rank-correlation coefficients between the dependent variable of interest and the eight independent variables for the hyperbolic models. The hyperbolic model with the highest correlation coefficient was chosen for use in regression analysis.

Linear, inverse, semilog, and hyperbolic models estimate the mean value of the dependent variable. Residuals (deviations of the observed data from the regression line) for these models are approximately normally distributed; consequently, these models also estimate the median value of the dependent variable.

Although least squares regression is done for the log-log model, as shown in equation 6, the log-log model is not commonly presented in this form. More often the equation for the log-log model is presented in exponential form (as in tables 14–28) so that the retransformed dependent variable is expressed in common units rather than in the logarithmic units of the dependent variable as in the log-log form. Residuals for the exponential form of the log-log model are approximately log-normally distributed. Consequently, the exponential form estimates the median value of the retransformed dependent variable but gives biased (low) estimates of the mean (Miller, 1984, p. 124).

The smearing method (Duan, 1983) can be used to correct the exponential form of the log-log model to give unbiased estimates of the mean. A bias corrector is calculated on the basis of scatter of the residuals. The greater the scatter of the residuals, the greater the bias corrector. Unbiased estimates of the mean of the retransformed dependent variable can be obtained by multiplying the estimate of the median obtained from the predictive equation for the log-log model by the bias corrector.

Using the smearing method, the log-log model (eq. 6) is equivalent to

$$Y = 10^a X^b (\Sigma\ 10^R)/n, \quad (8)$$

where

n = the number of data pairs used to develop the predictive equation,
R = the residual error for each data pair in logarithmic units (base-10),
$(\Sigma 10^R)/n$ = the bias corrector for the log-log model, and
X, Y, a, and b are as previously defined.

Examples of the forms of the models are shown in figure 11 for the relation between specific conductance and streamflow at White River at Petersburg (station WR48). PROC REG (SAS Institute Inc., 1982b, p. 41) was used to

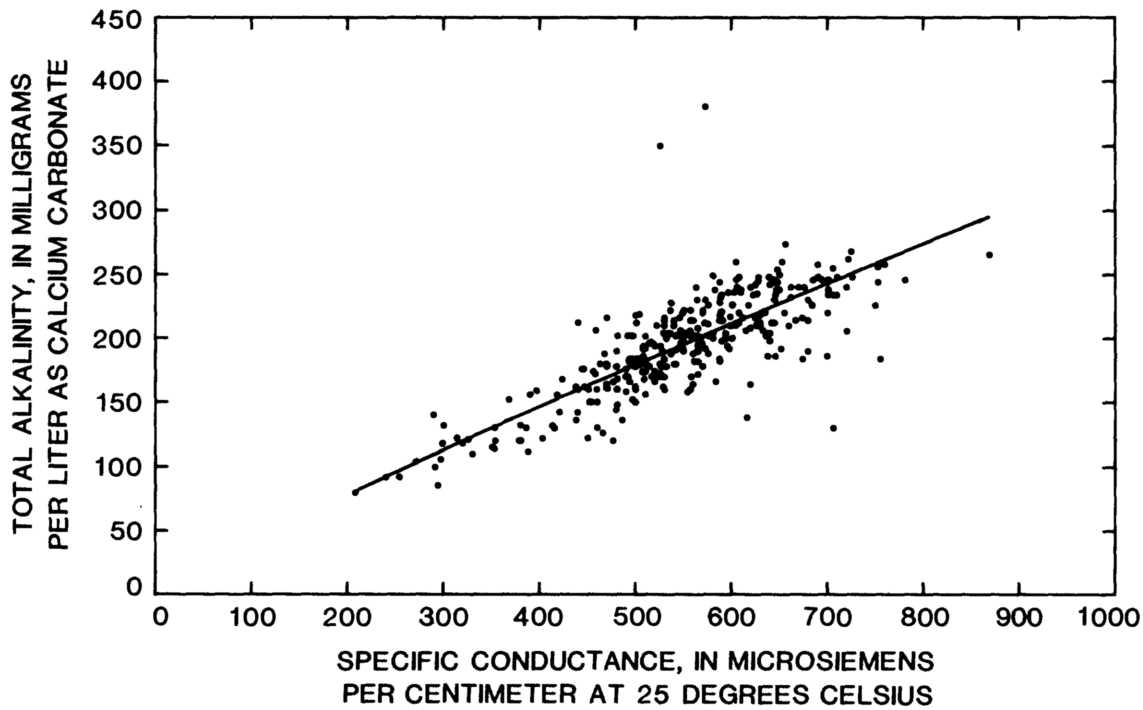

Figure 10*A*. Positive functional relation between total alkalinity concentration and specific conductance at Wabash River at Montezuma (station WB228).

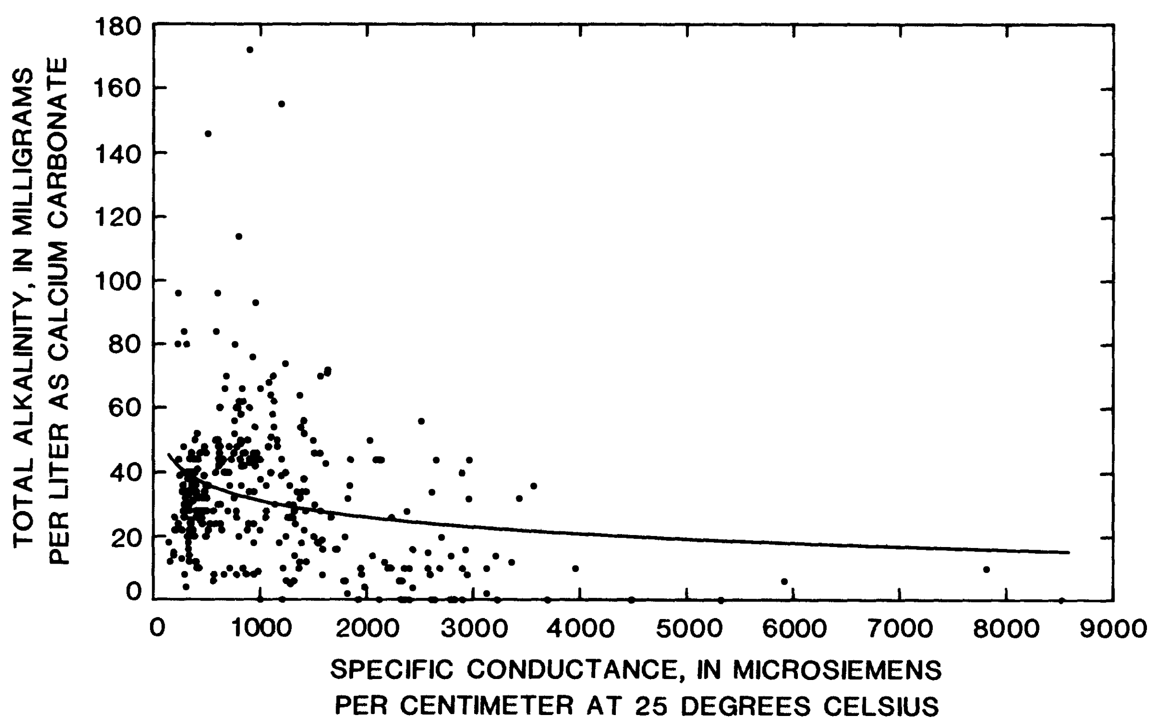

Figure 10*B*. Negative functional relation between total alkalinity concentration and specific conductance at Patoka River near Princeton (station P19). Specific conductance greater than 9,000 μS/cm at 25°C is not shown.

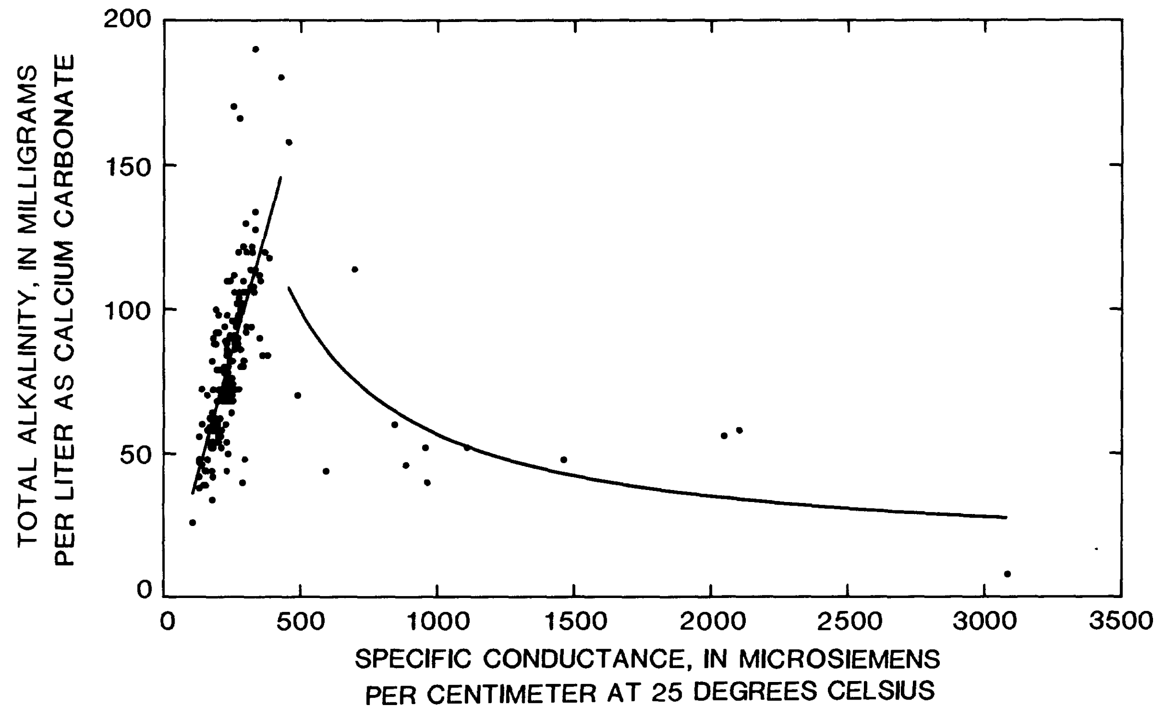

Figure 10C. Positive and negative functional relation between total alkalinity concentration and specific conductance at Patoka River at Jasper (station P86).

calculate least squares estimates for the coefficients in the linear regression models. In addition, PROC REG was used to calculate the coefficient of determination (R-square), the standard error of regression, Cook's D influence statistic, and the residuals and to test the statistical significance of the regression.

Criteria for Selecting the Best Model

The model that best described the functional relation between the dependent variable Y and the independent variable X was selected on the basis of the following criteria:

1. The significance level of the regression. For a model to be considered, p (the probability of obtaining a statistically significant relation by chance where, in fact, there is no relation) must be less than 5 percent ($p<0.05$).
2. The standard error of regression, in percent (Ep). Ep is an index of the standard deviation of the measured values from the regression line. The smaller the value of Ep, the better the regression line "fits" the data. For all models except the log-log model, Ep is calculated as the root mean square deviation of sample points from the regression line (Es) divided by the mean of the dependent variable times 100. For log-log models, Ep is from Hardison (1971, table 1, p. C229).
3. The coefficient of determination (R-square). R-square is a measure of the proportion of the variability in the dependent variable explained by the regression (Haan, 1977, p. 184). R-square ranges from 1.00 (for a regression that completely explains the variability in the dependent variable) to 0.00 (for a regression that explains none of the variability in the dependent variable). R-square was used as a criterion to select among linear, inverse, semilog, and hyperbolic models but was not used for log-log models. In the log-log model, the dependent variable has been transformed to a base-10 logarithm and the R-square cannot be compared directly with those from the other models (Sall, 1981, p. 2–9).
4. Residual analysis. Deviations of the measured values from the regression line (residuals) were plotted to see if the assumptions of regression were met. These assumptions are that the residuals are independent and are normally distributed with a mean of zero and a constant variance (Walpole and Myers, 1978, p. 285). Only the assumption that the residuals have a mean of zero is required for the use of the predictive equation. The other assumptions are necessary for estimating confidence intervals and testing hypotheses (Haan, 1977, p. 186). The assumption of normality was tested by using the normal option of PROC UNIVARIATE (SAS Institute Inc., 1982a, p. 580). The assumption of constant variance was tested by using the Spearman option of PROC CORR to determine the correlation between the absolute value of the residuals and the independent variable. The assumption of independence was not tested.

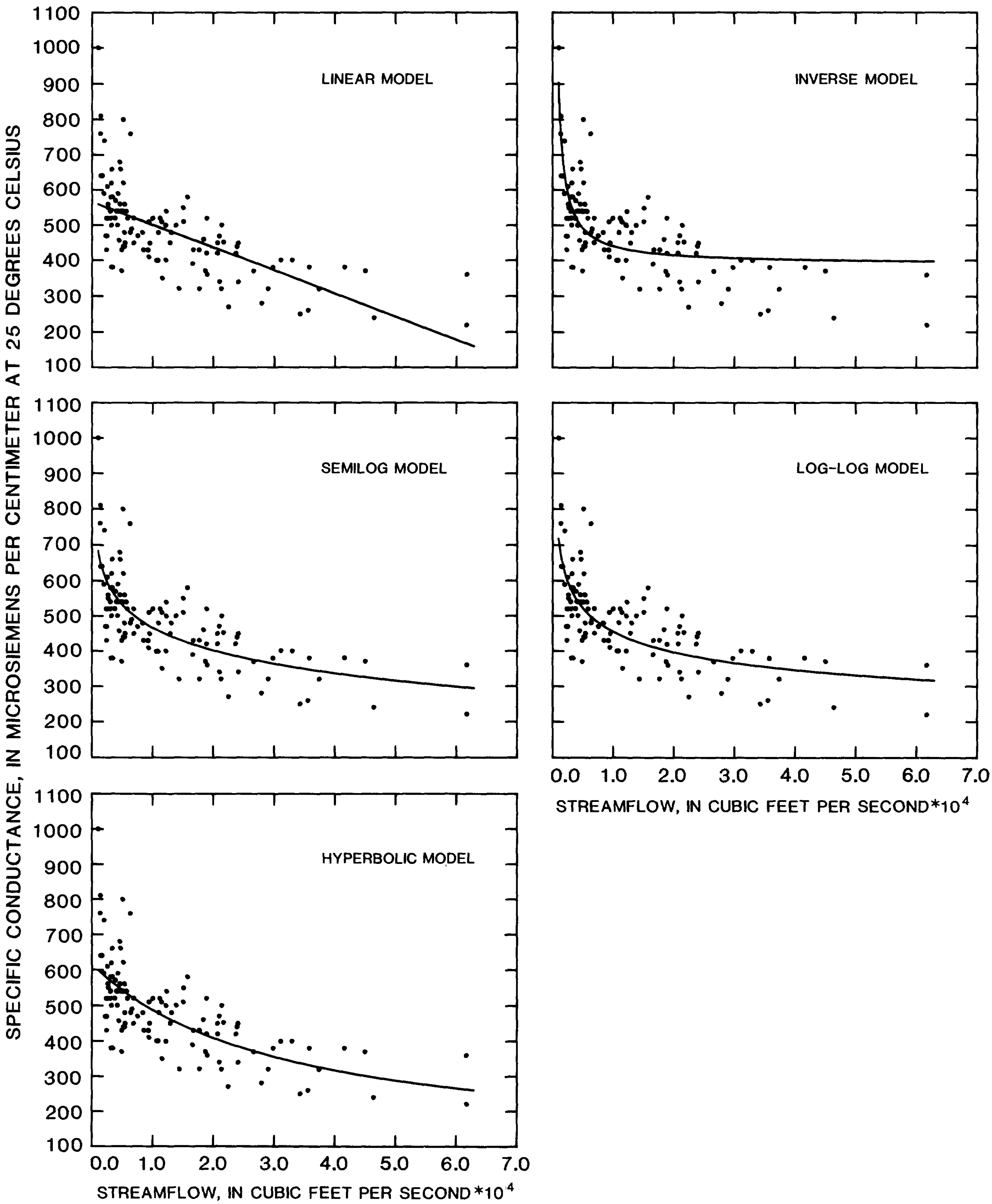

Figure 11. Linear, inverse, semilog, log-log, and hyperbolic models of the relation between specific conductance and streamflow at White River at Petersburg (station WR48).

5. Graphical analysis. Data points were plotted, and the regression line was drawn through the data points. The plot was inspected to ensure that the line fit the data over the entire range of the independent variable.
6. Influence statistic. Cook's D influence statistic was scrutinized, and models where one or more data points were extremely influential were not favored.

Predictive Equations

Predictive equations and statistics for all statistically significant water-quality functional relations are shown in tables 14–28. Units for the standard error of regression are logarithmic for the log-log model and arithmetic for all other models. Units for the mean of the independent variable are arithmetic for linear models, reciprocal for inverse and hyperbolic models, and logarithmic for semilog and log-log models. Units for the sum of squares of the independent variable are squares of the units for the mean of the independent variable.

Slope, Goodness-of-Fit, and Reliability of Functional Relations and Predictive Equations

The slope of a regression line defining a functional relation indicates whether two water-quality variables vary directly (positive slope) or inversely (negative slope). Slope is determined from the predictive equation and is the same as the sign of the b regression coefficient for linear (eq. 3), semilog (eq. 5), and log-log (eq. 6, 8) models. The slope of the relation for the inverse model (eq. 4) is opposite the sign of the b regression coefficient. Predictive equations for the hyperbolic model (eq. 7) must be graphed to determine the slope of the functional relation.

The goodness-of-fit of a functional relation and, therefore, the ability of the predictive equation to reliably estimate the response variable are dependent on the significance of the regression, the standard error of the regression, and the coefficient of determination. Relations are best where the regression is highly significant ($p<0.01$), the standard error of regression is small, and the coefficient of determination is large. Relations are poorest where the regression is significant ($p<0.05$), the standard error of regression is large, and the coefficient of determination is small. Relations fail to exist where the regression is not significant ($p>0.05$).

Regional Relations

Two distinct groups of data are apparent in a plot of dissolved-solids concentration against specific conductance. Predictive equations were developed separately for specific conductance between 60 and 740 μS/cm at 25°C and between 750 and 6,100 μS/cm at 25°C (table 14). The slope of the regression lines defining the regional relation is the primary difference between the predictive equations for the two ranges of specific conductance. The positive relation between dissolved-solids concentration and specific conductance is very good (R-square of 0.92 and 0.95, Ep of 13.4 and 14.4 percent). The two log-log equations in table 14 can be used to predict dissolved-solids concentration in the coal-mining region with confidence.

Two groups of data are apparent in a plot of sulfate concentration against specific conductance, as was true for the regional relation between dissolved-solids concentration and specific conductance. Predictive equations were developed for specific conductance between 40 and 740 μS/cm at 25°C and between 750 and 6,100 μS/cm at 25°C (table 15). Sulfate concentration was positively related to specific conductance. The regional relation was much better for the high range of specific conductance (R-square of 0.85, Ep of 24.6 percent) than for the low range (R-square of 0.36, Ep of 57.8 percent).

Relations At Stations

The slope and the statistical significance of functional relations between water-quality variables at U.S. Geological Survey gaging stations and at Indiana State Board of Health stations are reported in tables 29 and 30. Of 186 relations investigated, 143 were statistically significant.

Specific conductance was inversely related to streamflow at all 37 stations (tables 29, 30). The consistent results indicate that the processes controlling specific conductance may be the same at all stations. Specific conductance is higher in baseflow than in precipitation, and the negative functional relation between specific conductance and streamflow is probably caused by dilution during high flow. The log-log and the hyperbolic models were most applicable to the relations between specific conductance and streamflow. R-square ranged from 0.10 to 0.88 and Ep ranged from 12.9 to 48.9 percent (tables 16, 17).

The relations between pH and streamflow were statistically significant at 9 of 21 stations. Six of the significant relations were negative and three were positive. The hyperbolic model was most applicable to the relations between pH and streamflow. R-square for the significant relations ranged from 0.02 to 0.46 and Ep ranged from 2.7 to 15.0 percent (table 18).

Only 7 of 21 relations between pH and specific conductance were statistically significant. Positive and negative relations were observed. R-square for the significant relations ranged from 0.01 to 0.23 and Ep ranged from 3.3 to 14.4 percent (table 19). Differences in the slope and the significance of the relations indicate that the processes controlling pH are complex and require interpretation on a site-specific rather than a regional scale.

All the relations between total alkalinity concentration and streamflow and between total alkalinity concentration and specific conductance were statistically significant. Except for Patoka River near Princeton (station P19), total alkalinity concentration decreased as streamflow increased; at that station total alkalinity concentration was directly related to streamflow. The hyperbolic model was most applicable to the relations between total alkalinity concentration and streamflow. R-square ranged from 0.10 to 0.72 and Ep ranged from 12.3 to 69.6 percent (table 20).

Total alkalinity concentration was directly related to specific conductance at all stations except Patoka River at Jasper (station P86) and Patoka River near Princeton (station P19). The relation at Patoka River at Jasper was positive and negative (fig. 10*C*), and the relation at Patoka River near Princeton was negative (fig. 10*B*). The processes controlling total alkalinity concentration at these two stations are different from those at the other stations. The semilog model was most applicable to the relations between total alkalinity concentration and specific conductance. R-square ranged from 0.07 to 0.80 and Ep ranged from 11.6 to 70.5 percent (table 21).

Sulfate concentration was inversely related to streamflow at all stations. The semilog model was most applicable to the relations between sulfate concentration and streamflow. R-square ranged from 0.12 to 0.64 and Ep ranged from 13.5 to 60.3 percent (table 22).

Sulfate concentration was directly related to specific conductance at all stations. R-square ranged from 0.09 to 0.73 and Ep ranged from 12.5 to 43.7 percent (table 23).

Suspended-solids concentration was directly related to streamflow at all but two stations on the Patoka River. The lack of significant relations at these stations is an indication that the processes controlling suspended-solids concentration are different in nature or magnitude from the processes controlling suspended-solids concentration at the other stations. The log-log model was most applicable to the relations between suspended-solids concentration and streamflow, but the relations are poor. R-square for the significant relations ranged from 0.17 to 0.37 and Ep ranged from 79.4 to 140 percent (table 24).

Total iron concentration was directly related to streamflow at six of eight stations. R-square for the significant relations ranged from 0.10 to 0.78 and Ep ranged from 42.5 to 79.4 percent (table 25).

Total iron concentration was directly related to suspended-solids concentration at all eight stations. The log-log and the linear models were most applicable to the relations between total iron concentration and suspended-solids concentration. R-square ranged from 0.36 to 0.91 and Ep ranged from 25.8 to 47.3 percent (table 26).

Total manganese concentration was inversely related to streamflow at only two of eight stations. Both stations were on the Patoka River. R-square for these two relations was 0.47 and 0.60, and Ep was 63.7 and 55.6 percent (table 27).

The relations between total manganese and specific conductance were significant at three of eight stations. At two stations on the Patoka River the relations were positive, and at East Fork White River at Williams (station EW77) the relation was negative. R-square for the significant relations ranged from 0.22 to 0.81 and Ep ranged from 38.8 to 61.1 percent (table 28).

Confidence Limits

The standard error of regression, the sum of squares of the independent variable, and the mean of the independent variable are reported to allow the reader to calculate an estimate of the confidence limits for predicted water quality. By calculating confidence limits, the reliability of predicted water quality at a particular value of the independent variable can be estimated. This is often more useful than a single measure of reliability (such as Ep) for the entire equation.

Two kinds of confidence limits can be calculated: limits for the predicted individual response and limits for the predicted mean or median response. Confidence limits for the predicted individual response of the dependent variable at a particular value of the independent variable give the expected range (confidence interval) within which the true value should lie. For example, a single future measurement of specific conductance at a particular streamflow would be expected to fall within the range of specific conductance estimated by this type of confidence limits.

Confidence limits for the predicted mean or median response of the dependent variable at a particular value of the independent variable give the expected range within which the true mean or median value should lie. For example, the average of a large number of future measurements of specific conductance at a particular streamflow would be expected to fall within the range of mean or median specific conductance estimated by this type of confidence limits. Confidence limits for the predicted mean or median response are smaller than confidence limits for the predicted individual response.

Calculation and interpretation of confidence limits is dependent on the type of model. The dependent variable in linear, inverse, hyperbolic, and semilog models is untransformed, and confidence limits can be calculated for the predicted individual response and for the predicted mean response of the dependent variable. Confidence limits for these models are symmetric about the predicted response.

The dependent variable in log-log models is transformed to the base-10 logarithm; consequently, confidence limits are calculated on the log-transformed variable and reexpressed in untransformed units. Confidence limits for the predicted mean response cannot be calculated for the log-log model. However, confidence limits for the predicted individual response and for the predicted median response can be calculated. Confidence limits for the log-log model are nonsymmetric about the predicted response.

Confidence limits for the predicted individual response or for the predicted mean or median response of the dependent variable at one value of the independent variable can be estimated by using the following formula (Walpole and Myers, 1978, p. 292–294):

$$CL=\hat{Y}\pm t_{\alpha/2}Es\sqrt{f+\frac{1}{n}+\frac{(X-\bar{X})^2}{Sxx}}, \qquad (9)$$

where

- CL = the upper or lower confidence limit,
- $\hat{Y}$ = the predicted response of the dependent variable for X,
- $\alpha=(1-P/100)$, where P is the desired percent probability for the confidence limit,
- $t_{\alpha/2}$ = the value of the t distribution with $n-2$ degrees of freedom and $[100(1-\alpha)]$ percent probability,
- Es = the standard error of regression,
- f = a factor equal to 1 for predicted individual response or equal to 0 for predicted mean or median response,
- n = the number of data pairs,
- X = a value of the independent variable,
- $\bar{X}$ = the mean of the independent variable, and
- Sxx = the sum of squares of the independent variable $[\Sigma X^2-(\Sigma X)^2/n]$.

Confidence limits for the predicted individual response and for the predicted mean or median response of the dependent variable over the entire range of the independent variable can be estimated by calculating the confidence limits at several discrete points over the range of the independent variable. The upper and lower confidence limits for the predictive equation are estimated by connecting the points above the regression line and those below the regression line to form confidence bands (figs. 12, 13).

Interpretation of confidence limits can be confusing. Ninety-five-percent confidence limits imply that the probability that these limits contain the true value or true mean or median value is 95 percent. This is not to say that the true value is contained by these confidence limits 95 percent of the time. The true value is a fixed number and must be either inside or outside the confidence limits 100 percent of the time. Use and interpretation of confidence limits in regression are discussed in Haan (1977, p. 161–166, 186–192) and in Sokal and Rohlf (1969, p. 138–142, 420–427).

Procedures used for calculating an estimate of the confidence limits for models where the dependent variable is untransformed and is log-transformed follow.

Calculation of Confidence Limits for Models with Untransformed Dependent Variables

This section is an example of the computational procedure used to calculate an estimate of the confidence limits for the relation between specific conductance and streamflow at Crooked Creek near Santa Claus (station 03303400). The predictive equation is a semilog model (table 16); therefore, specific conductance in microsiemens per centimeter at 25 degrees Celsius is the dependent variable and the base-10 logarithm of streamflow in cubic feet per second is the independent variable. Several values of mean specific conductance (SC) are predicted for several values of streamflow (Q) from the equation $SC=504.8-107.7(\log_{10} Q)$. Maximum and minimum streamflows are included to adequately define the relation as in the table that follows:

Streamflow, Q (ft^3/s)	*Independent variable, X ($\log_{10} ft^3/s$)*	*Predicted dependent variable, $\hat{Y}$ (μS/cm at 25°C)*	*Predicted mean specific conductance, SC (μS/cm at 25°C)*
0.03	−1.523	668.8	668.8
.10	−1.000	612.5	612.5
.30	− .5229	561.1	561.1
1.0	.0000	504.8	504.8
3.0	.4771	453.4	453.4
10	1.000	397.1	397.1
36	1.556	337.2	337.2

The values of mean specific conductance and streamflow are plotted and the points are connected to define the relation described by the predictive equation (fig. 12). The equation for the confidence limits (CL) for the predicted individual response of the dependent variable ($\hat{Y}$) is

$$CL=\hat{Y}\pm t_{\alpha/2}Es\sqrt{f+\frac{1}{n}+\frac{(X-\bar{X})^2}{Sxx}},$$

and the variables are as defined in equation 9. From table 16, n=43, $\bar{X}$=0.1354 $\log_{10}$ ft^3/s, Sxx=32.82 $(\log_{10} ft^3/s)^2$, Es=84.75 μS/cm at 25° C, and f=1.0. For a 95-percent confidence limit, α= 0.05. The value of the t distribution, with 41 degrees of freedom ($n-2$) and 95-percent probability $[100(1-\alpha)]$, $t_{\alpha/2}$ is 2.019 (Rohlf and Sokal, 1969, p. 159–161). For a streamflow of 0.03 ft^3/s ($X=-1.523$, $\hat{Y}$=668.8), the 95-percent confidence limits for the predicted individual specific conductance are

$$CL = 668.8 \pm (2.019)(84.75)\sqrt{1.0 + \frac{1}{43} + \frac{(-1.523-0.1354)^2}{32.82}},$$

or

$$CL = 668.8 \pm 180.0,$$

or

CL upper = 668.8 + 180.0 = 848.8 µS/cm at 25°C, and
CL lower = 668.8 − 180.0 = 488.8 µS/cm at 25°C.

The 95-percent confidence limits for the predicted mean specific conductance are calculated as above except that f = 0.0:

$$CL = 668.8 \pm 56.0,$$

or

CL upper = 668.8 + 56.0 = 724.8 µS/cm at 25° C, and
CL lower = 668.8 − 56.0 = 612.8 µS/cm at 25°C.

Confidence limits similarly constructed for other values of streamflow and mean specific conductance are shown in the table that follows:

Streamflow, Q (ft^3/s)	Predicted mean specific conductance, SC (µS/cm at 25°C)	Predicted individual specific conductance: Upper confidence limit, CL upper (µS/cm at 25°C)	Predicted individual specific conductance: Lower confidence limit, CL lower (µS/cm at 25°C)
0.10	612.5	788.9	436.1
.30	561.1	735.3	386.9
1.0	504.8	677.9	331.7
3.0	453.4	626.8	280.0
10	397.1	572.1	222.1
36	337.2	515.4	159.0

Streamflow, Q (ft^3/s)	Predicted mean specific conductance, SC (µS/cm at 25°C)	Predicted mean specific conductance: Upper confidence limit, CL upper (µS/cm at 25°C)	Predicted mean specific conductance: Lower confidence limit, CL lower (µS/cm at 25°C)
0.10	612.5	655.3	569.7
.30	561.1	593.8	528.4
1.0	504.8	531.2	478.4
3.0	453.4	481.4	425.4
10	397.1	433.8	360.4
36	337.2	387.0	287.4

Confidence limits are plotted and the points are connected to estimate the 95-percent confidence limits for the predicted individual and mean specific conductance (fig. 12).

Calculation of Confidence Limits for Models with Log-Transformed Dependent Variables

This section is an example of the computational procedure used to calculate an estimate of the confidence limits for the relation between specific conductance and streamflow at Pigeon Creek at Evansville (station 03322100). The predictive equation is a log-log model (table 16); therefore, the base-10 logarithm of specific conductance in microsiemens per centimeter at 25 degrees Celsius is the dependent variable and the base-10 logarithm of streamflow in cubic feet per second is the independent variable. Several values of median specific conductance (SC) are predicted for several values of streamflow (Q) from the equation $SC = 3{,}238(Q)^{-0.3077}$. Maximum and minimum streamflows are included to adequately define the relation as in the table that follows:

Streamflow, Q (ft^3/s)	Independent variable, X ($\log_{10} ft^3/s$)	Predicted dependent variable, $\hat{Y}$ ($\log_{10}$ µS/cm at 25°C)	Predicted median specific conductance, SC (µS/cm at 25°C)
4.7	0.6721	3.303	2,011
10	1.000	3.203	1,594
50	1.699	2.988	971.6
100	2.000	2.895	785.0
500	2.699	2.680	478.4
1,000	3.000	2.587	386.5
5,720	3.757	2.354	226.0

The values of median specific conductance and streamflow are plotted and the points are connected to define the relation described by the predictive equation (fig. 13). Confidence limits (CL) for the predicted individual response of the dependent variable ($\hat{Y}$) are calculated from the following equation and then are retransformed. The equation is

$$CL = \hat{Y} \pm t_{\alpha/2} Es \sqrt{f + \frac{1}{n} + \frac{(X-\bar{X})^2}{Sxx}},$$

and the variables are defined in equation 9. From table 16, $n = 53$, $\bar{X} = 2.311$ $\log_{10}$ ft^3/s, $Sxx = 36.19$ ($\log_{10}$ $ft^3/s)^2$, $Es = 0.1564$ $\log_{10}$ µS/cm at 25°C, and $f = 1.0$. For a 95-percent confidence limit, $\alpha = 0.05$. The value of the t distribution, with 51 degrees of freedom ($n-2$) and 95-percent probability [$100(1-\alpha)$], $t_{\alpha/2}$ is 2.007 (Rohlf and Sokal, 1969, p. 159–161). For a streamflow of 4.7 ft^3/s ($X = 0.6721$, $\hat{Y} = 3.303$), the 95-percent confidence limits for the predicted individual specific conductance are

$$CL = 3.303 \pm (2.007)(0.1564)\sqrt{1.0 + \frac{1}{53} + \frac{(0.6721-2.311)^2}{36.19}},$$

or

$$CL = 3.303 \pm 0.328,$$

or

CL upper = 3.303 + 0.328 = 3.631 $\log_{10}$ µS/cm at 25°C or 4,277 µS/cm at 25°C, and

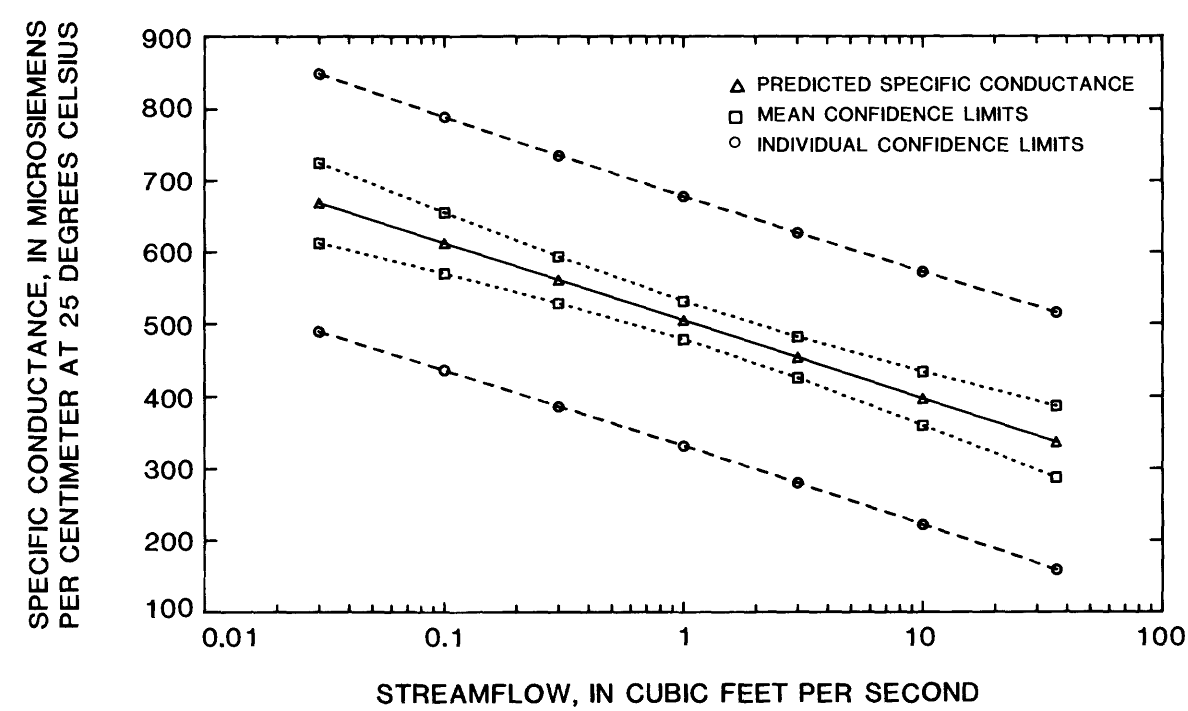

Figure 12. Estimated 95-percent confidence limits for the predicted individual and mean specific conductance at Crooked Creek near Santa Claus (station 03303400).

CL lower = 3.303−0.328 = 2.975 $\log_{10}$ µS/cm at 25°C or 943.7 µS/cm at 25°C.

The 95-percent confidence limits for the predicted median specific conductance are calculated as above except f = 0.0:

$$CL = 3.303 \pm 0.096,$$

or

CL upper = 3.303+0.096 = 3.399 $\log_{10}$ µS/cm at 25°C or 2,505µS/cm at 25°C, and

CL lower = 3.303−0.096 = 3.207 $\log_{10}$ µS/cm at 25°C or 1,611 µS/cm at 25°C.

Confidence limits similarly constructed for other values of streamflow and median specific conductance are shown in the table that follows:

		Predicted individual specific conductance	
Streamflow, Q (ft³/s)	Predicted median specific conductance, SC (µS/cm at 25°C)	Upper confidence limit, CL upper (µS/cm at 25°C)	Lower confidence limit, CL lower (µS/cm at 25°C)
10	1,594	3,366	756.6
50	971.6	2,025	467.3
100	785.0	1,630	378.2
500	478.4	994.2	230.4
1,000	386.5	805.1	185.4
5,720	226.0	478.3	106.7

		Predicted median specific conductance	
Streamflow, Q (ft³/s)	Predicted median specific conductance, SC (µS/cm at 25°C)	Upper confidence limit, CL upper (µS/cm at 25°C)	Lower confidence limit, CL lower (µS/cm at 25°C)
10	1,594	1,922	1,325
50	971.6	1,101	859.7
100	785.0	873.1	706.2
500	478.4	534.1	428.9
1,000	386.5	439.7	339.5
5,720	226.0	276.0	185.0

Confidence limits are plotted and the points are connected to estimate the 95-percent confidence limits for the predicted individual and median specific conductance (fig. 13).

Use of Predictive Equations

Predictive equations and statistics can be used to predict water-quality constituents and properties and to assign confidence limits to the predictions for known values of streamflow, specific conductance, and (or) suspended-solids concentration. The equations can be used to predict water quality during droughts or floods. Annual loads of chemicals can be estimated by using the predictive equations and records of daily mean streamflow or records of

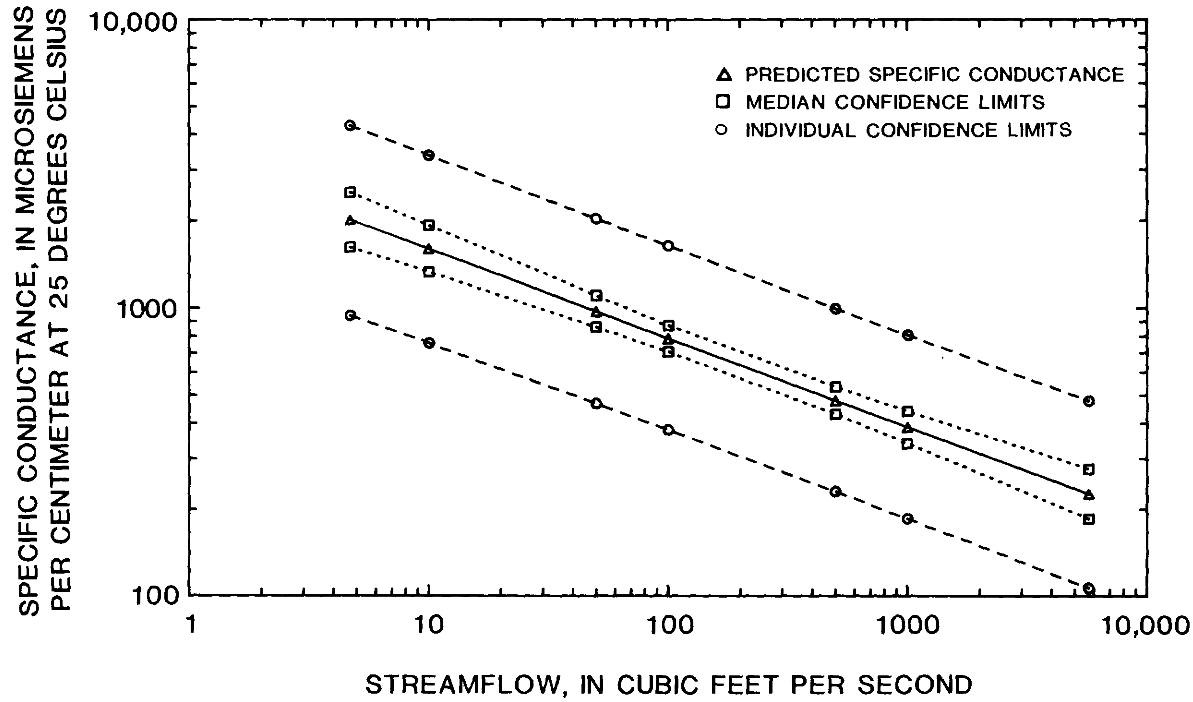

Figure 13. Estimated 95-percent confidence limits for the predicted individual and median specific conductance at Pigeon Creek at Evansville (station 03322100).

daily mean specific conductance. Similarly, duration or frequency curves of chemical concentration can be estimated by using streamflow duration and the predictive equations. The reliability of annual loads or frequency curves is dependent on the goodness-of-fit of the functional relation and the accuracy of the streamflow or specific conductance data. Predictive equations can be used to adjust chemical concentrations to account for the effect of streamflow on chemical concentration. Flow-adjusted concentrations of water-quality constituents then could be tested for time trends by using the method of Smith and others (1982).

The type of confidence limit used for the predictions discussed above depends on the objective of the user. For example, if the user wants to predict the average concentration of a constituent that occurs whenever a particular streamflow is attained, the predicted mean or median response confidence limit must be used. However, if the user wants to predict the concentration of a constituent during a particular flood, the predicted individual response confidence limit must be used.

More than one equation is available for predicting some of the water-quality constituents and properties. In this case, the equation for the best functional relation should be used for prediction. The best functional relation can be determined by calculating the confidence limits for the predicted response of the dependent variable. The relation with the smallest confidence limits should be used for predicting water quality.

The predictive equation should not be used beyond the range of data that was used to develop the equation. Predictions obtained by use of some of the equations are unreasonably large or negative beyond the range of data for the independent variable. Confidence limits are smallest at the mean of the independent variable and become larger away from the mean. Extrapolation of the equation beyond the range of data for the independent variable could result in extremely large confidence limits and could increase the chance for large errors.

SUMMARY AND CONCLUSIONS

The Surface Mining Control and Reclamation Act of 1977 requires that applications for coal-mining permits contain information about the water quality of streams at and near a proposed mine. Water-quality information for streams near the mine must be provided by an appropriate Federal or State agency and must be in sufficient detail to identify seasonal variations. The U.S. Geological Survey and the Indiana State Board of Health have data on the water quality of streams and rivers in the coal-mining region that can be used to provide some of the information required by the act.

Statistical analysis is used as a tool for obtaining useful information from the large quantity of surface-water-quality data. Statistical summaries of water-quality data by station and by season provide information on the spatial and seasonal variations in water quality. Schematic plots of water-quality data and plots of seasonal median values of water-quality data are presented and similarities or differences in water quality are described. Simple linear regression is used to investigate the functional relations between water-quality variables and to develop equations for predicting water quality. Linear, inverse, semilog, log-log, and hyperbolic regression models are evaluated and the model that best describes the relation between water-quality variables is used for the predictive equation. This report gives statistics that allow the user to determine the reliability of predicted water quality by estimating confidence limits.

Stations on the Patoka River exhibited most of the extremes of the water-quality data. These extremes included the lowest streamflow, the highest and lowest specific conductance, the lowest pH, the lowest alkalinity concentration, the highest and lowest suspended-solids concentration, and the highest total manganese concentration. Water quality in the Patoka River was more variable than that in the East Fork White River, White River, or Wabash River. Stations on the Patoka River had the most variable specific conductance, pH, and concentrations of total alkalinity, sulfate, suspended solids, and total manganese, but had the least variable total iron concentrations.

Median streamflow was least during fall at 15 of 16 stations having drainage areas greater than 1,000 mi^2 but was least during summer at 17 of 21 stations having drainage areas less than 1,000 mi^2. Median specific conductance was least during summer at 9 of 9 stations on the Wabash River, but was least during winter or spring (the seasons of greatest streamflow) at 27 of the remaining 28 stations. Specific conductance and concentrations of alkalinity and sulfate typically were most variable during winter, whereas streamflow was most variable during fall or summer.

Regional relations between dissolved-solids concentration and specific conductance, and between sulfate concentration and specific conductance, were investigated using data from 132 stations located throughout the coal-mining region. Two groups of data were apparent and predictive equations were developed separately for specific conductances of less than 740 μS/cm at 25°C and greater than 750 μS/cm at 25°C. The positive relation between dissolved-solids concentration and specific conductance is very good (R-square of 0.92 and 0.95, standard error of regression (Ep) of 13.4 and 14.4 percent) and can be used to predict dissolved-solids concentration with confidence. The positive relation between sulfate concentration and specific conductance was better for the high range of specific conductance (R-square of 0.85, Ep of 24.6 percent) than for the low range (R-square of 0.36, Ep of 57.8 percent).

Of 186 relations between water-quality variables at U.S. Geological Survey gaging stations and at Indiana State Board of Health stations that were investigated, 143 were statistically significant. Specific conductance and concentrations of total alkalinity and sulfate were negatively related to streamflow at all stations except for a positive relation between total alkalinity concentration and streamflow at Patoka River near Princeton. Concentrations of total alkalinity and sulfate were positively related to specific conductance at all stations except for a negative relation at Patoka River near Princeton and for a positive and negative relation at Patoka River at Jasper. Most of these relations are good and will give reliable predictions of water quality. The poorest relations are typically at stations in the Patoka River watershed. Suspended-solids concentration was positively related to streamflow at all but two stations on the Patoka River. These relations are poor and will give less reliable predictions of suspended-solids concentration.

The goodness-of-fit of a functional relation and the ability of the predictive equation to reliably predict water quality varies among relations and among stations. Predictive equations were developed for all statistically significant functional relations. The reliability of predicted water quality can best be determined by calculating an estimate of the confidence limits. Examples of the procedure used to calculate confidence limits are presented to facilitate use of this method of determining reliability.

Information about surface-water quality in and near the coal-mining region of Indiana may have transfer value to other areas in the Interior Coal Province. Water-quality information at stations on the Wabash River can be used to describe the water quality of the general area in applications for mining permits in eastern Illinois. The seasonal patterns of water quality described in this report are probably similar to the seasonal patterns of water quality in the coal-mining regions of Illinois and western Kentucky. Predictive equations for the regional relations between dissolved-solids concentration and specific conductance and between sulfate concentration and specific conductance are probably valid for the coal-mining regions of Illinois and western Kentucky. Although the predictive equations for the relations between water-quality variables at individual stations have little transfer value, the slope and goodness-of-fit of the relations at stations in Indiana are probably representative of those in other mined areas of the Interior Coal Province.

Statistical analysis, as used in this report, is only one of many tools that are necessary for interpreting water quality. Statistical analysis may show that water quality is different among stations or seasons, but field studies are needed to determine why water quality is different. Regression analysis may show a relation between water-quality variables, but regression gives little insight into the processes or mechanisms that cause the relation. Statistical analysis is an effective tool that can be used to identify relations or characteristics of water quality that warrant additional study. Perhaps it is this use of statistical analysis that will contribute most to our understanding of water resources.

REFERENCES CITED

American Public Health Association, American Water Works Association, and Water Pollution Control Federation, 1975, Standard methods for the examination of water and wastewater (14th ed.): Washington, D.C., American Public Health Association, 1,193 p.

Clark, G.D., ed., 1980, The Indiana water resource, availability, uses, and needs: Indianapolis, State of Indiana, Governor's Water Resource Study Commission, 508 p.

Corbett, D.M., 1965, Water supplied by coal surface mines, Pike County, Indiana: Indiana Water Resources Research Center Report of Investigations no. 1, 67 p.

———1969, Acid mine-drainage problem of the Patoka River watershed, southwestern Indiana: Indiana Water Resources Research Center Report of Investigations no. 4, 173 p.

Corbett, D.M., and Agnew, A.F., 1968, Coal mining effect on Busseron Creek watershed, Sullivan County, Indiana: Indiana Water Resources Research Center Report of Investigations no. 2, 187 p.

Duan, Naihua, 1983, Smearing estimate: A nonparametric retransformation method: Journal of the American Statistical Association, v. 78, no. 383, p. 605-610.

Engberg, R.A., 1983, A statistical analysis of the quality of surface water in Nebraska: U.S. Geological Survey Water-Supply Paper 2179, 252 p.

Gray, H.H., 1979, The Mississippian and Pennsylvanian (Carboniferous) Systems in the United States—Indiana: U.S. Geological Survey Professional Paper 1110–K, p. K1–K20.

Gutschick, R.C., 1966, Bedrock geology, *in* Lindsey, A.A., ed., Natural features of Indiana: Indianapolis, Indiana Academy of Science and Indiana State Library, p. 1–20.

Haan, C.T., 1977, Statistical methods in hydrology: Ames, Iowa State University Press, 378 p.

Hardison, C.H., 1971, Prediction error of regression estimates of streamflow characteristics at ungaged sites: U.S. Geological Survey Professional Paper 750–C, p. C228–C236.

Hem, J.D., 1970, Study and interpretation of the chemical characteristics of natural water (2d ed.): U.S. Geological Survey Water-Supply Paper 1473, 363 p.

Hoggatt, R.E., 1975, Drainage areas of Indiana streams: U.S. Geological Survey, 231 p.

Horner, R.G., 1976, Statistical summaries of Indiana streamflow data: U.S. Geological Survey Water-Resources Investigations 75–35, 526 p.

Indiana State Board of Health, 1957–1980, Water quality monitoring, rivers and streams: Indiana State Board of Health Monitor Station Records (published annually).

Integrated Software Systems Corporation, 1981, DISSPLA user's manual, current with version 9.0: San Diego, Calif., Integrated Software Systems Corp., variable pagination.

———1983, TELLAGRAF user's manual, version 4.5: San Diego, Calif., Integrated Software Systems Corp., variable pagination.

Knapton, J.R., and Ferreira, R.F., 1980, Statistical analyses of surface-water-quality variables in the coal area of southeastern Montana: U.S. Geological Survey Water-Resources Investigations 80–40, 134 p.

Miller, D.M., 1984, Reducing transformation bias in curve fitting: American Statistician, v. 38, no. 2, p. 124–126.

National Oceanic and Atmospheric Administration, 1973, Monthly normals of temperature, precipitation, and heating and cooling degree days, 1941–70, Indiana: Asheville, N.C., National Climatic Center, Climatography of the United States, no. 81.

Office of Surface Mining, 1979, Surface coal mining and reclamation operations permanent regulatory program: Federal Register, v. 44, no. 50, bk. 3, p. 15311–15463.

Peters, J.G., 1981, Effects of surface mining on water quality in a small watershed, Sullivan County, Indiana: U.S. Geological Survey Open-File Report 81–543, 61 p.

Powell, R.L., 1980, Map of southwestern Indiana showing areas strip mined for coal: Indiana Department of Natural Resources, Geological Survey Miscellaneous Map 15.

Purdue University Water Resources Research Center and Geosciences Research Associates, Inc., 1980, An inventory of groundwater data and aquifer assessment for Indiana: U.S. Environmental Protection Agency, Region V, 45 p., 34 pls.

Renn, D.E., 1983, Quality of surface water in the coal-mining region, southwestern Indiana, October 1979 to September 1980: U.S. Geological Survey Open-File Report 83–680, 95 p.

Renn, D.E., Ragone, S.E., and Wilber, W.G., 1980, Quality of surface water in the coal-mining region, southwestern Indiana, March and May 1979: U.S. Geological Survey Open-File Report 80–970, 65 p.

Rickert, D.A., and Hines, W.G., 1975, A practical framework for river-quality assessment: U.S. Geological Survey Circular 715–A, 17 p.

Rohlf, F.J., and Sokal, R.R., 1969, Statistical tables: San Francisco, W.H. Freeman and Co., 253 p.

Sall, John, 1981, SAS regression applications: Cary, N.C., SAS Institute Technical Report A–102, variable pagination.

SAS Institute Inc., 1982a, SAS user's guide, Basics (1982 ed.): Cary, N.C., SAS Institute Inc., 923 p.

———1982b, SAS user's guide, Statistics (1982 ed.): Cary, N.C., SAS Institute Inc., 584 p.

Schaal, L.A., 1959, The climate of Indiana, *in* Climates of the States, v. 1: U.S. Department of Commerce, National Oceanic and Atmospheric Administration, 486 p.

Schneider, A.F., 1966, Physiography, *in* Lindsey, A.A., ed., Natural features of Indiana: Indianapolis, Indiana Academy of Science and Indiana State Library, p. 40–56.

Skougstad, M.W., Fishman, M.J., Friedman, L.C., Erdmann, D.E., and Duncan, S.S., eds., 1979, Methods for determination of inorganic substances in water and fluvial sediments: Techniques of Water-Resources Investigations of the United States Geological Survey, Book 5, Chapter A1, 626 p.

Smith, R.A., Hirsch, R.M., and Slack, J.R., 1982, A study of trends in total phosphorus measurements at NASQAN stations: U.S. Geological Survey Water-Supply Paper 2190, 34 p.

Sokal, R.R., and Rohlf, F.J., 1969, Biometry, the principles and practice of statistics in biological research: San Francisco, Calif., W.H. Freeman and Co., 776 p.

Stewart, J.A., 1983, Low-flow characteristics of Indiana streams: U.S. Geological Survey Open-File Report 82–1007, 277 p.

Tukey, J.W., 1977, Exploratory data analysis: Reading, Mass., Addison-Wesley, 688 p.

U.S. Geological Survey, 1958–1982, Water resources data for Indiana, water years 1957–81: U.S. Geological Survey Water-Data Reports (published annually).

Walpole, R.E., and Myers, R.H., 1978, Probability and statistics for engineers and scientists (2d ed.): New York, MacMillan, 580 p.

Wangsness, D.J., 1982, Reconnaissance of stream biota and physical and chemical water quality in areas of selected land use in the coal-mining region, southwestern Indiana, 1979–80: U.S. Geological Survey Open-File Report 82–566, 43 p.

Wangsness, D.J., and others, 1981a, Hydrology of area 33, eastern region, Interior Coal Province, Indiana and Kentucky: U.S. Geological Survey Water-Resources Investigations/Open-File Report 81–423, 84 p.

———1981b, Hydrology of area 32, eastern region, Interior Coal Province, Indiana: U.S. Geological Survey Water-Resources Investigations/Open-File Report 81–498, 76 p.

———1983, Hydrology of area 30, eastern region, Interior Coal Province, Indiana and Illinois: U.S. Geological Survey Water-Resources Investigations/Open-File Report 82–1005, 82 p.

Wayne, W.J., 1966, Ice and land, *in* Lindsey, A.A., ed., Natural features of Indiana: Indianapolis, Indiana Academy of Science and Indiana State Library, p. 21–39.

Weir, C.E., 1973, Coal resources of Indiana: Indiana Department of Natural Resources, Geological Survey Bulletin 42–I, 40 p.

Wentz, D.A., and Steele, T.D., 1980, Analysis of stream quality in the Yampa River basin, Colorado and Wyoming: U.S. Geological Survey Water-Resources Investigations 80–8, 161 p.

Wilber, W.G., and Boje, R.R., 1982, Reconnaissance for determining effects of land use and surficial geology on concentrations of selected elements on streambed materials from the coal-mining region, southwestern Indiana, October 1979 to March 1980: U.S. Geological Survey Water-Resources Investigations 82–4013, 39 p.

Wilber, W.G., Crawford, C.G., Renn, D.E., Ragone, S.E., and Wangsness, D.J., 1980, Preliminary assessment of the factors affecting water quality in the coal-mining region, southwestern Indiana, March to October 1979, *in* Warner, R.E., and Clark, P.E., eds., Water resources and land-use management in Indiana, A symposium, Marshall, Ind., June 12–14, 1980, Proceedings: Indiana Water Resources Association, p. 215–234.

Zogorski, J.S., Ramey, D.S., Lambert, P.W., Martin, J.D., and Warner, R.E., 1981, Hydrologic evaluation of a hypothetical coal-mining site near Chrisney, Spencer County, Indiana: U.S. Geological Survey Open-File Report 80–1107, 133 p.

TABLES 1–30

Table 1. Streamflow at selected U.S. Geological Survey gaging stations

[Data from U.S. Geological Survey, 1975, 1979, 1982; Stewart, 1983]

Station	Station name	Drainage area (mi^2)	Period of recorded streamflow	Average streamflow[1] (ft^3/s)	Minimum daily streamflow (ft^3/s)	Maximum streamflow (ft^3/s)	Percent of time daily mean streamflow equaled or exceeded[2]					
							95	80	60	40	20	5
							Streamflow value equaled or exceeded (ft^3/s)					
03303300[3]	Middle Fork Anderson River at Bristow	39.8	1961-81	57.3	0.00	6,360	0.25	3.0	15	37	85	336
03303400	Crooked Creek near Santa Claus[4]	7.86	1969-81	11.3	.00	4,100	.00	.10	.93	3.5	12	53
03322100	Pigeon Creek at Evansville[4]	323	1960-81	348	1.0	12,100	4.1	14	40	116	408	1,560
03335500	Wabash River at Lafayette	7,267	1923-81	6,404	399	131,000	827	1,440	2,540	4,330	9,040	23,700
03336000	Wabash River at Covington	8,218	1939-81	7,284	487	147,000	982	1,790	3,110	5,250	10,600	25,300
03340500	Wabash River at Montezuma[4]	11,118	1927-81	9,664	571	184,000	1,210	2,180	3,880	6,810	14,100	33,700
03341500	Wabash River at Terre Haute[4]	12,265	1905-06 1927-81	10,670	701	189,000	1,450	2,540	4,420	7,820	15,800	36,100
03342000	Wabash River at Riverton[4]	13,161	1938-81	11,620	858	201,000	1,570	2,810	4,990	8,480	17,400	38,600
03342100	Busseron Creek near Hymera	16.7	1966-81	18.4	.00	1,890	.03	.22	1.4	6.0	24	80
03342150	West Fork Busseron Creek near Hymera[4]	14.4	1966-81	13.5	.00	1,930	.06	.26	1.2	3.8	12	58
03342250	Mud Creek near Dugger[4]	11.9	1966-81	14.1	.40	1,270	1.3	2.4	4.7	8.7	16	48
03342300	Busseron Creek near Sullivan[4]	138	1966-81	145	.90	6,050	3.4	8.7	24	61	170	656
03342360	Buttermilk Creek near Sullivan[4]	17.6	1974-78	--------	.03	594	------	------	------	------	------	------
03342500	Busseron Creek near Carlisle[4]	228	1943-81	222	.00	8,800	1.9	8.1	25	70	227	1,200
03343000	Wabash River at Vincennes[4]	13,706	1929-81	11,810	770	189,000	1,690	2,890	5,090	8,970	18,200	38,300
03354000	White River near Centerton	2,444	1930-32 1946-81	2,401	131	50,500	313	492	885	1,580	3,110	8,770
03360000[5]	Eel River at Bowling Green	830	1931-81	870	11	34,000	38	101	230	574	1,510	3,010
03360500	White River at Newberry[4]	4,688	1928-81	4,694	200	76,900	453	839	1,590	3,110	6,640	17,800
03371500	East Fork White River near Bedford	3,861	1939-81	3,869	138	75,700	335	601	1,230	2,480	5,540	13,600
03373500	East Fork White River at Shoals	4,927	1903-06 1908-16 1923-81	5,418	64	160,000	375	740	1,540	3,490	8,010	21,000
03374000	White River at Petersburg[4]	11,125	1927-81	11,668	573	183,000	1,080	2,040	3,890	8,030	17,400	42,100
03374500[6]	Patoka River near Cuzco	171	1961-81	220	.00	14,700	.80	5.9	27	92	271	1,150
03375500	Patoka River at Jasper	262	1947-81	360	.00	14,100	1.1	9.5	39	147	541	1,670
03375800	Hall Creek near St. Anthony	21.8	1970-81	33.3	.00	11,500	.07	.91	4.4	12	31	120
03376260	Flat Creek near Otwell[4]	21.3	1964-81	22.8	.00	1,680	.00	.66	2.8	6.4	18	84
03376300	Patoka River at Winslow[4]	603	1963-74	678	.50	15,500	4.1	21	100	395	1,260	2,670
03376350	South Fork Patoka River near Spurgeon[4]	42.8	1964-81	49.7	.00	5,900	4.9	8.4	16	29	58	179
03376500	Patoka River near Princeton[4]	822	1934-81	1,009	.00	18,700	10	40	139	596	1,850	3,870

[1] Average of annual mean streamflows.
[2] Streamflow duration based on the period of record excluding data from the 1979-81 water years.
[3] Streamflow duration based on 1970-78 water years.
[4] Station receives drainage from surface coal mines.
[5] Streamflow duration based on 1956-78 water years.
[6] Streamflow duration based on 1962-76 water years.

Table 2. Number of specific conductance measurements and period of record at U.S. Geological Survey gaging stations

Station	Station name	Latitude (N.)	Longitude (W.)	Drainage area[1] (mi^2)	Specific conductance: Period of record	Specific conductance: Number of measurements
03303300	Middle Fork Anderson River at Bristow	38°08'19"	86°43'16"	39.8	1969-75	55
03303400	Crooked Creek near Santa Claus[2]	38°07'05"	86°53'24"	7.86	1969-74	44
03322100	Pigeon Creek at Evansville[2]	38°00'14"	87°32'19"	323	1969-73	53
03342100	Busseron Creek near Hymera	39°12'54"	87°18'41"	16.7	1969-75	81
03342150	West Fork Busseron Creek near Hymera[2]	39°11'10"	87°19'44"	14.4	1969-74	64
03342250	Mud Creek near Dugger[2]	39°06'28"	87°16'42"	11.9	1969-75	76
03342300	Busseron Creek near Sullivan[2]	39°04'33"	87°23'11"	138	1969-74	75
03342360	Buttermilk Creek near Sullivan[2]	39°03'58"	87°21'32"	17.6	1974-75	18
03342500	Busseron Creek near Carlisle[2]	38°58'26"	87°25'33"	228	1969-74	68
03360000	Eel River at Bowling Green	39°22'58"	87°01'14"	830	1969-73	25
03375500	Patoka River at Jasper	38°24'49"	86°52'36"	262	1969-73	39
03375800	Hall Creek near St. Anthony	38°21'45"	86°49'43"	21.8	1970-74	35
03376260	Flat Creek near Otwell[2]	38°26'12"	87°07'52"	21.3	1969-75	49
03376300	Patoka River at Winslow[2]	38°22'48"	87°13'00"	603	1969-74	42
03376350	South Fork Patoka River near Spurgeon[2]	38°17'50"	87°15'39"	42.8	1969-73	46
03376500	Patoka River near Princeton[2]	38°23'30"	87°32'55"	822	1969-73	44

[1] Drainage areas from Hoggatt (1975).
[2] Station receives drainage from surface coal mines.

Table 3. Number of water-quality measurements and period of record at Indiana State Board of Health stations

Station	Station name	Latitude (N.)	Longitude (W.)	Drainage area[1] (mi^2)	Period of record	Number of water-quality measurements						
						Specific conductance	pH	Total alkalinity	Sulfate	Suspended solids	Total iron	Total manganese
EW77	East Fork White River at Williams	38°47'49"	86°39'54"	4,720	1971-80	115	80	13	90	115	45	34
EW56	East Fork White River at Shoals	38°40'02"	86°47'33"	4,927	1957-72	366	278	354	0	376	0	0
WR166	White River at Spencer	39°17'17"	86°44'45"	2,988	1957-80	406	353	365	95	412	11	35
WR130	White River at Bloomfield[2]	39°01'39"	86°58'00"	4,468	1957-70	325	254	334	0	333	0	0
WR80	White River at Edwardsport[2]	38°47'42"	87°14'29"	5,014	1957-80	446	337	339	91	455	0	33
WR48	White River at Petersburg[2]	38°30'42"	87°17'18"	11,125	1971-80	117	80	13	91	117	74	34
WR19	White River at Hazelton[2]	38°29'27"	87°33'50"	11,305	1957-72	344	282	352	0	351	0	0
P86	Patoka River at Jasper	38°23'15"	86°55'39"	275	1963-70	188	141	188	0	188	0	0
P76	Patoka River near Jasper	38°19'45"	86°58'00"	434	1971-80	118	79	4	81	118	80	51
P33	Patoka River near Oakland City[2]	38°22'38"	87°22'14"	733	1973-80	82	58	4	77	82	50	47
P19	Patoka River near Princeton[2]	38°23'23"	87°32'56"	822	1957-70	339	271	343	0	351	0	0
P14	Patoka River at Patoka[2]	38°23'54"	89°35'55"	838	1971-72	24	17	1	0	24	0	0
WB301	Wabash River at Lafayette	40°25'10"	86°53'51"	7,267	1957-80	371	330	348	96	379	0	0
WB260	Wabash River at Covington	40°08'24"	87°24'20"	8,218	1957-72	269	193	279	0	279	0	0
WB245	Wabash River near Cayuga[2]	39°57'08"	87°25'12"	10,000	1973-80	47	65	0	92	45	0	0
WB228	Wabash River at Montezuma[2]	39°47'33"	87°22'28"	11,118	1957-80	365	324	327	93	371	0	0
WB219	Wabash River at Clinton[2]	39°39'25"	87°24'00"	11,715	1976-80	46	38	0	46	46	12	1
WB214	Wabash River at Terre Haute[2]	39°28'39"	87°25'24"	12,265	1957-70	268	238	286	0	286	0	0
WB207	Wabash River at Terre Haute[2]	39°30'30"	87°24'49"	12,256	1973-80	44	60	0	89	42	0	0
WB194	Wabash River near Terre Haute[2]	39°24'10"	87°29'39"	12,423	1971-77	77	49	0	55	77	11	12
WB128	Wabash River at Vincennes[2]	38°42'26"	87°31'09"	13,706	1957-80	382	336	339	89	389	46	7

[1] Drainage areas estimated from Hoggatt (1975).
[2] Station recieves drainage from surface coal mines.

Table 4. Seasonal streamflow at U.S. Geological Survey gaging stations

[Data are the daily mean streamflows on days when water-quality measurements were made]

Station	Station name	Season[1]	Number of meas-urements	Mean[2] (ft^3/s)	Median[2] (ft^3/s)	Coef-ficient of var-iation (percent)	Minimum (ft^3/s)	Maximum (ft^3/s)
03303300	Middle Fork Anderson River at Bristow	All data	59	94	27	292	0.01	1,800
		Winter	14	137	47	204	18	1,100
		Spring	18	176	55	238	6.0	1,800
		Summer	14	5.4	2.5	136	.01	26.5
		Fall	13	28	16	122	.16	104
03303400	Crooked Creek near Santa Claus	All data	55	20	2.0	365	.00	424
		Winter	13	72	11	197	.63	424
		Spring	15	7.5	3.2	133	.09	36
		Summer	13	.42	.04	293	.00	4.5
		Fall	14	3.5	1.2	159	.00	16
03322100	Pigeon Creek at Evansville	All data	60	896	266	155	4.7	5,720
		Winter	12	864	435	98	76	2,630
		Spring	24	1,640	698	111	28	5,720
		Summer	12	159	39	175	9.7	990
		Fall	12	189	46	212	4.7	1,430
03342100	Busseron Creek near Hymera	All data	87	22	9.5	140	.01	137
		Winter	22	26	15	118	.30	93
		Spring	24	27	13	110	1.2	115
		Summer	21	8.5	.40	212	.01	70
		Fall	20	27	7.0	152	.03	137
03342150	West Fork Busseron Creek near Hymera	All data	67	32	2.7	285	.04	497
		Winter	14	12	5.0	160	.80	63
		Spring	21	50	7.9	233	1.4	497
		Summer	16	3.4	.21	344	.04	48
		Fall	16	54	.68	233	.06	426
03342250	Mud Creek near Dugger	All data	87	25	7.8	223	1.3	319
		Winter	19	16	11	103	2.7	67
		Spring	28	54	15	161	3.1	319
		Summer	20	3.4	2.9	73	1.4	13
		Fall	20	12	5.8	158	1.3	67
03342300	Busseron Creek near Sullivan	All data	88	331	102	186	2.6	4,590
		Winter	23	588	222	170	11	4,590
		Spring	26	440	259	112	24	1,750
		Summer	19	28	13	141	3.7	153
		Fall	20	182	42	132	2.6	700
03342360	Buttermilk Creek near Sullivan	All data	18	83	28	160	4.8	526
		Winter	5	53	19	109	13	149
		Spring	5	217	229	91	31	526
		Summer	3	5.4	5.1	13	4.8	6.2
		Fall	5	25	25	75	5.8	51
03342500	Busseron Creek near Carlisle	All data	73	418	87	197	4.6	5,580
		Winter	18	791	275	169	24	5,580
		Spring	18	447	144	158	35	2,860
		Summer	18	93	24	280	4.6	1,130
		Fall	19	346	58	139	7.4	1,450

Table 4. Seasonal streamflow at U.S. Geological Survey gaging stations—Continued

Station	Station name	Season[1]	Number of meas-urements	Mean[2] (ft³/s)	Median[2] (ft³/s)	Coef-ficient of var-iation (percent)	Minimum (ft³/s)	Maximum (ft³/s)
03360000	Eel River at Bowling Green	All data	39	1,250	622	127	45	7,010
		Winter	10	2,850	2,560	75	189	7,010
		Spring	10	1,340	903	81	303	3,330
		Summer	9	251	152	129	45	1,080
		Fall	10	466	184	128	50	1,820
03375500	Patoka River at Jasper	All data	43	448	133	179	1.8	4,220
		Winter	9	1,230	637	116	120	4,220
		Spring	13	475	294	87	12	1,210
		Summer	12	103	19	176	1.8	602
		Fall	9	84	59	98	2.8	218
03375800	Hall Creek near St. Anthony	All data	42	21	5.1	177	.00	171
		Winter	9	46	12	136	2.9	171
		Spring	11	28	18	106	.41	105
		Summer	9	6.3	.39	260	.00	50
		Fall	13	6.4	3.8	156	.00	31
03376260	Flat Creek near Otwell	All data	56	10	3.9	182	.00	100
		Winter	13	24	6.5	140	1.8	100
		Spring	15	9.3	9.2	85	1.3	27
		Summer	14	3.1	2.7	108	.23	14
		Fall	14	5.9	2.6	185	.00	42
03376300	Patoka River at Winslow	All data	46	899	356	130	1.1	5,500
		Winter	12	1,710	1,520	88	214	5,500
		Spring	13	1,180	976	95	63	3,530
		Summer	9	124	83	115	1.1	457
		Fall	12	365	162	150	2.0	1,930
03376350	South Fork Patoka River near Spurgeon	All data	48	42	20	152	4.1	343
		Winter	11	45	38	65	15	90
		Spring	14	82	54	127	13	343
		Summer	10	14	14	46	4.1	24
		Fall	13	17	13	63	6.5	36
03376500	Patoka River near Princeton	All data	49	1,630	1,190	122	20	9,930
		Winter	12	1,450	1,330	44	674	2,830
		Spring	16	2,890	2,280	100	118	9,930
		Summer	10	874	140	140	40	3,670
		Fall	11	704	419	98	20	1,690

[1] Winter is December 21–March 20, spring is March 21–June 20, summer is June 21–September 20, and fall is September 21–December 20.

[2] Mean and median are rounded to the number of significant figures for individual measurements of the same magnitude.

Table 5. Seasonal specific conductance at U.S. Geological Survey gaging stations

Station	Station name	Season[1]	Number of meas-urements	Mean[2] (µS/cm at 25° C)	Median[2] (µS/cm at 25° C)	Coef-ficient of var-iation (percent)	Minimum (µS/cm at 25° C)	Maximum (µS/cm at 25° C)
03303300	Middle Fork Anderson River at Bristow	All data	55	189	170	39	120	650
		Winter	12	178	158	28	140	310
		Spring	16	163	160	15	120	220
		Summer	14	219	183	58	120	650
		Fall	13	201	200	20	145	280
03303400	Crooked Creek near Santa Claus	All data	43	490	500	26	150	760
		Winter	9	383	375	37	150	620
		Spring	14	462	440	22	320	700
		Summer	8	596	595	7	550	690
		Fall	12	532	530	21	350	760
03322100	Pigeon Creek at Evansville	All data	53	780	685	65	110	2,100
		Winter	9	758	660	72	335	2,100
		Spring	21	489	465	54	110	1,080
		Summer	12	1,000	980	54	200	2,100
		Fall	11	1,110	1,050	48	300	2,000
03342100	Busseron Creek near Hymera	All data	81	300	218	28	135	500
		Winter	19	306	320	29	185	500
		Spring	22	308	323	27	165	500
		Summer	20	280	285	31	135	460
		Fall	20	308	320	29	170	440
03342150	West Fork Busseron Creek near Hymera	All data	64	884	778	54	180	1,950
		Winter	14	692	745	32	295	1,000
		Spring	18	590	585	38	210	1,130
		Summer	16	1,250	1,360	39	250	1,950
		Fall	16	1,020	983	55	180	1,900
03342250	Mud Creek near Dugger	All data	76	2,060	1,910	35	825	4,400
		Winter	18	1,600	1,540	26	900	2,575
		Spring	20	1,740	1,700	29	825	2,700
		Summer	19	2,680	2,600	26	1,700	4,400
		Fall	19	2,190	2,200	31	1,100	3,100
03342300	Busseron Creek near Sullivan	All data	75	1,100	1,000	57	160	2,600
		Winter	17	748	680	50	255	1,520
		Spring	20	855	780	49	160	1,600
		Summer	18	1,690	1,840	35	600	2,600
		Fall	20	1,130	1,240	57	400	2,150
03342360	Buttermilk Creek near Sullivan	All data	18	1,270	1,200	62	430	3,300
		Winter	5	875	800	43	430	1,330
		Spring	5	901	750	43	480	1,400
		Summer	3	2,200	2,000	46	1,300	3,300
		Fall	5	1,490	1,350	59	540	2,700
03342500	Busseron Creek near Carlisle	All data	67	958	910	55	215	2,350
		Winter	17	685	630	48	255	1,280
		Spring	18	782	783	44	215	1,430
		Summer	17	1,460	1,300	36	450	2,300
		Fall	15	908	640	59	420	2,350
03360000	Eel River at Bowling Green	All data	24	422	450	24	140	570
		Winter	5	308	320	37	140	450
		Spring	6	418	433	22	280	530
		Summer	7	451	475	17	290	520
		Fall	6	489	473	12	425	570

Table 5. Seasonal specific conductance at U.S. Geological Survey gaging stations—Continued

Station	Station name	Season[1]	Number of meas- urements	Mean[2] (µS/cm at 25° C)	Median[2] (µS/cm at 25° C)	Coef- ficient of var- iation (percent)	Minimum (µS/cm at 25° C)	Maximum (µS/cm at 25° C)
03375500	Patoka River at Jasper	All data	39	228	225	34	90	600
		Winter	6	173	168	27	125	235
		Spring	12	198	208	24	90	260
		Summer	12	245	253	13	190	300
		Fall	9	282	235	45	150	600
03375800	Hall Creek near St. Anthony	All data	35	246	245	18	160	360
		Winter	6	229	215	19	185	285
		Spring	10	220	218	17	170	300
		Summer	8	263	268	21	160	360
		Fall	11	266	265	12	225	320
03376260	Flat Creek near Otwell	All data	49	1,440	1,400	51	205	4,000
		Winter	10	864	665	71	205	1,840
		Spring	14	1,370	1,300	28	900	2,200
		Summer	12	1,870	1,730	44	480	4,000
		Fall	13	1,550	1,300	49	390	2,800
03376300	Patoka River at Winslow	All data	42	362	333	34	165	725
		Winter	10	284	270	26	195	415
		Spring	13	319	320	32	165	580
		Summer	8	431	410	26	285	570
		Fall	11	436	400	31	275	725
03376350	South Fork Patoka River near Spurgeon	All data	45	2,910	3,000	32	1,180	4,500
		Winter	9	2,330	2,200	38	1,180	3,500
		Spring	14	2,460	2,570	34	1,300	3,500
		Summer	9	3,630	3,600	15	2,900	4,500
		Fall	13	3,300	3,400	24	1,980	4,500
03376500	Patoka River near Princeton	All data	43	823	560	77	270	2,430
		Winter	9	475	415	34	320	855
		Spring	14	576	460	52	270	1,400
		Summer	9	1,240	1,540	57	330	2,200
		Fall	11	1,080	610	79	410	2,430

[1]Winter is December 21–March 20, spring is March 21–June 20, summer is June 21–September 20, and fall is September 21–December 20.
[2]Mean and median are rounded to the number of significant figures for individual measurements of the same magnitude.

Table 6. Seasonal streamflow at Indiana State Board of Health stations

[Data are estimates of the daily mean streamflows on days when water-quality measurements were made]

Station	Station name	Season[1]	Number of meas-urements	Mean[2] (ft^3/s)	Median[2] (ft^3/s)	Coef-ficient of var-iation (percent)	Minimum (ft^3/s)	Maximum (ft^3/s)
EW77	East Fork White River	All data	112	5,390	3,570	94	394	23,100
	at Williams	Winter	25	9,250	8,690	69	394	23,100
		Spring	34	6,520	5,940	72	1,100	20,200
		Summer	27	2,470	2,070	68	541	6,840
		Fall	26	3,220	1,570	103	507	10,900
EW56	East Fork White River	All data	377	4,880	2,190	151	278	58,600
	at Shoals	Winter	89	8,240	4,010	135	278	58,600
		Spring	95	7,300	5,190	93	1,340	35,400
		Summer	99	2,460	1,200	156	341	29,000
		Fall	94	1,790	828	154	278	18,300
WR166	White River at	All data	469	3,130	1,590	134	242	32,200
	Spencer	Winter	111	4,600	2,630	100	242	19,300
		Spring	120	4,320	3,180	104	763	32,200
		Summer	125	1,950	948	179	277	27,400
		Fall	113	1,710	770	192	252	27,900
WR130	White River at	All data	334	4,250	2,080	137	343	41,100
	Bloomfield	Winter	83	6,440	3,640	106	343	24,300
		Spring	80	6,180	4,750	97	1,000	39,100
		Summer	91	2,770	1,330	197	416	41,100
		Fall	80	1,750	958	139	378	14,000
WR80	White River at	All data	452	5,340	2,590	136	385	54,100
	Edwardsport	Winter	109	8,160	4,420	101	385	32,700
		Spring	114	7,300	5,490	108	1,120	54,100
		Summer	120	3,220	1,570	170	467	38,500
		Fall	109	2,810	1,250	197	425	46,900
WR48	White River at	All data	114	13,200	9,330	94	1,050	61,700
	Petersburg	Winter	26	20,100	18,300	66	1,050	46,400
		Spring	32	18,300	18,100	78	3,050	61,700
		Summer	29	6,950	4,930	93	1,960	35,600
		Fall	27	7,400	3,800	100	1,350	29,000
WR19	White River at	All data	369	10,900	5,780	132	855	105,000
	Hazelton	Winter	85	17,600	10,400	118	1,000	105,000
		Spring	95	16,400	12,600	86	3,340	78,200
		Summer	98	5,720	3,210	113	1,000	35,500
		Fall	91	4,700	2,330	148	855	50,900
P86	Patoka River at	All data	188	272	48	181	.00	2,610
	Jasper	Winter	48	527	212	133	1.6	2,610
		Spring	47	386	198	128	6.0	2,470
		Summer	50	77	9.4	233	.21	745
		Fall	43	88	13	271	.00	1,340
P76	Patoka River near	All data	118	695	240	157	2.0	8,310
	Jasper	Winter	24	1,450	1,420	77	38	3,250
		Spring	34	862	398	168	17	8,310
		Summer	32	163	52	200	2.5	1,670
		Fall	28	450	81	154	2.0	2,850
P33	Patoka River near	All data	81	1,080	804	110	31	6,820
	Oakland City	Winter	14	1,610	1,500	61	74	3,940
		Spring	21	1,670	1,350	100	174	6,820
		Summer	24	508	226	119	31	1,920
		Fall	22	785	399	108	32	2,710

Table 6. Seasonal streamflow at Indiana State Board of Health stations—Continued

Station	Station name	Season[1]	Number of measurements	Mean[2] (ft^3/s)	Median[2] (ft^3/s)	Coefficient of variation (percent)	Minimum (ft^3/s)	Maximum (ft^3/s)
P19	Patoka River near Princeton	All data	354	918	243	167	4.3	14,500
		Winter	81	1,700	1,180	131	38	14,500
		Spring	88	1,440	1,140	109	30	11,100
		Summer	96	342	76	213	5.8	5,220
		Fall	89	310	60	186	4.3	2,590
P14	Patoka River at Patoka	All data	24	658	464	96	20	2,190
		Winter	5	1,360	1,540	56	314	2,190
		Spring	8	655	464	77	58	1,590
		Summer	5	353	127	106	29	793
		Fall	6	331	100	129	20	1,010
WB301	Wabash River at Lafayette	All data	444	6,550	3,800	128	610	88,000
		Winter	88	10,500	6,430	100	730	49,600
		Spring	126	9,480	6,130	113	1,270	88,000
		Summer	117	3,590	2,360	95	610	19,200
		Fall	113	3,310	2,100	106	610	21,800
WB260	Wabash River at Covington	All data	280	7,020	3,750	119	660	47,000
		Winter	59	10,800	6,850	99	900	47,000
		Spring	77	11,100	7,240	86	2,190	39,800
		Summer	69	3,350	2,290	94	660	16,600
		Fall	75	3,240	2,290	115	675	25,800
WB245	Wabash River near Cayuga	All data	90	10,000	7,020	90	1,250	48,600
		Winter	19	16,500	13,600	77	2,200	48,600
		Spring	26	12,400	11,000	67	1,900	39,700
		Summer	25	6,690	4,590	75	1,830	22,900
		Fall	20	4,850	3,720	80	1,250	15,500
WB228	Wabash River at Montezuma	All data	439	10,300	6,250	105	940	56,800
		Winter	88	16,400	11,200	84	1,200	56,000
		Spring	125	14,600	11,400	80	2,110	56,800
		Summer	112	5,920	3,500	106	940	34,000
		Fall	114	5,210	3,230	101	955	33,700
WB219	Wabash River at Clinton	All data	43	10,400	7,920	87	1,240	38,000
		Winter	9	12,400	8,000	105	1,240	38,000
		Spring	13	13,200	11,600	69	2,250	29,800
		Summer	12	9,200	6,520	88	2,220	30,400
		Fall	9	5,960	6,480	42	2,580	8,900
WB214	Wabash River at Terre Haute	All data	288	10,600	5,840	119	910	88,000
		Winter	68	14,900	7,930	120	1,540	88,000
		Spring	77	15,500	11,000	78	3,520	63,800
		Summer	72	5,960	3,560	113	910	42,500
		Fall	71	5,760	3,000	124	1,230	41,300
WB207	Wabash River at Terre Haute	All data	86	12,500	8,800	85	1,300	51,000
		Winter	16	21,900	20,100	65	1,300	51,000
		Spring	26	15,100	14,400	63	2,360	32,500
		Summer	24	8,710	5,950	79	2,320	31,800
		Fall	20	6,270	4,940	77	1,360	21,100

Table 6. Seasonal streamflow at Indiana State Board of Health stations—Continued

Station	Station name	Season[1]	Number of measurements	Mean[2] (ft^3/s)	Median[2] (ft^3/s)	Coefficient of variation (percent)	Minimum (ft^3/s)	Maximum (ft^3/s)
WB194	Wabash River near Terre Haute	All data	77	13,200	9,280	82	1,380	51,700
		Winter	17	20,100	17,000	65	5,050	51,700
		Spring	22	16,000	14,600	64	2,390	42,800
		Summer	20	7,110	4,440	69	2,350	17,300
		Fall	18	9,980	5,720	97	1,380	34,900
WB128	Wabash River at Vincennes	All data	440	12,600	7,970	103	1,000	80,900
		Winter	103	17,300	11,700	91	1,000	80,900
		Spring	116	18,500	14,600	76	4,210	73,600
		Summer	115	8,020	5,180	100	1,440	46,400
		Fall	106	6,410	3,670	114	1,390	55,600

[1]Winter is December 21-March 20, spring is March 21-June 20, summer is June 21-September 20, and fall is September 21-December 20.
[2]Mean and median are rounded to the number of significant figures for individual measurements of the same magnitude.

Table 7. Seasonal specific conductance at Indiana State Board of Health stations

Station	Station name	Season[1]	Number of meas- urements	Mean[2] (µS/cm at 25° C)	Median[2] (µS/cm at 25° C)	Coef- ficient of var- iation (percent)	Minimum (µS/cm at 25° C)	Maximum (µS/cm at 25° C)
EW77	East Fork White River at Williams	All data	115	430	420	24	180	680
		Winter	26	425	400	31	180	680
		Spring	34	410	420	20	220	560
		Summer	27	407	420	18	210	580
		Fall	28	480	505	21	300	630
EW56	East Fork White River at Shoals	All data	366	433	433	25	179	1,140
		Winter	89	431	429	25	179	650
		Spring	92	391	397	22	199	580
		Summer	92	411	420	24	190	847
		Fall	93	498	520	21	271	1,140
WR166	White River at Spencer	All data	406	678	668	26	192	1,330
		Winter	98	656	640	30	192	1,270
		Spring	102	595	603	20	230	890
		Summer	104	695	703	24	274	1,040
		Fall	102	764	779	21	388	1,330
WR130	White River at Bloomfield	All data	325	594	590	27	168	1,040
		Winter	83	571	557	32	168	939
		Spring	79	502	494	21	235	758
		Summer	84	614	614	22	236	952
		Fall	79	690	700	21	320	1,040
WR80	White River at Edwardsport	All data	446	579	580	26	167	1,330
		Winter	110	569	561	31	219	1,080
		Spring	113	518	510	20	241	740
		Summer	113	569	588	22	167	830
		Fall	110	661	667	24	264	1,330
WR48	White River at Petersburg	All data	117	485	480	26	220	1,000
		Winter	27	477	420	38	240	1,000
		Spring	32	446	450	19	220	620
		Summer	29	481	480	17	260	660
		Fall	29	540	540	24	320	800
WR19	White River at Hazelton	All data	344	493	498	25	210	1,060
		Winter	82	480	480	29	211	758
		Spring	86	431	438	20	230	590
		Summer	90	487	503	19	210	706
		Fall	86	575	579	21	274	1,060
P86	Patoka River at Jasper	All data	188	303	240	106	106	3,080
		Winter	48	255	216	79	106	1,460
		Spring	47	305	221	126	130	2,100
		Summer	50	285	249	60	130	962
		Fall	43	374	276	121	156	3,080
P76	Patoka River near Jasper	All data	118	257	240	37	120	640
		Winter	24	213	190	31	120	350
		Spring	33	220	220	21	120	350
		Summer	32	288	260	38	150	640
		Fall	29	302	280	35	140	600

Table 7. Seasonal specific conductance at Indiana State Board of Health stations—Continued

Station	Station name	Season[1]	Number of meas- urements	Mean[2] (µS/cm at 25° C)	Median[2] (µS/cm at 25° C)	Coef- ficient of var- iation (percent)	Minimum (µS/cm at 25° C)	Maximum (µS/cm at 25° C)
P33	Patoka River near Oakland City	All data	82	659	486	82	110	2,990
		Winter	14	432	350	59	110	890
		Spring	21	505	420	56	200	1,230
		Summer	24	828	680	66	270	2,710
		Fall	23	762	450	98	210	2,990
P19	Patoka River near Princeton	All data	339	1,340	930	135	146	21,200
		Winter	80	737	516	72	146	2,430
		Spring	87	737	620	60	240	2,130
		Summer	86	1,650	1,240	139	157	21,200
		Fall	86	2,220	1,690	109	190	19,500
P14	Patoka River at Patoka	All data	24	989	720	70	360	2,760
		Winter	5	516	410	40	360	870
		Spring	8	855	705	72	370	2,330
		Summer	5	1,210	1,010	75	530	2,760
		Fall	6	1,370	1,300	52	640	2,600
WB301	Wabash River at Lafayette	All data	371	552	550	19	228	880
		Winter	74	559	571	27	240	870
		Spring	105	535	546	17	228	780
		Summer	92	507	512	13	267	627
		Fall	100	605	603	15	412	880
WB260	Wabash River at Covington	All data	269	557	554	19	257	847
		Winter	59	560	590	26	257	837
		Spring	76	528	538	17	274	775
		Summer	62	521	520	11	386	690
		Fall	72	615	625	16	270	847
WB245	Wabash River near Cayuga	All data	47	612	600	19	400	920
		Winter	8	678	685	27	420	920
		Spring	14	592	599	10	500	740
		Summer	14	525	545	14	400	610
		Fall	11	698	670	11	580	840
WB228	Wabash River at Montezuma	All data	365	560	560	20	208	920
		Winter	73	556	558	27	240	920
		Spring	104	540	553	17	208	755
		Summer	89	519	520	13	299	674
		Fall	99	619	628	16	300	890
WB219	Wabash River at Clinton	All data	46	618	595	22	340	1,040
		Winter	9	697	660	32	470	1,040
		Spring	13	601	590	14	490	770
		Summer	12	506	520	16	340	630
		Fall	12	690	710	10	570	820
WB214	Wabash River at Terre Haute	All data	268	558	564	19	230	955
		Winter	67	564	600	25	249	801
		Spring	73	530	545	17	260	796
		Summer	61	528	543	15	230	706
		Fall	67	610	610	13	460	955

Table 7. Seasonal specific conductance at Indiana State Board of Health stations—Continued

Station	Station name	Season[1]	Number of meas- urements	Mean[2] (µS/cm at 25° C)	Median[2] (µS/cm at 25° C)	Coef- ficient of var- iation (percent)	Minimum (µS/cm at 25° C)	Maximum (µS/cm at 25° C)
WB207	Wabash River at Terre Haute	All data	44	597	580	19	320	900
		Winter	6	607	530	35	370	900
		Spring	14	602	595	12	500	720
		Summer	13	515	510	15	320	640
		Fall	11	684	710	9	560	790
WB194	Wabash River near Terre Haute	All data	77	591	590	20	280	1,010
		Winter	17	621	610	24	280	860
		Spring	22	567	580	14	420	720
		Summer	20	532	540	14	370	660
		Fall	18	657	635	20	460	1,010
WB128	Wabash River at Vincennes	All data	382	555	560	20	206	870
		Winter	91	575	594	25	250	870
		Spring	97	526	543	18	233	760
		Summer	99	517	540	17	206	680
		Fall	95	606	613	16	323	830

[1]Winter is December 21-March 20, spring is March 21-June 20, summer is June 21-September 20, and fall is September 21-December 20.

[2]Mean and median are rounded to the number of significant figures for individual measurements of the same magnitude.

Table 8. Seasonal pH at Indiana State Board of Health stations

Station	Station name	Season[1]	Number of meas- urements	Mean[2]	Median[2]	Coef- ficient of var- iation (percent)	Minimum	Maximum
EW77	East Fork White River at Williams	All data	80	7.7	7.7	6	6.3	8.8
		Winter	20	7.6	7.6	6	6.5	8.2
		Spring	28	7.7	7.8	7	6.3	8.8
		Summer	16	7.7	7.7	6	6.5	8.7
		Fall	16	7.7	7.7	6	6.8	8.6
EW56	East Fork White River at Shoals	All data	278	7.9	7.9	5	6.6	9.1
		Winter	57	7.8	7.8	5	7.1	8.6
		Spring	68	7.9	8.0	5	7.2	8.7
		Summer	80	7.9	8.0	5	7.0	9.1
		Fall	73	7.8	7.8	6	6.6	8.6
WR166	White River at Spencer	All data	353	7.8	7.8	5	6.2	8.8
		Winter	73	7.7	7.8	5	7.0	8.5
		Spring	92	7.7	7.8	5	6.7	8.4
		Summer	99	7.9	7.9	6	6.2	8.8
		Fall	89	7.7	7.8	6	6.6	8.8
WR130	White River at Bloomfield	All data	254	7.9	8.0	6	6.4	9.8
		Winter	54	7.8	7.8	5	6.4	8.4
		Spring	60	7.9	8.0	5	7.0	8.6
		Summer	75	8.1	8.0	6	7.2	9.8
		Fall	65	7.9	8.0	5	6.8	8.6
WR80	White River at Edwardsport	All data	337	7.9	7.9	6	6.8	9.1
		Winter	72	7.7	7.7	4	7.0	8.4
		Spring	87	7.8	7.9	6	7.0	9.1
		Summer	93	8.0	8.0	6	7.0	8.9
		Fall	85	7.8	7.8	6	6.8	8.6
WR48	White River at Petersburg	All data	80	7.8	7.8	6	6.8	8.8
		Winter	17	7.6	7.7	6	6.8	8.2
		Spring	27	7.8	7.8	6	6.8	8.8
		Summer	17	7.8	7.8	6	6.8	8.6
		Fall	19	7.9	8.0	6	7.0	8.6
WR19	White River at Hazelton	All data	282	7.9	7.9	5	6.7	9.3
		Winter	53	7.8	7.8	5	6.9	8.7
		Spring	72	7.8	7.8	5	6.7	8.6
		Summer	82	7.9	8.0	5	7.0	9.3
		Fall	75	7.9	7.9	6	6.7	9.2
P86	Patoka River at Jasper	All data	141	7.3	7.2	9	5.0	9.1
		Winter	30	7.5	7.4	6	6.2	8.3
		Spring	32	7.4	7.4	7	5.9	8.3
		Summer	42	7.5	7.3	9	6.6	9.1
		Fall	37	7.0	7.1	10	5.0	8.4
P76	Patoka River near Jasper	All data	79	7.3	7.2	7	6.4	8.9
		Winter	16	7.2	7.2	7	6.4	7.9
		Spring	30	7.3	7.2	7	6.5	8.5
		Summer	14	7.3	7.4	9	6.6	8.9
		Fall	19	7.1	7.1	4	6.7	7.8
P33	Patoka River near Oakland City	All data	58	7.1	7.0	5	6.4	8.1
		Winter	9	6.9	6.8	6	6.4	7.5
		Spring	17	7.1	7.1	5	6.6	8.1
		Summer	14	7.1	7.0	6	6.5	8.0
		Fall	18	7.0	7.0	3	6.7	7.4

Table 8. Seasonal pH at Indiana State Board of Health stations—Continued

Station	Station name	Season[1]	Number of measurements	Mean[2]	Median[2]	Coefficient of variation (percent)	Minimum	Maximum
P19	Patoka River near Princeton	All data	271	6.8	7.1	17	3.0	9.0
		Winter	51	7.3	7.2	9	5.0	9.0
		Spring	62	7.3	7.4	8	5.0	8.4
		Summer	82	6.6	6.9	18	3.1	8.6
		Fall	76	6.1	6.5	22	3.0	8.1
P14	Patoka River at Patoka	All data	17	7.3	7.3	7	6.5	8.4
		Winter	5	6.9	6.8	7	6.5	7.7
		Spring	8	7.5	7.5	5	6.9	8.0
		Summer	1	8.4	8.4	--	8.4	8.4
		Fall	3	7.3	7.0	9	6.8	8.0
WB301	Wabash River at Lafayette	All data	330	7.9	7.9	6	6.6	9.5
		Winter	61	7.8	7.8	5	6.6	8.4
		Spring	99	7.9	7.9	6	6.7	9.0
		Summer	85	7.9	8.0	6	6.6	9.5
		Fall	85	7.9	7.9	6	6.8	8.9
WB260	Wabash River at Covington	All data	193	7.9	7.9	6	6.7	9.6
		Winter	37	7.8	7.8	4	7.0	8.4
		Spring	51	7.8	7.9	5	6.7	8.6
		Summer	50	8.0	8.0	7	6.7	9.6
		Fall	55	7.9	7.9	6	6.8	9.0
WB245	Wabash River near Cayuga	All data	65	7.8	7.9	6	6.5	8.6
		Winter	12	7.8	7.8	7	6.5	8.6
		Spring	20	7.7	7.8	7	6.7	8.5
		Summer	17	7.8	7.9	6	7.0	8.5
		Fall	16	7.8	7.8	5	6.8	8.5
WB228	Wabash River at Montezuma	All data	324	7.9	7.9	6	6.6	9.8
		Winter	60	7.8	7.8	5	6.6	8.7
		Spring	89	7.9	7.9	6	6.8	9.0
		Summer	88	8.0	7.9	7	6.8	9.8
		Fall	87	8.0	8.0	5	7.1	9.2
WB219	Wabash River at Clinton	All data	38	7.7	7.8	6	6.5	8.6
		Winter	6	7.4	7.3	7	6.5	8.0
		Spring	12	7.7	7.8	6	6.7	8.3
		Summer	10	7.6	7.5	5	7.0	8.2
		Fall	10	7.9	7.8	3	7.7	8.6
WB214	Wabash River at Terre Haute	All data	238	8.0	8.0	4	6.9	8.6
		Winter	61	7.8	7.8	3	7.3	8.3
		Spring	67	7.9	7.9	3	7.4	8.6
		Summer	57	8.1	8.1	4	6.9	8.6
		Fall	53	8.2	8.2	3	7.5	8.6
WB207	Wabash River at Terre Haute	All data	60	7.8	7.9	6	6.5	8.7
		Winter	9	7.8	8.1	8	6.5	8.4
		Spring	19	7.8	7.9	6	6.9	8.7
		Summer	16	7.7	7.6	7	6.7	8.6
		Fall	16	8.0	7.9	3	7.6	8.4

Table 8. Seasonal pH at Indiana State Board of Health stations—Continued

Station	Station name	Season[1]	Number of measurements	Mean[2]	Median[2]	Coefficient of variation (percent)	Minimum	Maximum
WB194	Wabash River near Terre Haute	All data	49	8.0	8.0	6	6.8	8.7
		Winter	9	8.1	8.3	5	7.3	8.6
		Spring	17	7.8	7.9	7	6.8	8.7
		Summer	10	7.9	8.1	6	6.9	8.3
		Fall	13	8.0	8.1	5	7.5	8.6
WB128	Wabash River at Vincennes	All data	336	7.9	7.9	6	6.4	9.8
		Winter	70	7.8	7.8	5	6.4	8.4
		Spring	87	7.8	7.8	6	6.7	8.9
		Summer	92	8.0	8.0	5	6.6	8.9
		Fall	87	7.9	7.9	6	6.8	9.8

[1]Winter is December 21-March 20, spring is March 21-June 20, summer is June 21-September 20, and fall is September 21-December 20.

[2]Mean and median are rounded to the number of significant figures for individual measurements of the same magnitude.

Table 9. Seasonal total alkalinity concentration at Indiana State Board of Health stations

Station	Station name	Season[1]	Number of meas- urements	Mean[2] (mg/L as $CaCO_3$)	Median[2] (mg/L as $CaCO_3$)	Coef- ficient of var- iation (percent)	Min- imum (mg/L as $CaCO_3$)	Max- imum (mg/L as $CaCO_3$)
EW77	East Fork White River at Williams	All data	13	180	200	22	120	230
		Winter	4	190	200	14	160	220
		Spring	4	150	140	26	120	200
		Summer	3	180	200	27	120	210
		Fall	2	230	230	4	220	230
EW56	East Fork White River at Shoals	All data	354	170	170	27	62	350
		Winter	85	170	170	32	62	310
		Spring	87	150	150	25	78	250
		Summer	93	170	170	22	76	350
		Fall	89	200	210	21	78	330
WR166	White River at Spencer	All data	365	220	230	20	62	340
		Winter	90	220	230	25	62	320
		Spring	86	200	210	20	94	260
		Summer	98	230	240	15	120	280
		Fall	91	240	250	16	110	340
WR130	White River at Bloomfield	All data	334	200	210	24	44	330
		Winter	83	190	190	31	44	330
		Spring	80	180	180	23	78	280
		Summer	91	210	220	19	90	270
		Fall	80	230	240	17	76	290
WR80	White River at Edwardsport	All data	339	190	200	25	52	350
		Winter	84	190	180	31	74	350
		Spring	82	170	170	22	86	250
		Summer	92	190	200	22	52	280
		Fall	81	220	230	19	76	280
WR48	White River at Petersburg	All data	13	190	200	32	100	330
		Winter	5	200	210	46	100	330
		Spring	3	160	140	27	130	210
		Summer	3	180	180	9	160	200
		Fall	2	220	220	7	210	230
WR19	White River at Hazelton	All data	352	180	180	25	60	320
		Winter	81	170	160	31	60	280
		Spring	87	150	160	23	82	220
		Summer	97	170	170	17	91	230
		Fall	87	210	210	20	86	320
P86	Patoka River at Jasper	All data	188	79	76	36	8	190
		Winter	48	64	61	31	26	120
		Spring	47	73	70	29	42	160
		Summer	50	90	90	32	40	180
		Fall	43	91	92	36	8	190
P76	Patoka River near Jasper	All data	4	73	71	18	60	88
		Winter	0	---	---	--	---	---
		Spring	2	62	62	5	60	64
		Summer	1	88	88	--	88	88
		Fall	1	78	78	--	78	78
P33	Patoka River near Oakland City	All data	4	63	73	35	30	76
		Winter	1	30	30	--	30	30
		Spring	1	76	76	--	76	76
		Summer	1	72	72	--	72	72
		Fall	1	74	74	--	74	74

Table 9. Seasonal total alkalinity concentration at Indiana State Board of Health stations—Continued

Station	Station name	Season[1]	Number of measurements	Mean[2] (mg/L as $CaCO_3$)	Median[2] (mg/L as $CaCO_3$)	Coefficient of variation (percent)	Minimum (mg/L as $CaCO_3$)	Maximum (mg/L as $CaCO_3$)
P19	Patoka River near Princeton	All data	343	32	30	73	0	170
		Winter	81	36	33	65	0	170
		Spring	87	39	39	50	5	150
		Summer	91	29	24	87	0	160
		Fall	84	25	20	94	0	110
P14	Patoka River at Patoka	All data	1	53	53	--	53	53
		Winter	1	53	53	--	53	53
		Spring	0	---	---	--	---	---
		Summer	0	---	---	--	---	---
		Fall	0	---	---	--	---	---
WB301	Wabash River at Lafayette	All data	348	200	200	23	60	450
		Winter	70	190	200	29	84	310
		Spring	95	180	190	20	60	260
		Summer	89	190	190	18	96	360
		Fall	94	220	230	19	110	450
WB260	Wabash River at Covington	All data	279	190	200	21	64	410
		Winter	58	190	190	28	64	270
		Spring	77	180	180	19	94	230
		Summer	69	190	180	19	110	410
		Fall	75	220	230	12	120	260
WB228	Wabash River at Montezuma	All data	327	200	200	21	80	380
		Winter	63	180	190	26	86	270
		Spring	91	180	190	21	80	350
		Summer	83	190	180	17	120	380
		Fall	90	220	230	14	120	270
WB214	Wabash River at Terre Haute	All data	286	200	200	23	78	590
		Winter	68	200	210	28	78	300
		Spring	76	190	190	18	100	340
		Summer	71	190	190	30	78	590
		Fall	71	220	220	13	120	270
WB128	Wabash River at Vincennes	All data	339	190	190	21	58	280
		Winter	82	190	190	30	90	280
		Spring	84	180	180	18	88	220
		Summer	91	180	180	17	58	230
		Fall	82	210	210	15	86	260

[1]Winter is December 21–March 20, spring is March 21–June 20, summer is June 21–September 20, and fall is September 21–December 20.
[2]Mean and median are rounded to the number of significant figures for individual measurements of the same magnitude.

Table 10. Seasonal sulfate concentration at Indiana State Board of Health stations

Station	Station name	Season[1]	Number of meas- urements	Mean[2] (mg/L)	Median[2] (mg/L)	Coef- ficient of var- iation (percent)	Min- imum (mg/L)	Max- imum (mg/L)
EW77	East Fork White River at Williams	All data	90	37	36	26	19	85
		Winter	20	40	40	16	26	50
		Spring	26	35	36	13	26	42
		Summer	22	36	32	46	19	85
		Fall	22	38	39	15	28	47
WR166	White River at Spencer	All data	95	63	62	27	28	110
		Winter	21	59	54	38	28	110
		Spring	25	59	57	23	39	91
		Summer	26	63	65	26	32	110
		Fall	23	71	74	19	40	100
WR80	White River at Edwardsport	All data	91	71	69	30	24	160
		Winter	21	66	59	31	37	110
		Spring	25	64	62	19	33	82
		Summer	22	69	70	31	24	110
		Fall	23	85	86	28	46	160
WR48	White River at Petersburg	All data	91	55	51	29	23	130
		Winter	20	55	51	33	30	100
		Spring	24	50	48	23	35	78
		Summer	23	58	55	35	23	130
		Fall	24	58	60	23	28	79
P76	Patoka River near Jasper	All data	81	37	36	33	16	100
		Winter	16	38	39	26	22	55
		Spring	22	35	34	19	22	50
		Summer	23	34	35	32	16	63
		Fall	20	42	38	44	22	100
P33	Patoka River near Oakland City	All data	77	230	150	89	53	1,000
		Winter	14	170	120	66	59	370
		Spring	20	160	110	65	56	460
		Summer	22	280	210	81	69	1,000
		Fall	21	260	130	100	53	1,000
WB301	Wabash River at Lafayette	All data	96	63	62	23	39	140
		Winter	16	65	55	40	39	140
		Spring	28	60	61	16	43	79
		Summer	28	60	58	18	43	97
		Fall	24	70	69	16	52	110
WB245	Wabash River near Cayuga	All data	92	68	70	25	34	140
		Winter	18	68	63	31	34	98
		Spring	26	64	66	19	45	86
		Summer	25	64	64	22	39	89
		Fall	23	79	75	24	55	140
WB228	Wabash River at Montezuma	All data	93	67	69	21	30	110
		Winter	19	65	68	28	30	98
		Spring	26	62	64	18	43	87
		Summer	24	63	65	20	31	90
		Fall	24	76	75	14	56	110
WB219	Wabash River at Clinton	All data	46	67	72	23	27	98
		Winter	9	69	76	37	27	98
		Spring	13	66	67	19	46	85
		Summer	12	60	59	24	29	76
		Fall	12	75	75	8	63	85

Table 10. Seasonal sulfate concentration at Indiana State Board of Health stations—Continued

Station	Station name	Season[1]	Number of meas-urements	Mean[2] (mg/L)	Median[2] (mg/L)	Coef-ficient of var-iation (percent)	Min-imum (mg/L)	Max-imum (mg/L)
WB207	Wabash River at Terre Haute	All data	89	67	68	21	31	100
		Winter	16	62	58	25	45	100
		Spring	26	64	66	19	46	91
		Summer	24	64	65	21	31	91
		Fall	23	76	76	14	56	100
WB194	Wabash River near Terre Haute	All data	55	70	71	21	40	110
		Winter	10	64	57	28	40	92
		Spring	17	69	70	17	52	92
		Summer	14	68	71	20	40	86
		Fall	14	79	77	19	58	110
WB128	Wabash River at Vincennes	All data	89	69	72	20	29	100
		Winter	19	70	62	27	45	100
		Spring	24	65	65	20	29	86
		Summer	23	66	69	19	39	92
		Fall	23	76	76	10	58	87

[1]Winter is December 21–March 20, spring is March 21–June 20, summer is June 21–September 20, and fall is September 21–December 20.

[2]Mean and median are rounded to the number of significant figures for individual measurements of the same magnitude.

Table 11. Seasonal suspended-solids concentration at Indiana State Board of Health stations

Station	Station name	Season[1]	Number of meas- urements	Mean[2] (mg/L)	Median[2] (mg/L)	Coef- ficient of var- iation (percent)	Min- imum (mg/L)	Max- imum (mg/L)
EW77	East Fork White River at Williams	All data	115	60	32	156	3	773
		Winter	26	72	29	114	3	320
		Spring	34	71	33	183	11	773
		Summer	27	62	40	147	18	500
		Fall	28	35	24	126	3	200
EW56	East Fork White River at Shoals	All data	376	56	31	150	1	770
		Winter	89	58	22	146	1	480
		Spring	94	74	46	142	1	770
		Summer	99	58	35	140	6	668
		Fall	94	32	20	148	1	370
WR166	White River at Spencer	All data	412	79	42	223	1	2,930
		Winter	97	70	27	179	3	918
		Spring	101	91	58	111	10	800
		Summer	111	108	52	262	10	2,930
		Fall	103	43	21	234	1	980
WR130	White River at Bloomfield	All data	333	101	56	188	2	2,380
		Winter	83	81	52	142	2	682
		Spring	79	138	81	142	18	1,430
		Summer	91	135	65	207	16	2,380
		Fall	80	45	35	98	2	310
WR80	White River at Edwardsport	All data	455	104	74	116	3	1,230
		Winter	110	96	60	138	5	1,070
		Spring	114	134	96	106	19	1,230
		Summer	120	125	81	96	10	650
		Fall	111	58	46	94	3	400
WR48	White River at Petersburg	All data	117	99	71	100	8	600
		Winter	27	107	72	121	9	600
		Spring	32	83	68	68	15	300
		Summer	29	147	93	85	18	450
		Fall	29	60	54	63	8	150
WR19	White River at Hazelton	All data	351	108	68	126	4	1,180
		Winter	82	112	65	131	5	934
		Spring	85	132	96	114	14	1,180
		Summer	97	124	74	123	19	1,050
		Fall	87	63	44	107	4	376
P86	Patoka River at Jasper	All data	188	56	25	204	1	896
		Winter	48	53	21	212	1	706
		Spring	47	80	37	177	10	896
		Summer	50	62	22	209	8	690
		Fall	43	25	18	90	1	110
P76	Patoka River near Jasper	All data	118	115	84	125	2	1,300
		Winter	24	133	47	203	2	1,300
		Spring	33	108	96	63	7	370
		Summer	32	153	116	72	26	540
		Fall	29	65	64	74	4	180
P33	Patoka River near Oakland City	All data	82	97	71	114	4	840
		Winter	14	91	70	89	8	280
		Spring	21	72	69	52	22	150
		Summer	24	163	120	107	20	840
		Fall	23	57	40	69	4	150

Table 11. Seasonal suspended-solids concentration at Indiana State Board of Health stations—Continued

Station	Station name	Season[1]	Number of meas- urements	Mean[2] (mg/L)	Median[2] (mg/L)	Coef- ficient of var- iation (percent)	Min- imum (mg/L)	Max- imum (mg/L)
P19	Patoka River near Princeton	All data	351	86	27	308	1	3,400
		Winter	81	88	40	179	1	900
		Spring	86	115	44	203	7	1,550
		Summer	95	109	18	391	3	3,400
		Fall	89	30	12	154	1	238
P14	Patoka River at Patoka	All data	24	91	47	172	7	780
		Winter	5	51	40	56	20	94
		Spring	8	164	68	157	20	780
		Summer	5	78	47	89	20	190
		Fall	6	37	35	71	7	80
WB301	Wabash River at Lafayette	All data	379	75	37	177	1	1,360
		Winter	74	73	28	155	1	548
		Spring	104	106	47	189	2	1,360
		Summer	98	87	49	122	11	828
		Fall	103	33	21	119	1	290
WB260	Wabash River at Covington	All data	279	77	47	144	2	984
		Winter	59	81	30	163	2	792
		Spring	77	111	59	145	14	984
		Summer	68	84	68	67	7	336
		Fall	75	34	31	72	4	128
WB245	Wabash River near Cayuga	All data	45	82	59	91	6	340
		Winter	8	67	53	103	6	190
		Spring	13	84	70	57	16	180
		Summer	13	131	86	75	52	340
		Fall	11	31	30	48	8	60
WB228	Wabash River at Montezuma	All data	371	100	56	159	3	1,520
		Winter	73	137	39	185	3	1,520
		Spring	102	132	69	144	5	1,220
		Summer	94	91	70	76	6	472
		Fall	102	51	38	112	4	436
WB219	Wabash River at Clinton	All data	46	111	61	135	4	780
		Winter	9	86	36	144	4	380
		Spring	13	102	80	58	40	256
		Summer	12	216	89	112	50	780
		Fall	12	35	28	52	10	71
WB214	Wabash River at Terre Haute	All data	286	84	47	157	2	1,200
		Winter	67	63	29	157	3	674
		Spring	76	116	56	135	2	990
		Summer	72	111	62	156	6	1,200
		Fall	71	43	38	94	7	313
WB207	Wabash River at Terre Haute	All data	42	112	62	113	6	630
		Winter	6	150	81	118	8	480
		Spring	13	101	76	79	21	310
		Summer	12	171	120	98	20	630
		Fall	11	39	39	39	6	62

Table 11. Seasonal suspended-solids concentration at Indiana State Board of Health stations—Continued

Station	Station name	Season[1]	Number of measurements	Mean[2] (mg/L)	Median[2] (mg/L)	Coefficient of variation (percent)	Minimum (mg/L)	Maximum (mg/L)
WB194	Wabash River near Terre Haute	All data	77	97	80	74	4	370
		Winter	17	88	76	100	12	370
		Spring	22	116	98	59	27	320
		Summer	20	106	92	63	20	280
		Fall	18	70	58	84	4	260
WB128	Wabash River at Vincennes	All data	389	128	82	136	1	1,800
		Winter	91	130	71	189	1	1,800
		Spring	96	144	99	118	8	1,450
		Summer	106	155	96	106	36	980
		Fall	96	78	68	71	8	414

[1]Winter is December 21-March 20, spring is March 21-June 20, summer is June 21-September 20, and fall is September 21-December 20.

[2]Mean and median are rounded to the number of significant figures for individual measurements of the same magnitude.

Table 12. Seasonal total iron concentration at Indiana State Board of Health stations

Station	Station name	Season[1]	Number of meas-urements	Mean[2] (µg/L)	Median[2] (µg/L)	Coef-ficient of var-iation (percent)	Min-imum (µg/L)	Max-imum (µg/L)
EW77	East Fork White River at Williams	All data	45	780	600	72	200	3,000
		Winter	12	1,200	1,000	73	200	3,000
		Spring	11	810	600	54	200	1,600
		Summer	10	670	650	38	300	1,200
		Fall	12	470	450	44	200	900
WR166	White River at Spencer	All data	11	1,100	700	89	300	3,000
		Winter	3	830	700	73	300	1,500
		Spring	2	750	750	9	700	800
		Summer	3	2,200	2,800	55	800	3,000
		Fall	3	430	400	35	300	600
WR48	White River at Petersburg	All data	74	1,600	1,200	72	280	5,600
		Winter	16	1,700	1,700	68	280	3,800
		Spring	20	1,400	1,300	45	400	2,700
		Summer	20	2,300	1,600	68	600	5,600
		Fall	18	920	950	40	340	1,800
P76	Patoka River near Jasper	All data	80	2,200	1,800	72	300	8,300
		Winter	16	1,900	1,100	105	800	8,300
		Spring	22	1,900	1,600	52	900	4,800
		Summer	22	3,200	2,400	58	300	7,200
		Fall	20	1,600	1,700	53	600	4,300
P33	Patoka River near Oakland City	All data	50	2,400	2,000	62	900	6,600
		Winter	12	2,700	2,200	50	1,000	4,800
		Spring	12	1,900	2,000	38	900	3,400
		Summer	13	3,000	2,000	60	1,000	6,100
		Fall	13	2,100	1,500	85	940	6,600
WB219	Wabash River at Clinton	All data	12	1,200	800	79	200	3,500
		Winter	2	1,100	1,100	116	200	2,000
		Spring	4	930	900	24	700	1,200
		Summer	3	2,000	1,800	74	600	3,500
		Fall	3	670	700	23	500	800
WB194	Wabash River near Terre Haute	All data	11	1,800	1,000	105	600	7,100
		Winter	3	3,000	1,200	119	700	7,100
		Spring	4	1,100	950	31	900	1,600
		Summer	2	2,500	2,500	40	1,800	3,200
		Fall	2	750	750	28	600	900
WB128	Wabash River at Vincennes	All data	46	2,300	1,600	86	200	9,600
		Winter	13	2,700	1,700	70	200	6,500
		Spring	12	1,500	1,300	52	400	2,700
		Summer	10	3,500	2,400	79	700	9,600
		Fall	11	1,600	1,100	97	500	6,000

[1]Winter is December 21–March 20, spring is March 21–June 20, summer is June 21–September 20, and fall is September 21–December 20.
[2]Mean and median are rounded to the number of significant figures for individual measurements of the same magnitude.

Table 13. Seasonal total manganese concentration at Indiana State Board of Health stations

Station	Station name	Season[1]	Number of meas-urements	Mean[2] (µg/L)	Median[2] (µg/L)	Coef-ficient of var-iation (percent)	Min-imum (µg/L)	Max-imum (µg/L)
EW77	East Fork White River at Williams	All data	34	130	120	46	40	280
		Winter	9	130	120	40	40	190
		Spring	9	110	110	40	70	210
		Summer	7	150	130	48	90	260
		Fall	9	120	100	55	50	280
WR166	White River at Spencer	All data	35	160	130	54	70	550
		Winter	9	170	120	85	70	550
		Spring	9	130	130	38	80	240
		Summer	7	160	130	43	80	270
		Fall	10	160	160	27	100	250
WR80	White River at Edwardsport	All data	33	260	200	86	100	1,300
		Winter	9	210	190	43	100	330
		Spring	9	310	180	120	140	1,300
		Summer	7	360	260	52	220	660
		Fall	8	180	160	30	120	280
WR48	White River at Petersburg	All data	34	180	160	40	70	410
		Winter	9	200	160	49	90	410
		Spring	8	150	150	23	110	220
		Summer	8	230	210	32	160	390
		Fall	9	150	140	32	70	220
P76	Patoka River near Jasper	All data	51	680	480	87	80	2,500
		Winter	12	280	200	92	80	1,000
		Spring	13	390	430	43	90	600
		Summer	14	1,200	1,100	33	700	2,000
		Fall	12	790	400	104	140	2,500
P33	Patoka River near Oakland City	All data	47	2,200	1,700	87	150	7,700
		Winter	11	1,100	630	99	190	3,800
		Spring	11	1,500	1,200	63	220	2,900
		Summer	13	2,900	3,100	54	150	5,600
		Fall	12	3,000	2,200	89	460	7,700
WB219	Wabash River at Clinton	All data	1	100	100	--	100	100
		Winter	1	100	100	--	100	100
		Spring	0	-----	-----	--	---	-----
		Summer	0	-----	-----	--	---	-----
		Fall	0	-----	-----	--	---	-----
WB194	Wabash River near Terre Haute	All data	12	150	140	48	50	300
		Winter	3	140	80	95	50	300
		Spring	3	140	110	43	100	210
		Summer	3	180	200	28	120	210
		Fall	3	140	160	33	90	180
WB128	Wabash River at Vincennes	All data	7	170	160	30	110	240
		Winter	1	160	160	--	160	160
		Spring	2	120	120	12	110	130
		Summer	2	180	180	39	130	230
		Fall	2	210	210	20	180	240

[1]Winter is December 21-March 20, spring is March 21-June 20, summer is June 21-September 20, and fall is September 21-December 20.
[2]Mean and median are rounded to the number of significant figures for individual measurements of the same magnitude.

Table 14. Equations for predicting the regional relation between dissolved-solids concentration and specific conductance

[DS, dissolved-solids concentration, in milligram per liter; SC, specific conductance, in microsiemen per centimeter at 25°C; p, the probability of obtaining a significant relation by chance where, in fact, there is no relation; **, the relation is significant at p<0.01]

Predictive equation	Model	Bias corrector for log-log models, $(\Sigma 10^{R})/n$	Coefficient of determination, R-square	Standard error of regression[1,2], Es ($\log_{10}$ mg/L)	Standard error of regression[1,2], Ep (percent)	Sum of squares of independent variable, Sxx ($\log_{10}$ µS/cm at 25° C)^2	Mean of independent variable, $\overline{X}$ ($\log_{10}$ µS/cm at 25° C)	Number of data pairs, n	Number of stations	Range of specific conductance used to develop the predictive equation (µS/cm at 25° C)
$DS=2.000(SC)^{0.8136}$	Log-log	1.009	0.92**	5.817×10^{-2}	13.4	12.45	2.591	208	61	60-740
$DS=0.2154(SC)^{1.180}$	Log-log	1.010	.95**	6.229×10^{-2}	14.4	13.32	3.287	260	86	750-6,100

[1] The standard error of regression (Ep) is from Hardison (1971, table 1, p. C229).
[2] The standard error regression (Es) for log-log models in for the log-log form and not for the exponential form show in column one of this table. Es is reported to allow the reader to estimate confidence limits for the log-log model.

Table 15. Equations for predicting the regional relation between sulfate concentration and specific conductance

[SO_4, sulfate concentration, in milligram per liter; SC, specific conductance, in microsiemen per centimeter at 25°C; p, the probability of obtaining a significant relation by chance where, in fact, there is no relation; **, the relation is significant at $p<0.01$]

Predictive equation	Model	Bias corrector for log-log models, $(\Sigma 10^R)/n$	Coefficient of determination, R-square	Standard error of regression[1,2,3], Es	Standard error of regression[1,2,3], Ep (percent)	Sum of squares of independent variable[4], Sxx	Mean of independent variable[5], $\overline{X}$	Number of data pairs, n	Number of stations	Range of specific conductance used to develop the predictive equation (µS/cm at 25° C)
$SO_4=1.262(SC)^{0.6367}$	Log-log	1.166	0.36**	0.2331	57.8	16.20	2.566	216	61	40-740
$SO_4=-169.5+0.6092(SC)$	Linear	-----	.85**	295.3	24.6	3.856×10^8	2,252	289	92	750-6,100

[1]The unit of measure for Es for the linear model is milligram per liter and for the log-log model is $\log_{10}$ milligram per liter.

[2]The standard error of regression in percent (Ep) for the linear model is the standard error of regression (Es) divided by the mean of the dependent variable times 100. Ep for the log-log model is from Hardison (1971, table 1, p. C229).

[3]The standard error of regression (Es) for the log-log model is for the log-log form and not for the exponential form shown in column one of this table. Es is reported to allow the reader to estimate confidence limits for the log-log model, and should not be compared with Es for the other model.

[4]The unit of measure for the linear model is the square of microsiemen per centimeter at 25° C and for the log-log model is the square of $\log_{10}$ microsiemen per centimeter at 25° C.

[5]The unit of measure for the linear model is microsiemen per centimeter at 25° C and for the log-log model is $\log_{10}$ microsiemen per centimeter at 25° C.

Table 16. Equations for predicting the relations between specific conductance and streamflow at U.S. Geological Survey gaging stations

[SC, specific conductance, in microsiemen per centimeter at 25°C; Q, streamflow, in cubic foot per second; p, the probability of obtaining a significant relation by chance where, in fact, there is no relation; *, the relation is significant at $p<0.05$; **, the relation is significant at $p<0.01$]

Station	Predictive equation	Model	Bias corrector for log-log models, $(\Sigma 10^R)/n$	Coefficient of determination, R-square	Standard error of regression[1,2,3], Es	Standard error of regression[1,2,3], Ep (percent)	Sum of squares of independent variable[4], Sxx	Mean of independent variable[5], $\bar{X}$	Number of data pairs, n	Range of streamflow used to develop the predictive equation (ft^3/s)
03303300	$SC=202.9(Q)^{-0.04285}$	Log-log	1.040	0.10*	0.1096	25.6	40.04	1.129	55	0.01-169
03303400	$SC=504.8-107.7(\log_{10} Q)$	Semilog	-----	.56**	84.75	17.3	32.82	.1354	43	.03-36
03322100	$SC=3,238(Q)^{-0.3077}$	Log-log	1.063	.73**	.1564	37.1	36.19	2.311	53	4.7-5,720
03342100	$SC=152.9+200.7\left\{\frac{1}{1+Q\times 10^{-1.5}}\right\}$	Hyperbolic	-----	.35**	69.50	23.1	5.096	.7346	81	.01-137
03342150	$SC=938.6(Q)^{-0.2330}$	Log-log	1.036	.78**	.1193	28.0	58.90	.4011	64	.04-426
03342250	$SC=3,195(Q)^{-0.2490}$	Log-log	1.022	.65**	9.194×10^{-2}	21.4	18.52	.8745	76	1.3-246
03342300	$SC=4,064(Q)^{-0.3541}$	Log-log	1.022	.88**	9.480×10^{-2}	22.1	38.63	1.815	75	2.6-1,750
03342360	$SC=698.5+8,583(1/Q)$	Inverse	-----	.60**	515.1	40.4	8.581×10^{-2}	6.704×10^{-2}	18	4.8-526
03342500	$SC=407.6+1,749\left\{\frac{1}{1+Q\times 10^{-1.5}}\right\}$	Hyperbolic	-----	.75**	268.4	28.0	4.491	.3148	67	4.6-2,860
03360000	$SC=483.7-6.161\times10^{-2}(Q)$	Linear	-----	.73**	54.56	12.9	4.668×10^{7}	997.1	24	45-5,930
03375500	$SC=307.7(Q)^{-0.07501}$	Log-log	1.041	.22**	.1208	28.4	26.61	2.014	39	1.8-4,220
03375800	$SC=166.3+105.0\left\{\frac{1}{1+Q\times 10^{-1.5}}\right\}$	Hyperbolic	-----	.31**	38.21	15.5	1.967	.7579	35	.12-137
03376260	$SC=57.37+2,091\left\{\frac{1}{1+Q\times 10^{-1}}\right\}$	Hyperbolic	-----	.45**	546.4	38.0	2.592	.6602	49	.23-100
03376300	$SC=1,011(Q)^{-0.1852}$	Log-log	1.015	.74**	7.567×10^{-2}	17.5	18.78	2.535	42	3.0-3,530
03376350	$SC=1,090+3,253\left\{\frac{1}{1+Q\times 10^{-1.5}}\right\}$	Hyperbolic	-----	.50**	666.9	22.9	1.775	.5598	45	4.1-343
03376500	$SC=6,386(Q)^{-0.3506}$	Log-log	1.086	.71**	.1517	36.1	18.73	2.817	43	20-9,930

[1]The unit of measure for Es for all models except log-log is microsiemen per centimeter at 25° C and for the log-log models is $\log_{10}$ microsiemen per centimeter at 25° C.

[2]The standard error of regression in percent (Ep) for all models except log-log is the standard error of regression (Es) divided by the mean of the dependent variable times 100. Ep for the log-log models is from Hardison (1971, table 1, p. C229).

[3]The standard error of regression (Es) for log-log models is for the log-log form and not for the exponential form shown in column two of this table. Es is reported to allow the reader to estimate confidence limits for the log-log model, and should not be compared with Es for the other models.

[4]The unit of measure for the linear model is the square of cubic foot per second, for the hyperbolic and the inverse models is the square of the reciprocal of cubic foot per second, and for the log-log and the semilog models is the square of $\log_{10}$ cubic foot per second.

[5]The unit of measure for the linear model is cubic foot per second, for the hyperbolic and the inverse models is the reciprocal of cubic foot per second, and for the log-log and the semilog models is $\log_{10}$ cubic foot per second.

Table 17. Equations for predicting the relations between specific conductance and streamflow at Indiana State Board of Health stations

[SC, specific conductance, in microsiemen per centimeter at 25°C; Q, streamflow, in cubic foot per second; p, the probability of obtaining a significant relation by chance where, in fact, there is no relation; **, the relation is significant at p<0.01]

Station	Predictive equation	Model	Bias corrector for log-log models, $(\Sigma 10^{R})/n$	Coefficient of determination, R-square	Standard error of regression[1,2,3], Es	Standard error of regression[1,2,3], Ep (percent)	Sum of squares of independent variable[4], Sxx	Mean of independent variable[5], $\bar{X}$	Number of data pairs, n	Range of streamflow used to develop the predictive equation (ft^3/s)
EW77	$SC=480.3-1.023\times10^{-2}(Q)$	Linear	-----	0.27**	85.17	20.0	2.817×10^{9}	5,387	112	394-23,100
EW56	$SC=162.0+357.8\left\{\frac{1}{1+Q\times10^{-4}}\right\}$	Hyperbolic	-----	.42**	82.25	19.0	13.85	.7576	366	278-58,600
WR166	$SC=1,625-295.7(\log_{10} Q)$	Semilog	-----	.61**	109.1	16.1	83.76	3.209	403	242-32,200
WR130	$SC=1,559-286.9(\log_{10} Q)$	Semilog	-----	.71**	85.36	14.4	70.52	3.363	325	343-41,100
WR80	$SC=1,430-246.3(\log_{10} Q)$	Semilog	-----	.58**	99.62	17.3	97.89	3.461	443	385-54,100
WR48	$SC=1,332-216.4(\log_{10} Q)$	Semilog	-----	.52**	86.98	18.1	19.58	3.938	114	1,050-61,700
WR19	$SC=1,256-201.6(\log_{10} Q)$	Semilog	-----	.59**	78.93	16.0	74.41	3.786	344	855-105,000
P86	$SC=369.0(Q)^{-0.09734}$	Log-log	1.162	.20**	.1868	45.0	166.8	1.700	186	.10-2,610
P76	$SC=536.3(Q)^{-0.1495}$	Log-log	1.018	.68**	8.191×10^{-2}	19.0	72.98	2.300	117	2.0-8,310
P33	$SC=4,183(Q)^{-0.3334}$	Log-log	1.100	.52**	.1986	48.2	30.80	2.707	81	31-6,820
P19	$SC=7,416(Q)^{-0.3735}$	Log-log	1.127	.68**	.2007	48.9	210.9	2.424	339	4.9-14,500
P14	$SC=8,004(Q)^{-0.3931}$	Log-log	1.020	.88**	9.029×10^{-2}	20.9	8.853	2.518	24	20-2,190
WB301	$SC=110.4+514.7\left\{\frac{1}{1+Q\times10^{-4.5}}\right\}$	Hyperbolic	-----	.36**	85.50	15.5	5.743	.8559	368	610-88,000
WB260	$SC=611.9-7.743\times10^{-3}(Q)$	Linear	-----	.38**	84.72	15.2	1.922×10^{10}	7,153	269	660-47,000
WB245	$SC=674.0-7.680\times10^{-3}(Q)$	Linear	-----	.23**	105.9	17.5	2.363×10^{9}	8,768	44	1,830-30,700
WB228	$SC=621.0-6.182\times10^{-3}(Q)$	Linear	-----	.40**	83.35	14.9	4.445×10^{10}	1.020×10^{4}	362	940-56,800
WB219	$SC=2,130(Q)^{-0.1427}$	Log-log	1.017	.28**	8.251×10^{-2}	19.2	5.421	3.874	43	1,240-38,000
WB214	$SC=184.1+474.4\left\{\frac{1}{1+Q\times10^{-4.5}}\right\}$	Hyperbolic	-----	.49**	75.76	13.6	6.501	.7883	268	910-88,000
WB207	$SC=666.6-6.871\times10^{-3}(Q)$	Linear	-----	.32**	97.35	16.5	3.696×10^{9}	1.118×10^{4}	41	1,300-39,800
WB194	$SC=663.0-5.476\times10^{-3}(Q)$	Linear	-----	.25**	103.8	17.6	8.953×10^{9}	1.319×10^{4}	77	1,380-51,700
WB128	$SC=-214.3+850.8\left\{\frac{1}{1+Q\times10^{-5}}\right\}$	Hyperbolic	-----	.42**	86.05	15.5	2.764	.9029	379	1,000-80,900

[1] The unit of measure for Es for all models except log-log is microsiemen per centimeter at 25° C and for the log-log models is $\log_{10}$ microsiemen per centimeter at 25° C.

[2] The standard error of regression in percent (Ep) for all models except log-log is the standard error of regression (Es) divided by the mean of the dependent variable times 100. Ep for the log-log models is from Hardison (1971, table 1, p. C229).

[3] The standard error of regression (Es) for log-log models if for the log-log form and not for the exponential form shown in column two of this table. Es is reported to allow the reader to estimate confidence limits for the log-log model, and should not be compared with Es for the other models.

[4] The unit of measure for the linear models is the square of cubic foot per second, for the hyperbolic models the square of the reciprocal of cubic foot per second, and for the log-log and the semilog models is the square of $\log_{10}$ cubic foot per second.

[5] The unit of measure for the linear models is cubic foot per second, for the hyperbolic models is the reciprocal of cubic foot per second, and for the log-log and the semilog models is $\log_{10}$ cubic foot per second.

Table 18. Equations for predicting the relations between pH and streamflow at Indiana State Board of Health stations

[pH, pH; Q, streamflow, in cubic foot per second; p, the probability of obtaining a significant relation by chance where, in fact, there is no relation; **, the relation is significant at $p<0.01$; *, the relation is significant at $p<0.05$; NS, the relation is not significant at $p<0.05$]

Station	Predictive equation	Model	Coefficient of determination, R-square	Standard error of regression[1], Es	Standard error of regression[1], Ep (percent)	Sum of squares of independent variable[2], Sxx	Mean of independent variable[3], $\bar{X}$	Number of data pairs, n	Range of streamflow used to develop the predictive equation (ft^3/s)
EW77	----	---	NS	--	--	--	--	79	394-23,100
EW56	----	---	NS	--	--	--	--	278	278-46,800
WR166	----	---	NS	--	--	--	--	352	242-27,900
WR130	$pH=6.735+1.206\left\{\frac{1}{1+Q\times 10^{-5}}\right\}$	Hyperbolic	0.02*	0.4371	5.5	0.5189	0.9641	254	378-41,100
WR80	$pH=7.093+0.8668\left\{\frac{1}{1+Q\times 10^{-4.5}}\right\}$	Hyperbolic	.05**	.4400	5.6	4.638	.8815	336	407-46,900
WR48	$pH=7.079+0.9205\left\{\frac{1}{1+Q\times 10^{-4.5}}\right\}$	Hyperbolic	.10**	.4615	6.0	2.097	.7356	79	1,050-61,700
WR19	$pH=7.102+0.8291\left\{\frac{1}{1+Q\times 10^{-5}}\right\}$	Hyperbolic	.03**	.4186	5.3	1.908	.9187	282	855-92,400
P86	$pH=7.482-0.4456\left\{\frac{1}{1+Q\times 10^{-1}}\right\}$	Hyperbolic	.04*	.6225	8.5	12.38	.3184	139	.01-2,500
P76	----	---	NS	--	--	--	--	78	2.0-8,310
P33	----	---	NS	--	--	--	--	57	31-6,820
P19	$pH=7.475-1.812\left\{\frac{1}{1+Q\times 10^{-2}}\right\}$	Hyperbolic	.23**	1.014	15.0	25.73	.3864	271	4.3-11,100
P14	----	---	NS	--	--	--	--	17	20-2,190
WB301	----	---	NS	--	--	--	--	328	610-88,000
WB260	----	---	NS	--	--	--	--	193	660-47,000
WB245	----	---	NS	--	--	--	--	63	1,250-35,100
WB228	----	---	NS	--	--	--	--	322	940-56,800
WB219	----	---	NS	--	--	--	--	36	2,220-38,000
WB214	$pH=7.434+0.9437\left\{\frac{1}{1+Q\times 10^{-4}}\right\}$	Hyperbolic	.46**	.2173	2.7	10.67	.5918	238	910-88,000
WB207	----	---	NS	--	--	--	--	58	1,360-39,800
WB194	$pH=8.183-1.824\left\{\frac{1}{1+Q\times 10^{-3}}\right\}$	Hyperbolic	.13*	.4371	5.5	.4095	.1260	49	1,380-37,800
WB128	$pH=7.922-4.583\times 10^{-6}(Q)$	Linear	.02*	.4393	5.6	5.422×10^{10}	1.195×10^{4}	335	1,390-80,900

[1]The standard error of regression in percent (Ep) is the standard error of regression (Es) divided by the mean of the dependent variable times 100.

[2]The unit of measure for the linear model is the square of cubic foot per second and for the hyperbolic models is the square of the reciprocal of cubic foot per second.

[3]The unit of measure for the linear model is cubic foot per second and for the hyperbolic model is the reciprocal of cubic foot per second.

Table 19. Equations for predicting the relations between pH and specific conductance at Indiana State Board of Health stations

[pH, pH; SC, specific conductance, in microsiemen per centimeter at 25°C; p, the probability of obtaining a significant relation by chance where, in fact, there is no relation; **, the relation is significant at $p<0.01$; *, the relation is significant at $p<0.05$; NS, the relation is not significant at $p<0.05$]

Station	Predictive equation	Model	Coefficient of determination, R-square	Standard error of regression[1], Es	Standard error of regression[1], Ep (percent)	Sum of squares of independent variable[2], Sxx	Mean of independent variable[3], $\overline{X}$	Number of data pairs, n	Range of specific conductance used to develop the predictive equation (µS/cm at 25° C)
EW77	----	---	NS	--	--	--	--	80	220-680
EW56	----	---	NS	--	--	--	--	271	199-847
WR166	$pH=7.955-2.865\times10^{-4}(SC)$	Linear	0.01*	0.4184	5.4	9.188×10^{6}	681.8	312	230-1,330
WR130	----	---	NS	--	--	--	--	248	223-958
WR80	----	---	NS	--	--	--	--	331	219-1,330
WR48	$pH=8.212-207.2(1/SC)$	Inverse	.07*	.4652	6.0	3.019×10^{-5}	2.201×10^{-3}	80	220-1,000
WR19	----	---	NS	--	--	--	--	260	230-817
P86	----	---	NS	--	--	--	--	141	130-3,080
P76	----	---	NS	--	--	--	--	78	120-600
P33	----	---	NS	--	--	--	--	58	200-2,990
P19	$pH=11.24-1.477(\log_{10} SC)$	Semilog	.23**	.9847	14.4	34.71	2.993	260	157-21,200
P14	----	---	NS	--	--	--	--	17	360-2,600
WB301	----	---	NS	--	--	--	--	283	228-837
WB260	$pH=8.208-6.269\times10^{-4}(SC)$	Linear	.02*	.4305	5.5	1.925×10^{6}	561.2	187	257-837
WB245	----	---	NS	--	--	--	--	39	400-840
WB228	----	---	NS	--	--	--	--	270	208-920
WB219	$pH=6.653+1.690\times10^{-3}(SC)$	Linear	.19**	.3954	5.2	4.556×10^{5}	597.9	38	340-820
WB214	$pH=8.481-270.6(1/SC)$	Inverse	.20**	.2638	3.3	5.169×10^{-5}	1.868×10^{-3}	219	230-955
WB207	$pH=6.528+1.905\times10^{-3}(SC)$	Linear	.22**	.4035	5.3	4.173×10^{5}	585.3	35	320-840
WB194	----	---	NS	--	--	--	--	49	440-1,010
WB128	----	---	NS	--	--	--	--	297	206-870

[1]The standard error of regression in percent (Ep) is the standard error of regression (Es) divided by the mean of the dependent variable times 100.

[2]The unit of measure for the linear models is the square of microsiemen per centimeter at 25° C, for the inverse models is the square of the reciprocal of microsiemen per centimeter at 25° C, and for the semilog model is the square of $\log_{10}$ microsiemen per centimeter at 25° C.

[3]The unit of measure for the linear models is microsiemen per centimeter at 25° C, for the inverse models is the reciprocal of microsiemen per centimeter at 25° C, and for the semilog model is $\log_{10}$ microsiemen per centimeter at 25° C.

Table 20. Equations for predicting the relations between total alkalinity concentration and streamflow at Indiana State Board of Health stations

[Alk, total alkalinity concentration, in milligram per liter as calcium carbonate; Q, streamflow, in cubic foot per second; p, the probability of obtaining a significant relation by chance where, in fact, there is no relation; **, the relation is significant at $p<0.01$]

Station	Predictive equation	Model	Bias corrector for log-log models, $(\Sigma 10^{R})/n$	Coefficient of determination, R-square	Standard error of regression[1],[2],[3], Es	Standard error of regression, Ep (percent)	Sum of squares of independent variable[4], Sxx	Mean of independent variable[5], $\overline{X}$	Number of data pairs, n	Range of streamflow used to develop the predictive equation (ft^3/s)
EW77	$Alk=96.10+161.3\left\{\frac{1}{1+Q\times 10^{-3.5}}\right\}$	Hyperbolic	-----	0.72**	20.89	12.3	0.3526	0.4564	10	1,400-20,200
EW56	$Alk=46.84+168.5\left\{\frac{1}{1+Q\times 10^{-4}}\right\}$	Hyperbolic	-----	.51**	32.95	18.9	13.89	.7555	354	278-58,600
WR166	$Alk=124.2+153.7\left\{\frac{1}{1+Q\times 10^{-3.5}}\right\}$	Hyperbolic	-----	.53**	30.88	13.9	16.57	.6397	362	252-32,200
WR130	$Alk=487.8-85.16(\log_{10} Q)$	Semilog	-----	.66**	28.92	14.4	72.99	3.362	334	343-41,100
WR80	$Alk=41.20+203.8\left\{\frac{1}{1+Q\times 10^{-4}}\right\}$	Hyperbolic	-----	.63**	29.97	15.5	12.22	.7476	338	385-54,100
WR48	$Alk=2{,}993(Q)^{-0.3127}$	Log-log	1.023	.60**	9.859×10^{-2}	23.0	1.171	3.992	10	3,780-31,100
WR19	$Alk=437.2-69.41(\log_{10} Q)$	Semilog	-----	.55**	29.04	16.6	76.12	3.782	352	855-105,000
P86	$Alk=35.64+59.18\left\{\frac{1}{1+Q\times 10^{-2.5}}\right\}$	Hyperbolic	-----	.35**	22.80	28.9	14.52	.7319	186	.10-2,610
P19	$Alk=38.89-31.76\left\{\frac{1}{1+Q\times 10^{-1.5}}\right\}$	Hyperbolic	-----	.10**	22.39	69.6	18.93	.2107	343	4.3-14,500
WB301	$Alk=-7.439+235.7\left\{\frac{1}{1+Q\times 10^{-4.5}}\right\}$	Hyperbolic	-----	.44**	33.65	17.3	5.401	.8589	345	610-88,000
WB260	$Alk=10.85+215.3\left\{\frac{1}{1+Q\times 10^{-4.5}}\right\}$	Hyperbolic	-----	.47**	30.35	15.7	4.794	.8465	279	660-47,000
WB228	$Alk=-126.8+351.4\left\{\frac{1}{1+Q\times 10^{-5}}\right\}$	Hyperbolic	-----	.48**	29.26	15.0	2.057	.9164	327	940-56,800
WB214	$Alk=67.87+164.7\left\{\frac{1}{1+Q\times 10^{-4.5}}\right\}$	Hyperbolic	-----	.30**	39.01	19.7	6.722	.7932	286	910-88,000
WB128	$Alk=-108.7+326.2\left\{\frac{1}{1+Q\times 10^{-5}}\right\}$	Hyperbolic	-----	.49**	28.50	15.3	2.448	.9033	338	1,000-80,900

[1] The unit of measure for Es for all models except log-log is milligram per liter as calcium carbonate and for the log-log model is $\log_{10}$ milligram per liter as calcium carbonate.

[2] The standard error of regression in percent (Ep) for all models except log-log is the standard error of regression (Es) divided by the mean of the dependent variable times 100. Ep for the log-log model is from Hardison (1971, table 1, p. C229).

[3] The standard error or regression (Es) for the log-log model is for the log-log form and not for the exponential form shown in column two of this table. Es is reported to allow the reader to estimate confidence limits for the log-log model, and should not be compared with Es for the other models.

[4] The unit of measure for the hyperbolic models is the square of the reciprocal of cubic foot per second and for the log-log and the semilog models is the square of $\log_{10}$ cubic foot per second.

[5] The unit of measure for the hyperbolic models is the reciprocal of cubic foot per second and for the log-log and the semilog models is $\log_{10}$ cubic foot per second.

Table 21. Equations for predicting the relations between total alkalinity concentration and specific conductance at Indiana State Board of Health stations

[Alk, total alkalinity concentration, in milligram per liter as calcium carbonate; SC, specific conductance, in microsiemen per centimeter at 25°C; p, the probability of obtaining a significant relation by chance where, in fact, there is no relation; **, the relation is significant at $p<0.01$; *, the relation is significant at $p<0.05$]

Station	Predictive equation	Model	Bias corrector for log-log models, $(\Sigma 10^R)/n$	Coefficient of determination, R-square	Standard error of regression[1,2,3] Es	Standard error of regression[1,2,3] Ep (percent)	Sum of squares of independent variable[4], Sxx	Mean of independent variable[5], $\overline{X}$	Number of data pairs, n	Range of specific conductance used to develop the predictive equation (µS/cm at 25° C)
EW77	$Alk=-862.3+392.1(\log_{10} SC)$	Semilog	-----	0.75**	21.12	11.6	9.534×10^{-2}	2.664	13	310-630
EW56	$Alk=-712.0+337.9(\log_{10} SC)$	Semilog	-----	.65**	27.90	16.0	4.261	2.623	343	179-1,140
WR166	$Alk=-631.4+303.9(\log_{10} SC)$	Semilog	-----	.66**	26.18	11.8	5.171	2.810	355	192-1,330
WR130	$Alk=-675.9+318.1(\log_{10} SC)$	Semilog	-----	.67**	28.42	14.1	5.188	2.757	325	168-1,040
WR80	$Alk=-729.9+336.7(\log_{10} SC)$	Semilog	-----	.74**	24.84	12.8	5.131	2.743	330	167-1,330
WR48	$Alk=-1,317+552.3(\log_{10} SC)$	Semilog	-----	.80**	27.91	14.9	.1097	2.724	13	400-760
WR19	$Alk=-713.2+331.5(\log_{10} SC)$	Semilog	-----	.77**	20.99	12.0	4.514	2.679	343	210-1,060
P86	$Alk=0.3367(SC)^{0.9988}$	Log-log	1.024	.58**	9.539×10^{-2}	22.2	2.137	2.358	175	106-426
P86	$Alk=13.78+4.282\times10^{4}(1/SC)$	Inverse	-----	.46*	28.39	45.8	4.120×10^{-6}	1.126×10^{-3}	13	456-3,080
P19	$Alk=82.61-17.00(\log_{10} SC)$	Semilog	-----	.07**	22.82	70.5	41.41	2.955	329	146-21,200
WB301	$Alk=-816.2+370.3(\log_{10} SC)$	Semilog	-----	.55**	30.78	15.7	2.814	2.732	337	228-880
WB260	$Alk=-741.4+341.5(\log_{10} SC)$	Semilog	-----	.55**	28.03	14.5	2.217	2.737	268	257-847
WB228	$Alk=0.6462(SC)^{0.9040}$	Log-log	1.008	.70**	5.429×10^{-2}	12.6	2.599	2.732	316	208-869
WB214	$Alk=45.13+0.2743(SC)$	Linear	-----	.38**	37.39	18.9	2.990×10^{6}	558.1	268	230-955
WB128	$Alk=23.09+0.2966(SC)$	Linear	-----	.67**	23.06	12.4	3.950×10^{6}	548.8	330	206-826

[1] The unit of measure for Es for all models except log-log is milligram per liter as calcium carbonate and for the log-log models is $\log_{10}$ milligram per liter as calcium carbonate.

[2] The standard error of regression in percent (Ep) for all models except log-log is the standard error of regression (Es) divided by the mean of the dependent variable times 100. Ep for the log-log models is from Hardison (1971, table 1, p. C229).

[3] The standard error of regression (Es) for log-log models is for the log-log form and not for the exponential form shown in column two of this table. Es is reported to allow the reader to estimate confidence limits for the log-log model, and should not be compared with Es for the other models.

[4] The unit of measure for the linear models is the square of microsiemen per centimeter at 25° C, for the inverse model is the square of the reciprocal of microsiemen per centimeter at 25° C, and for the log-log and the semilog models is the square of $\log_{10}$ microsiemen per centimeter at 25° C.

[5] The unit of measure for the linear models is microsiemen per centimeter at 25° C, for the inverse model is the reciprocal of microsiemen per centimeter at 25° C, and for the log-log and semilog models is $\log_{10}$ microsiemen per centimeter at 25° C.

Table 22. Equations for predicting the relations between sulfate concentration and streamflow at Indiana State Board of Health stations

[SO_4, sulfate concentration, in milligram per liter; Q, streamflow, in cubic foot per second; p, the probability of obtaining a significant relation by chance where, in fact, there is no relation; **, the relation is significant at $p<0.01$]

Station	Predictive equation	Model	Bias corrector for log-log models, $(\Sigma 10^R)/n$	Coefficient of determination, R-square	Standard error of regression[1,2,3], Es	Standard error of regression[1,2,3], Ep (percent)	Sum of squares of independent variable[4], Sxx	Mean of independent variable[5], $\bar{X}$	Number of data pairs, n	Range of streamflow used to develop the predictive equation (ft^3/s)
EW77	$SO_4=66.73(Q)^{-0.07490}$	Log-log	1.023	0.12**	9.061×10^{-2}	21.0	17.60	3.575	87	394-23,100
WR166	$SO_4=167.7-31.13(\log_{10} Q)$	Semilog	-----	.64**	10.23	16.3	17.65	3.372	92	242-19,300
WR80	$SO_4=195.1-34.51(\log_{10} Q)$	Semilog	-----	.52**	14.94	21.2	17.12	3.607	88	407-38,500
WR48	$SO_4=154.6-25.17(\log_{10} Q)$	Semilog	-----	.43**	12.28	22.5	15.32	3.974	88	1,050-61,700
P76	$SO_4=55.80(Q)^{-0.08252}$	Log-log	1.036	.21**	.1182	27.8	41.92	2.397	80	3.5-3,250
P33	$SO_4=1,613(Q)^{-0.3582}$	Log-log	1.165	.46**	.2418	60.3	28.60	2.734	76	31-6,820
WB301	$SO_4=15.17+56.78\left\{\frac{1}{1+Q\times10^{-4.5}}\right\}$	Hyperbolic	-----	.19**	13.34	21.3	1.156	.8364	93	887-40,200
WB245	$SO_4=193.3-32.58(\log_{10} Q)$	Semilog	-----	.47**	12.79	18.8	11.98	3.843	89	1,250-48,600
WB228	$SO_4=45.77+64.07\left\{\frac{1}{1+Q\times10^{-3.5}}\right\}$	Hyperbolic	-----	.57**	9.392	14.2	2.523	.3211	90	1,200-54,100
WB219	$SO_4=197.7-33.90(\log_{10} Q)$	Semilog	-----	.59**	10.27	15.5	5.421	3.874	43	1,240-38,000
WB207	$SO_4=177.1-28.10(\log_{10} Q)$	Semilog	-----	.58**	8.924	13.5	11.93	3.947	86	1,300-51,000
WB194	$SO_4=183.9-28.61(\log_{10} Q)$	Semilog	-----	.54**	10.29	14.6	7.907	3.965	55	1,380-51,700
WB128	$SO_4=43.19+50.80\left\{\frac{1}{1+Q\times10^{-4}}\right\}$	Hyperbolic	-----	.54**	9.556	13.8	3.431	.5094	86	1,440-73,600

[1] The unit of measure for Es for all models except log-log is milligram per liter and for the log-log models is $\log_{10}$ milligram per liter.

[2] The standard error of regression in percent (Ep) for all models except log-log is the standard error of regression (Es) divided by the mean of the dependent variable times 100. Ep for the log-log models is from Hardison (1971, table 1, p. C229).

[3] The standard error of regression (Es) for log-log models is for the log-log form and not for the exponential form shown in column two of this table. Es is reported to allow the reader to estimate confidence limits for the log-log model, and should not be compared with Es for the other models.

[4] The unit of measure for the hyperbolic models is the square of the reciprocal of cubic foot per second, and for the log-log and the semilog models is the square of $\log_{10}$ cubic foot per second at 25° C.

[5] The unit of measure for the hyperbolic models is the reciprocal of cubic foot per second, and for the log-log and semilog models is $\log_{10}$ cubic foot per second .

Table 23. Equations for predicting the relations between sulfate concentration and specific conductance at Indiana State Board of Health stations

[SO_4, sulfate concentration, in milligram per liter; SC, specific conductance, in microsiemen per centimeter at 25°C; p, the probability of obtaining a significant relation by chance where, in fact, there is no relation; **, the relation is significant at $p<0.01$]

Station	Predictive equation	Model	Bias corrector for log-log models, $(\Sigma 10^R)/n$	Coefficient of determination, R-square	Standard error of regression[1,2,3], Es	Standard error of regression[1,2,3], Ep (percent)	Sum of squares of independent variable[4], Sxx	Mean of independent variable[5], $\overline{X}$	Number of data pairs, n	Range of specific conductance used to develop the predictive equation (µS/cm at 25° C)
EW77	$SO_4=7.292(SC)^{0.2661}$	Log-log	1.024	0.09**	9.224×10^{-2}	21.4	1.042	2.618	90	180-680
WR166	$SO_4=0.1131(SC)^{0.9617}$	Log-log	1.011	.73**	6.486×10^{-2}	15.1	.6614	2.863	55	340-1,270
WR80	$SO_4=-269.2+123.5(\log_{10} SC)$	Semilog	-----	.51**	14.83	20.9	1.329	2.753	91	290-1,080
WR48	$SO_4=0.6913(SC)^{0.7057}$	Log-log	1.023	.43**	9.384×10^{-2}	21.8	1.197	2.670	91	240-1,000
P76	$SO_4=13.29+9.800\times10^{-2}(SC)$	Linear	-----	.43**	9.384	25.4	5.409×10^{5}	241.1	81	120-600
P33	$SO_4=0.1786(SC)^{1.112}$	Log-log	1.143	.70**	.1817	43.7	4.531	2.676	75	110-1,750
WB301	$SO_4=112.3-2.767\times10^{4}(1/SC)$	Inverse	-----	.60**	7.746	12.5	5.041×10^{-6}	1.819×10^{-3}	45	380-870
WB245	$SO_4=-262.2+119.8(\log_{10} SC)$	Semilog	-----	.44**	11.35	16.1	.3144	2.779	47	400-920
WB228	$SO_4=-285.9+127.2(\log_{10} SC)$	Semilog	-----	.49**	11.46	16.7	.3554	2.788	48	360-920
WB219	$SO_4=-285.1+126.7(\log_{10} SC)$	Semilog	-----	.59**	10.27	15.3	.4074	2.781	46	340-1,040
WB207	$SO_4=117.5-2.817\times10^{4}(1/SC)$	Inverse	-----	.52**	10.22	14.9	6.012×10^{-6}	1.742×10^{-3}	44	320-900
WB194	$SO_4=20.95+8.523\times10^{-2}(SC)$	Linear	-----	.47**	11.01	15.6	7.791×10^{5}	581.1	55	280-1,010
WB128	$SO_4=-209.3+101.9(\log_{10} SC)$	Semilog	-----	.48**	10.66	14.7	.4998	2.768	52	300-870

[1] The unit of measure for Es for all models except log-log is milligram per liter and for the log-log models is $\log_{10}$ milligram per liter.

[2] The standard error of regression in percent (Ep) for all models except log-log is the standard error of regression (Es) divided by the mean of the dependent variable times 100. Ep for the log-log models is from Hardison (1971, table 1, p. C229).

[3] The standard error of regression (Es) for log-log models is for the log-log form and not for the exponential form shown in column two of this table. Es is reported to allow the reader to estimate confidence limits for the log-log model, and should not be compared with Es for the other models.

[4] The unit of measure for the linear models is the square of microsiemen per centimeter at 25° C, for the inverse model is the square of the reciprocal of microsiemen per centimeter at 25° C, and for the log-log and the semilog models is the square of $\log_{10}$ microsiemen per centimeter at 25° C.

[5] The unit of measure for the linear models is microsiemen per centimeter at 25° C, for the inverse model is the reciprocal of microsiemen per centimeter at 25° C, and for the log-log and semilog models is $\log_{10}$ microsiemen per centimeter at 25° C.

Table 24. Equations for predicting the relations between suspended-solids concentration and streamflow at Indiana State Board of Health stations

[SS, suspended-solids concentration, in milligram per liter; Q, streamflow, in cubic foot per second; p, the probability of obtaining a significant relation by chance where, in fact, there is no relation; *, the relation is significant at $p<0.05$; **, the relation is significant at $p<0.01$; NS, the relation is not significant at $p<0.05$]

Station	Predictive equation	Model	Bias corrector for log-log models, $(\Sigma 10^R)/n$	Coefficient of determination, R-square	Standard error of regression[1],[2], Es ($\log_{10}$ mg/L)	Standard error of regression[1],[2], Ep (percent)	Sum of squares of independent variable, Sxx ($\log_{10}$ ft^3/s)^2	Mean of independent variable, $\bar{X}$ ($\log_{10}$ ft^3/s)	Number of data pairs, n	Range of streamflow used to develop the predictive equation (ft^3/s)
EW77	$SS=0.3337(Q)^{0.5747}$	Log-log	1.403	0.35**	0.3458	92.0	21.25	3.535	112	394-23,100
EW56	$SS=0.6162(Q)^{0.5108}$	Log-log	1.362	.35**	.3597	99.4	98.85	3.375	376	278-58,600
WR166	$SS=0.6169(Q)^{0.5726}$	Log-log	1.597	.33**	.3769	106	85.96	3.203	409	242-32,200
WR130	$SS=0.6599(Q)^{0.5744}$	Log-log	1.443	.35**	.3662	102	72.61	3.360	333	343-41,100
WR80	$SS=1.702(Q)^{0.4662}$	Log-log	1.321	.31**	.3285	87.9	100.4	3.459	452	385-54,100
WR48	$SS=1.916(Q)^{0.3965}$	Log-log	1.360	.19**	.3431	93.1	19.58	3.938	114	1,050-61,700
WR19	$SS=1.164(Q)^{0.4697}$	Log-log	1.399	.30**	.3360	90.6	76.16	3.782	351	855-105,000
P86	$SS=10.46(Q)^{0.2506}$	Log-log	1.655	.27**	.3923	112	166.8	1.700	186	.10-2,610
P76	----	---	-----	NS	--	--	--	--	117	2.0-8,310
P33	----	---	-----	NS	--	--	--	--	81	31-6,820
P19	$SS=2.908(Q)^{0.4179}$	Log-log	2.365	.35**	.4512	140	223.1	2.399	351	4.3-14,500
P14	$SS=10.16(Q)^{0.2783}$	Log-log	1.698	.17*	.3910	112	8.853	2.518	24	20-2,190
WB301	$SS=0.1700(Q)^{0.6572}$	Log-log	1.516	.33**	.4036	119	68.63	3.578	376	610-88,000
WB260	$SS=0.7316(Q)^{0.4989}$	Log-log	1.404	.26**	.3704	103	52.63	3.620	279	660-47,000
WB245	$SS=0.1572(Q)^{0.6778}$	Log-log	1.264	.36**	.3183	84.3	4.950	3.822	42	1,830-30,700
WB228	$SS=0.6067(Q)^{0.5218}$	Log-log	1.446	.26**	.3812	107	67.15	3.787	368	940-56,800
WB219	$SS=7.065\times10^{-2}(Q)^{0.7716}$	Log-log	1.443	.37**	.3679	102	5.421	3.874	43	1,240-38,000
WB214	$SS=1.149(Q)^{0.4255}$	Log-log	1.538	.17**	.3961	114	50.50	3.808	286	910-88,000
WB207	$SS=0.4280(Q)^{0.5783}$	Log-log	1.357	.30**	.3292	88.2	5.043	3.921	39	1,300-39,800
WB194	$SS=0.9072(Q)^{0.4800}$	Log-log	1.240	.25**	.3035	79.4	10.03	3.977	77	1,380-51,700
WB128	$SS=1.052(Q)^{0.4891}$	Log-log	1.381	.24**	.3600	99.4	65.36	3.873	386	1,000-80,900

[1]The standard error of regression in percent (Ep) is from Hardison (1971, table 1, p. C229).

[2]The standard error or regression (Es) for log-log models is for the log-log form and not for the exponential form shown in column two of this table. Es is reported to allow the reader to estimate confidence limits for the log-log model.

Table 25. Equations for predicting the relations between total iron concentration and streamflow at Indiana State Board of Health stations

[Fe, total iron concentration, in microgram per liter; Q, streamflow, in cubic foot per second; p, the probability of obtaining a significant relation by chance where, in fact, there is no relation; *, the relation is significant at $p<0.05$; **, the relation is significant at $p<0.01$; NS, the relation is not significant at $p<0.05$]

Station	Predictive equation	Model	Bias corrector for log-log models, $(\Sigma 10^R)/n$	Coefficient of determination, R-square	Standard error of regression[1,2,3] Es	Standard error of regression[1,2,3] Ep (percent)	Sum of squares of independent variable[4], Sxx	Mean of independent variable[5], $\overline{X}$	Number of data pairs, n	Range of streamflow used to develop the predictive equation (ft^3/s)
EW77	$Fe=16.09(Q)^{0.4569}$	Log-log	1.084	0.62**	0.1770	42.5	10.44	3.491	45	394-20,600
WR166	----	---	-----	NS	--	--	--	--	11	242-4,960
WR48	$Fe=47.04(Q)^{0.3633}$	Log-log	1.196	.24**	.2516	63.2	10.68	3.988	71	1,050-61,700
P76	----	---	-----	NS	--	--	--	--	79	3.5-3,250
P33	$Fe=2,772-5.845\times10^{4}(1/Q)$	Inverse	-----	.10*	1,448	59.3	3.045×10^{-3}	5.649×10^{-3}	49	32-4,540
WB219	$Fe=1.788(Q)^{0.7145}$	Log-log	1.100	.64**	.2014	49.0	1.416	3.782	12	1,240-16,300
WB194	$Fe=257.0+0.1158(Q)$	Linear	-----	.78**	946.6	52.3	2.097×10^{9}	1.301×10^{4}	11	2,350-51,700
WB128	$Fe=38.01(Q)^{0.4069}$	Log-log	1.273	.22**	.3036	79.4	6.990	4.048	46	1,590-55,500

[1] The unit of measure for Es for all models except log-log is microgram per liter and for the log-log models is $\log_{10}$ microgram per liter.

[2] The standard error of regression in percent (Ep) for all models except log-log is the standard error of regression (Es) divided by the mean of the dependent variable times 100. Ep for the log-log models is from Hardison (1971, table 1, p. 229).

[3] The standard error of regression (Es) for log-log models is for the log-log form and not for the exponential form shown in column two of this table. Es is reported to allow the reader to estimate confidence limits for the log-log model, and should not be compared with Es for the other models.

[4] The unit of measure for the linear model is the square of cubic foot per second, for the inverse model is the square of the reciprocal of cubic foot per second, and for the log-log models is the square of $\log_{10}$ cubic foot per second.

[5] The unit of measure for the linear models is cubic foot per second, for the inverse model is the reciprocal of cubic foot per second, and for the log-log models is $\log_{10}$ cubic foot per second.

Table 26. Equations for predicting the relations between total iron concentration and suspended-solids concentration at Indiana State Board of Health stations

[Fe, total iron concentration, in microgram per liter; SS, suspended-solids concentration, in milligram per liter; p, the probability of obtaining a significant relation by chance where, in fact, there is no relation; **, the relation is significant at $p<0.01$]

Station	Predictive equation	Model	Bias corrector for log-log models, $(\Sigma 10^R)/n$	Coefficient of determination, R-square	Standard error of regression[1,2,3], Es	Standard error of regression[1,2,3], Ep (percent)	Sum of squares of independent variable[4], Sxx	Mean of independent variable[5], $\bar{X}$	Number of data pairs, n	Range of suspended solids concentration used to develop the predictive equation (mg/L)
EW77	$Fe=76.49(SS)^{0.6146}$	Log-log	1.034	0.83**	0.1187	27.9	7.732	1.494	45	3-240
WR166	$Fe=46.69(SS)^{0.7905}$	Log-log	1.028	.91**	.1104	25.8	1.706	1.561	11	10-180
WR48	$Fe=60.42(SS)^{0.6960}$	Log-log	1.122	.70**	.1660	39.7	9.563	1.896	74	9-450
P76	$Fe=260.6(SS)^{0.4446}$	Log-log	1.105	.51**	.1938	46.9	15.23	1.882	80	4-1,300
P33	$Fe=451.8(SS)^{0.3734}$	Log-log	1.114	.36**	.1953	47.3	7.303	1.761	50	4-280
WB219	Fe=-24.94+15.54(SS)	Linear	-----	.84**	382.0	33.2	3.108×10^4	75.58	12	4-210
WB194	Fe=-90.88+19.00(SS)	Linear	-----	.87**	709.2	39.2	8.765×10^4	93.62	11	19-370
WB128	Fe=-98.25+19.05(SS)	Linear	-----	.88**	313.6	32.3	9.869×10^3	56.14	7	7-140

[1] The unit of measure for Es for the linear models is microgram per liter and for the log-log models is $\log_{10}$ microgram per liter.

[2] The standard error of regression in percent (Ep) for the linear models is the standard error of regression (Es) divided by the mean of the dependent variable times 100. Ep for the log-log models is from Hardison (1971, table 1, p. C229).

[3] The standard error of regression (Es) for log-log models is for the log-log form and not for the exponential form shown in column two of this table. Es is reported to allow the reader to estimate confidence limits for the log-log model, and should not be compared with Es for the other models.

[4] The unit of measure for the linear models is the square of milligram per liter and for the log-log models is the square of $\log_{10}$ milligram per liter.

[5] The unit of measure for the linear models is milligram per liter and for the log-log models is $\log_{10}$ milligram per liter.

Table 27. Equations for predicting the relations between total manganese concentration and streamflow at Indiana State Board of Health stations

[Mn, total manganese concentration, in microgram per liter; Q, streamflow, in cubic foot per second; p, the probability of obtaining a significant relation by chance where, in fact, there is no relation; **, the relation is significant at $p<0.01$; NS, the relation is not significant at $p<0.05$]

Station	Predictive equation	Model	Coefficient of determination, R-square	Standard error of regression[1], Es (µg/L)	Standard error of regression[1], Ep (percent)	Sum of squares of independent variable[2], Sxx	Mean of independent variable[3], $\overline{X}$	Number of data pairs, n	Range of streamflow used to develop the predictive equation (ft^3/s)
EW77	----	---	NS	--	--	--	--	34	507-20,600
WR166	----	---	NS	--	--	--	--	35	286-14,100
WR80	----	---	NS	--	--	--	--	33	482-23,800
WR48	----	---	NS	--	--	--	--	34	1,350-46,400
P76	$Mn=2,111-609.0(\log_{10} Q)$	Semilog	0.60**	380.3	55.6	28.76	2.344	51	3.5-3,250
P33	$Mn=165.0+4,529\left\{\frac{1}{1+Q\times 10^{-2.5}}\right\}$	Hyperbolic	.47**	1,392	63.7	3.790	.4444	47	32-4,450
WB194	----	---	NS	--	--	--	--	12	1,380-51,700
WB128	----	---	NS	--	--	--	--	7	1,590-6,610

[1]The standard error of regression in percent (Ep) is the standard error of regression (Es) divided by the mean of the dependent variable times 100.

[2]The unit of measure for the hyperbolic model is the square of the reciprocal of cubic foot per second and for the semilog model is the square of $\log_{10}$ cubic foot per second.

[3]The unit of measure for the hyperbolic model is the reciprocal of cubic foot per second and for the semilog model is $\log_{10}$ cubic foot per second.

Table 28. Equations for predicting the relations between total manganese concentration and specific conductance at Indiana State Board of Health stations

[Mn, total manganese concentration, in microgram per liter; SC, specific conductance, in microsiemen per centimeter at 25°C; p, the probability of obtaining a significant relation by chance where, in fact, there is no relation; **, the relation is significant at $p<0.01$; NS, the relation is not significant at $p<0.05$]

Station	Predictive equation	Model	Bias corrector for log-log models, $(\Sigma 10^R)/n$	Coefficient of determination, R-square	Standard error of regression[1,2,3], Es	Standard error of regression[1,2,3], Ep (percent)	Sum of squares of independent variable[4], Sxx	Mean of independent variable[5], $\overline{X}$	Number of data pairs, n	Range of specific conductance used to develop the predictive equation (µS/cm at 25° C)
EW77	$Mn=1.072\times10^4(SC)^{-0.7615}$	Log-log	1.080	0.22**	0.1722	41.3	0.4601	2.582	34	180-680
WR166	----	---	-----	NS	--	--	--	--	11	630-1,100
WR80	----	---	-----	NS	--	--	--	--	33	290-1,050
WR48	----	---	-----	NS	--	--	--	--	34	240-810
P76	$Mn=-452.1+4.597(SC)$	Linear	-----	.52**	417.8	61.1	4.355×10^5	247.1	51	120-600
P33	$Mn=109.6+2.626(SC)$	Linear	-----	.81**	845.0	38.8	1.926×10^7	787.6	47	110-2,990
WB194	----	---	-----	NS	--	--	--	--	12	280-1,010
WB128	----	---	-----	NS	--	--	--	--	7	480-720

[1] The unit of measure for the linear models is microgram per liter and for the log-log model is $\log_{10}$ microgram per liter.
[2] The standard error of regression in percent (Ep) for the linear models is the standard error of regression (Es) divided by the mean of the dependent variable times 100. Ep for the log-log model is from Hardison (1971, table 1, p. C229).
[3] The standard error of regression (Es) for the log-log model is for the log-log form and not for the exponential form shown in column two of this table. Es is reported to allow the reader to estimate confidence limits for the log-log model, and should not be compared with Es for the other models.
[4] The unit of measure for the linear models is the square of microsiemen per centimeter at 25° C and for the log-log model is the square of $\log_{10}$ microsiemen per centimeter at 25° C.
[5] The unit of measure for the linear models is microsiemen per centimeter at 25° C and for the log-log model is $\log_{10}$ microsiemen per centimeter at 25° C.

Table 29. Slope and significance of the functional relations between specific conductance and streamflow at U.S. Geological Survey gaging stations

[–, a negative relation; p, the probability of obtaining a significant relation by chance where, in fact, there is no relation; *, the relation is significant at $p<0.05$; **, the relation is significant at $p<0.01$]

Station Number	Station Name	Functional relation between specific conductance and streamflow
03303300	Middle Fork Anderson River at Bristow	-*
03303400	Crooked Creek near Santa Claus	-**
03322100	Pigeon Creek at Evansville	-**
03342100	Busseron Creek near Hymera	-**
03342150	West Fork Busseron Creek near Hymera	-**
03342250	Mud Creek near Dugger	-**
03342300	Busseron Creek near Sullivan	-**
03342360	Buttermilk Creek near Sullivan	-**
03342500	Busseron Creek near Carlisle	-**
03360000	Eel River at Bowling Green	-**
03375500	Patoka River at Jasper	-**
03375800	Hall Creek near St. Anthony	-**
03376260	Flat Creek near Otwell	-**
03376300	Patoka River at Winslow	-**
03376350	South Fork Patoka River near Spurgeon	-**
03376500	Patoka River near Princeton	-**

Table 30. Slope and significance of the functional relations between water-quality variables at Indiana State Board of Health stations

[+, a positive relation; −, a negative relation; p, the probability of obtaining a significant relation by chance where, in fact, there is no relation; *, the relation is significant at $p<0.05$; **, the relation is significant at $p<0.01$; NS, the relation is not significant at $p<0.05$]

Functional relation between...	Station																				
	EW77	EW56	WR166	WR130	WR80	WR48	WR19	P86	P76	P33	P19	P14	WB301	WB260	WB245	WB228	WB219	WB214	WB207	WB194	WB128
Specific conductance and streamflow	-**	-**	-**	-**	-**	-**	-**	-**	-**	-**	-**	-**	-**	-**	-**	-**	-**	-**	-**	-**	-**
pH and streamflow	NS	NS	NS	-*	-**	-**	-**	+*	NS	NS	+**	NS	NS	NS	NS	NS	NS	-**	NS	+*	-*
pH and specific conductance	NS	NS	-*	NS	NS	+*	NS	NS	NS	NS	-**	NS	NS	-*	NS	NS	+**	+**	+**	NS	NS
Total alkalinity concentration and streamflow	-**	-**	-**	-**	-**	-**	-**	-**	--	--	+**	--	-**	-**	--	-**	--	-**	--	--	-**
Total alkalinity concentration and specific conductance[1]	+**	+**	+**	+**	+**	+**	+**	+**/-*	--	--	-**	--	+**	+**	--	+**	--	+**	--	--	+**
Sulfate concentration and streamflow	-**	--	-**	--	-**	-**	--	--	-**	-**	--	--	-**	--	-**	-**	-**	--	-**	-**	-**
Sulfate concentration and specific conductance	+**	--	+**	--	+**	+**	--	--	+**	+**	--	--	+**	--	+**	+**	+**	--	+**	+**	+**
Suspended-solids concentration and streamflow	+**	+**	+**	+**	+**	+**	+**	+**	NS	NS	+*	+**	+**	+**	+**	+**	+**	+**	+**	+**	+**
Total iron concentration and streamflow	+**	--	NS	--	--	+**	--	--	NS	+*	--	--	--	--	--	--	+**	--	--	+**	+**
Total iron concentration and suspended-solids concentration	+**	--	+**	--	--	+**	--	--	+**	+**	--	--	--	--	--	--	+**	--	--	+**	+**
Total manganese concentration and streamflow	NS	--	NS	--	NS	NS	--	--	-**	-**	--	--	--	--	--	--	--	--	--	NS	NS
Total manganese concentration and specific conductance	-**	--	NS	--	NS	NS	--	--	+**	+**	--	--	--	--	--	--	--	--	--	NS	NS

[1] At station P86, the functional relation between total alkalinity concentration and specific conductance was positive from 106 to 426 µS/cm at 25° C but was negative when specific conductance exceeded 450 µS/cm at 25° C.

METRIC CONVERSION FACTORS

The inch-pound units used in this report can be converted to metric units by use of the following factors:

Multiply Inch-Pound Units	By	To Obtain Metric Units
cubic foot per second (ft^3/s)	0.02832	cubic meter per second (m^3/s)
cubic foot per second per square mile ($ft^3/s/mi^2$)	0.01093	cubic meter per second per square kilometer ($m^3/s/km^2$)
inch (in.)	25.40	millimeter (mm)
square mile (mi^2)	2.590	square kilometer (km^2)
degree Fahrenheit (°F)	5/9(°F-32°)	degree Celsius (°C)